This is to certify that the

dissertation entitled

MICROWAVE PROCESSING AND DIELECTRIC DIAGNOSIS
OF POLYMERS AND COMPOSITES USING A
SINGLE-MODE RESONANT CAVITY TECHNIQUE
presented by

Jinder Jow

has been accepted towards fulfillment
of the requirements for

Ph.D. degree in CHE

Major professor

Date October 14, 1988.

MICROWAVE PROCESSING AND DIELECTRIC DIAGNOSIS OF POLYMERS AND COMPOSITES USING A SINGLE-MODE RESONANT CAVITY TECHNIQUE

By

Jinder Jow

A DISSERTATION

Submitted to

Michigan State University

in partial fulfillment of the requirements

for the degree of

DOCTOR OF PHILOSOPHY

Department of Chemical Engineering

1988

ABSTRACT

MICROWAVE PROCESSING AND DIELECTRIC DIAGNOSIS OF POLYMERS AND COMPOSITES USING A SINGLE-MODE RESONANT CAVITY TECHNIQUE

By

Jinder Jow

The objectives of this research are to develop microwave coupling and dielectric measurement systems for processing of materials, and to understand microwave power absorption and heat transfer inside the materials. A single-mode resonant cavity technique has been developed to simultaneously heat the materials and measure material dielectric properties at 2.45 GHz. Dielectric measurements are made using the TM_{012}-mode material-cavity perturbation technique. However, only small samples can be processed and diagnosed due to the perturbation limitations and the cavity size. Two consistent and repeatable methods (single and swept frequency methods) are used to measure material dielectric properties. Dielectric properties of epoxy/amine resins are measured using the single frequency method during microwave curing and using the swept frequency method during cooling. Dielectric properties of epoxy/amine resins decrease as the extent of cure increases. Dielectric loss factors of nonreacting polymers (Nylon 66 and pure epoxy) as a function of temperature are also obtained. The dielectric loss factor of polymers increases with increasing temperature before reaching the maximum dielectric loss but decreases thereafter.

Continuous and computer-controlled pulsed microwave power systems have been developed to process nonreacting materials, reacting polymers, and composites. This controlled pulsed power has been utilized to eliminate the exothermic temperature peak, maintain constant temperature-time profiles, and measure dielectric loss factors during curing of epoxy/amine resins. Curing time of epoxy/amine resins using pulsed microwave energy is longer than that using thermal energy at a given temperature. However, the slow reaction can be compensated at a higher cure temperature using controlled pulsed power.

For microwave processing of low thermal conductivity polymers or composites, a temperature gradient is eventually built up due to surface heat loss, slow heat conduction, and changes in loss factor with temperature and electric field strength with loss factor inside the materials. The electric field strength inside the resonant cavity always decreases as the material loss factor increases. Microwave heating is fast, controllable, selective, and outward, but not necessarily uniform. Uniform microwave heating of low thermal conductivity materials can be achieved by insulating the material boundary, fast heating, increasing the material thermal conductivity, or combining microwave and thermal methods during the heating process.

ACKNOWLEDGMENTS

The author wishes to express his sincere appreciation to his academic advisor, Dr. Martin C. Hawley for his general guidance. Appreciation is also given to Dr. Jes Asmussen for his valuable guidance in understanding the microwave cavity technique. The author is grateful to Ron Fritz for the microwave system set-up and Mark C. Finzel for his helpful discussion and proofreading in several publications. The author also wishes to thank his undergraduate assistant, Tom Kern, for assisting some of the experiments, and his brother, Tzong C. Jow, for his family support. Special thanks would like to be expressed to the author's wife, Shu-Chen Chiang for her continued love, encouragement and sacrifice during his graduate research years.

This work was supported in part by the U.S. Army under contract number DAAG46-85-K-0006 and the Navy university initiative program on thick-section composites administrated by University of Illinois.

TABLE OF CONTENTS

LIST OF TABLES

LIST OF FIGURES

CHAPTER ONE

INTRODUCTION

1.1 Research Scope

Microwave processing of polymers and composites is an alternative to conventional thermal processing. In the thermal process, heat is nonselective and conducted from the material boundaries to the material interiors. Heat produced by the exothermic curing reaction can significantly induce temperature gradients inside the materials. This non-uniformity in the temperature/position/time profile can build up thermal stress and create mechanical defects within the polymer or composite part. Curing time is also very long and temperature gradients inside the materials are steeper when the materials are thick than when they are thin. However, microwave energy can be directly transferred to the lossy materials and heat thick materials quickly. Heat is then conducted from the material interior to the cold material boundary. Microwaves can concentrate heating of polymers and composites within the higher lossy constituent or interface rather than the lower lossy surrounding materials. The exothermic heat can also be eliminated by controlling the input power cycle. The advantages of using microwave heating for processing of polymers and composites are: (1) fast, direct, and outward heating, (2) selective heating dependent upon the magnitude of loss factor of constituents in materials, and (3) increased control of material temperature/time profile and input power cycles to optimize the reaction process. These advantages may cause microwave heated

polymers and composites to have superior mechanical characteristics when compared with thermally heated materials.

Continuous microwave cure of thermosetting resins has been investigated using multi-mode microwave ovens and wave guides. These experiments show that greater rapidity of cure and direct heating can be obtained using microwave heating. However, the multi-mode ovens and wave guides are usually low energy efficiency devices. They can not efficiently control or simultaneously diagnose the heating process. Thermoset cures are also very difficult to monitor up to the end of reaction due to conversion of viscous liquids to crosslinked solids. Dielectric diagnosis is one of a few nondestructive, sensitive and convenient techniques available for studying the entire cure process. Dielectric measurements at a given temperature and frequency can be used to relate dielectric properties to the extent of cure in order to monitor the cure process. Another important factor of using dielectric analysis in this research is the ability of diagnosing the reaction under microwave energy radiation.

A continuous microwave processing and dielectric diagnosis technique using a single-mode resonant cavity is developed here to efficiently transfer microwave energy into the loaded materials and to diagnose the curing process. Three typical material temperature-time stages occur in the continuous microwave curing processes: (1) initial rapid temperature rise by directly heating the monomers, (2) a significant temperature peak due to the exothermic curing reaction, and (3) free convective cooling at the end of reaction. Exothermic heat usually increases the temperature gradient inside the samples during the curing. Neither continuous microwave nor thermal process can be effectively controlled in order to maintain constant temperature-time

profiles through the entire process. Therefore, this single-mode resonant cavity system is further aided with computer data acquisition and control. The computer-aided system with feedback temperature control can diagnose the curing process, eliminate the exothermic heat, and maintain constant material temperature-time profiles by pulsing the input power. This controlled pulsed microwave system can also process thermosetting resins at a higher cure temperature without thermal degradation when compared with thermal or continuous microwave process.

1.2 Concept of Microwave Processing and Dielectric Diagnosis

Incident electromagnetic fields can interact with conductive and nonconductive materials. The fundamental electromagnetic property of nonmagnetic materials for microwave heating and diagnosis is complex permittivity ($\epsilon_t^* = \epsilon_t' - \epsilon_t''j$). In general, the complex permittivity of materials consists of two major components: ionic and dipolar contributions. The dipolar contribution is due to the motion of dipoles. The ionic contribution is due to the motion of ions or electrons. The real part of the complex permittivity is permittivity ϵ_t' (dielectric constant), which is related to the energy stored in the materials. The imaginary part of the complex permittivity is loss factor ϵ_t'', which is related to energy dissipated as heat in the materials. The loss factor of materials is generally due to contributions by dielectric loss factor ϵ'' (the motion of dipoles) and conductivity σ (the motion of charges) as described in Equation 1.1. The loss factor is a function of material structures and compositions, angular frequency, temperature, and pressure. The electromagnetic energy absorption P_m of materials is dependent on the angular frequency,

the material loss factor, and the square of the electric field strength inside the material as described in Equation 1.2.

$$\epsilon_t'' = \epsilon'' + \sigma/\omega\epsilon_o \tag{1.1}$$

$$P_m = 0.5\ \omega\ \epsilon_o\ (\epsilon'' + \sigma/\omega\epsilon_o)\ |E|^2 \tag{1.2}$$

For conductive materials such as carbon fibers and acid solutions, microwave heating is mainly due to the interaction of the motion of ions or electrons with the electric field. However, for a perfect conductor, the electric field is reflected and no electric field is induced inside a perfect conductor at any frequency. Therefore, no electromagnetic energy will be dissipated even though the conductivity of the perfect conductor is infinite. For nonconductive materials such as polymers, glass fibers, and Kelvar fibers, dielectric heating is mainly due to the interaction of the motion of dipoles with the alternating electric field. However, semiconductors can have comparable conductive and dielectric heating at microwave frequencies. Since electromagnetic heating is strongly dependent upon the magnitude of loss factor of the constituents, selective and fast microwave heating can be used to fuse two materials into one, either surface-to-surface (composite processing) or edge-to-edge (sealing). The matrix material has low loss relative to the interface. The interface is an uncured adhesive material with high loss or is coated with a high lossy adhesive resin. Microwave energy is then directly transferred into the interface and cures the interface extremely rapidly, even though the matrix material is very thick.

In dielectric materials, the polar segments attempt to align up with the alternating electromagnetic field so that the normal random orientation of the dipoles becomes ordered. These ordered polar

segments tend to relax and oscillate with the field. The energy used to hold the dipoles in place is dissipated as heat into the material while the relaxation motion of dipoles is out of phase with the oscillation of the electric field. The alignment ability of these dipoles with the field is defined as dielectric constant, which is related to the energy stored in the material. The mobility of these dipoles under the alternating electric field is defined as dielectric loss factor, which is related to the energy dissipated in the material.

Thermoplastic and thermoset polymers, typical dielectric materials, are classified on the basis of their response to heating. Thermoplastic polymers melt on heating and solidify on cooling. Some common thermoplastic resins are PVC, PEEK, and Nylon, etc. On the other hand, thermosetting polymers are heated and irreversibly converted from fusible materials to infusible, rigid, crosslinked solids. Some common commercial thermosetting resins are epoxy resins, phenolics, amino resins, polyesters, polyurethanes, polyisocyanurates, silicones, polyimides, etc. These polymers do indeed have polar groups to interact with electromagnetic fields and exhibit dielectric relaxation at microwave frequencies, ranging from methyl groups, epoxide groups, hydroxyl groups, amino groups, and others. Microwave energy can be directly absorbed by these polar groups. The localized heating on the reactive polar sites can initiate or promote reactions which require heat. The population and mobility of the polar chains change as these reactive sites are consumed during reaction. The presence of these polar groups can be determined by dielectric loss factor measurements. The polar chains with lower dielectric loss do not absorb microwave energy as readily as those with higher dielectric loss. The rate of microwave energy absorption of materials is determined by the dielectric

loss factor and electric field strength. Therefore, the dielectric loss factor of materials can be an index of the extent of reaction as well as an index of microwave energy dissipation in the materials. Dielectric loss measurements can also be used to monitor the matrix curing process for composites (such as glass/epoxy) with low lossy additives relative to the matrix.

In conductive materials, the net charge due to electrons or ions is conducted inside the material under the alternating electric fields so that a conduction current is induced. Electromagnetic energy is dissipated into the materials while the conduction current is in phase with the electric field inside the materials. Dissipated energy is proportional to conductivity and the square of the electric field strength. The ability of inducing charge density inside materials under the alternating electric fields is defined as dielectric constant, which is related to the energy stored in the materials. The conduction of charge inside the materials is defined as conductivity, which is related to the energy dissipated in the materials. The presence of mobile ions or electrons can be determined by conductivity measurements. Therefore, for microwave processing of graphite/epoxy composites, energy is preferably absorbed by the conductive fibers and heat is conducted from the fiber to the matrix. Loss factor is mainly due to the fiber conductivity and can not be used to diagnose the curing process of the low lossy matrix relative to the fibers.

1.3 Specific Research Topics

This thesis research is directed towards development and investigation of microwave coupling and measurement systems for material

processing. Five specific topics are studied and discussed in the following chapters. The first research topic in Chapters 2 and 3 is to develop a continuous microwave processing and diagnostic technique of non-reacting and reacting materials. The second research topic in Chapter 4 is to study the continuous microwave curing and dielectric diagnosis of epoxy/amine resins at a microwave frequency of 2.45 GHz. The third research topic in Chapter 5 is to develop a computer-controlled pulsed microwave processing and diagnostic system and to study the effects on processing of epoxy/amine resins. The next research topic in Chapter 6 is to investigate controlled pulsed microwave heating of composite materials. The last research topic in Chapter 7 is to model and to understand the power absorption and heating characteristics during microwave heating of low thermal conductivity nonreacting polymeric materials (Nylon 66).

A microwave single-mode resonant cavity technique has been developed to heat the materials and diagnose the heating process. A cavity of 7.62 cm in radius was used and resonated with the microwave external circuit in the TM_{012} mode at 2.45 GHz. Two diagnostic techniques were employed in this system: on-line measurements of temperature and complex permittivity. Temperature measurements were made using fluoroptic thermometry. Complex permittivity measurements were made using the TM_{012}-mode material-cavity perturbation technique. Three types of microwave absorbing materials were used in this study: (1) nonreacting materials: Nylon 66, graphite, and pure epoxy, (2) reacting materials: epoxy/amine resins, and (3) composite materials: Nylon 66 with graphite, and epoxy with graphite and glass powders.

In Chapters 2 and 3, the continuous microwave heating and dielectric measurement of nonreacting and reacting materials is

developed using the single-mode resonant cavity technique [1-4]. The material-cavity perturbation technique is reviewed in Chapter 2. The TM_{012}-mode perturbation equations were derived and discussed. Two experimental methods (single and swept frequency methods) were used to simultaneously heat Nylon 66 rods and to measure the material dielectric properties. The microwave processing and diagnostic system as well as these two methods are fully described in this chapter [2]. In Chapter 3, the single frequency method used to process chemically reacting materials and to measure the complex permittivity is described [4]. Epoxy/amine resins were used in this study. Microwave curing of epoxy resins using waveguides and multi-mode cavities is also reviewed in Chapter 3.

In Chapter 4, fundamental models and experimental techniques for dielectric analysis of materials are reviewed. A literature survey on dielectric study on epoxy/amine resins below the microwave frequencies is also made. Dielectric data of epoxy/amine resins as a function of extent of cure and temperature were obtained and discussed using this single-mode resonant cavity technique [5,6].

In Chapter 5, the newly developed computer-controlled pulsed microwave processing and diagnostic system is described and discussed [7,8]. Temperature/position/time profiles of epoxy/amine cure using controlled pulsed power were compared with those using continuous microwave and thermal processing. Dielectric measurements and high temperature cure using controlled pulsed microwave power were demonstrated. The effects on cure kinetics and glass transition temperature using controlled pulsed microwave power were also investigated and compared with thermal cure.

In Chapter 6, temperature/position/time profiles of composites were

studied using the controlled pulsed power system [9]. The selective microwave heating is illustrated using rodlike composites of graphite/Nylon materials. The temperature/position/time profiles of epoxy with and without conductive and nonconductive powders using this controlled pulsed microwave heating were studied. A hybrid mode of microwave and thermal heating is also developed to heat low thermal conductive materials uniformly and quickly.

In Chapter 7, non-uniform temperature distribution and power absorption due to surface heat loss, slow heat conduction, and changes in the dielectric loss and the electric field strength were studied during microwave heating of low thermal conductivity materials [10]. Nylon 66, a nonreacting low thermal conductivity material, was used in this study. The dielectric loss factor of Nylon 66 as a function of temperature at 2.45 GHz was measured and modeled using a simple Debye dielectric relaxation model. The square of the electric field strength was also measured and related to the material dielectric loss. Microwave heating characteristics were then modeled and verified with the experimental data. Methods of improving microwave heating of low thermal conductivity materials are also discussed in this chapter.

The above research findings and achievements are summarized in Chapter 8. Suggestions for future work are proposed in Chapter 9.

CHAPTER TWO

MICROWAVE RESONANT CAVITY TECHNIQUE

2.1 Introduction

The long term objectives of this research are to develop microwave processing and diagnostic techniques to heat materials and to diagnose the heating process. Several types of microwave applicators can be used to heat materials: (1) transmission line, (2) wave guide, (3) non-resonant cavity, and (4) resonant cavity. However, the resonant cavity system can have higher energy efficiency to transfer microwave power into the processed materials. The resonant cavity system can also measure complex permittivity of the materials during heating and be adaptable for feedback control of the heating process.

Two microwave resonant cavity techniques have been used to simultaneously heat the material and measure material complex permittivity during heating. One method is a dual-mode technique which heats the material in a high power mode and measures the material complex permittivity in a low power diagnostic mode. The other method is a single-mode technique which heats and diagnoses the material in the same high power mode.

Couderc [11] has developed a dual-mode technique using a heating mode of TM_{010} at 2.45 GHz, and a diagnostic mode of TE_{111} at 3.1 GHz for spherical samples and TM_{012} at 3.7 GHz for rodlike samples. Temperature measurements of materials were made using an IR radiation thermometer. The sample was placed at the position of strongest electric fields for

both heating and diagnostic modes in a cylindrical cavity. The heating and the diagnostic modes were individually coupled without any cross-coupling. The accuracy of dielectric measurements using material-cavity perturbation was ±3% for ϵ' and ±15 % for ϵ''.

Dielectric measurement using material-cavity perturbation is also a suitable diagnostic method in the single-mode resonant cavity technique. Two methods are used to heat the material and to measure material complex permittivity using material-cavity perturbation: (1) swept frequency method, and (2) single frequency method. The swept frequency method measures conventional resonant frequency shifts and cavity Q factor changes from the resonance curve of a sweeping cavity at a fixed cavity length. The single frequency method measures the changes of the resonant cavity length and power ratio measurements at a single frequency. Both swept and single frequency methods have been applied on-line to diagnose and process chemically reacting materials (epoxy/amine resins) in a TM_{012}-mode resonant cavity [3,4]. However, most of the incident input power using the swept frequency method is reflected. The microwave power can be more efficiently transferred into the processed materials using the single frequency method. In the swept frequency method, the measurement accuracy of the resonant frequency shift and the cavity Q factor is limited by the resolution of the cavity resonance curve on the X-Y oscilloscope and frequency marker. Power ratio and cavity length measurements in the single frequency method are faster and more accurate. The microwave power input is also easily controlled using the single frequency method. Therefore, the single frequency method is more suitable to simultaneously heat the material and diagnose the heating process when compared with the swept frequency method.

The objective of this chapter is to develop a microwave single-mode resonant cavity technique to heat the materials and to measure the material complex permittivity during heating. This microwave processing and diagnostic system is fully described here. The sample temperatures are measured using a fluoroptic thermometer. Dielectric measurements using the material-cavity perturbation technique are reviewed and discussed. A nonreacting and microwave absorbing material rod used in this study is Nylon 66. A TM_{012} mode, which is suitable to process the rodlike sample, is used as a heating and diagnostic mode. A "tunable" cylindrical cavity is continuously resonated with the microwave external circuit in the TM_{012} mode during microwave heating of the sample at 2.45 GHz. Dielectric measurements using the single and swept frequency methods are presented. Dielectric measurements during microwave heating of Nylon 66 using these two methods are made and compared.

2.2 Microwave Processing and Diagnostic System

The microwave processing and diagnostic system has four basic components: (1) a tunable cavity, (2) an external microwave circuit, (3) a temperature sensing system, and (4) loaded materials. A schematic diagram of this system is shown in Figure 2.1.

2.2.1 Tunable cavity

A prototype tunable cavity is shown in Figure 2.2. The cavity is a cylindrical brass cylinder (15.25 cm i.d., 25.4 cm long, and 0.3175 cm thick) with an internal transverse brass circular shorting plate. This shorting plate inside the cavity is adjustable to provide a variable cavity length from 4.500 cm to 21.890 cm. One sample-insertion hole of

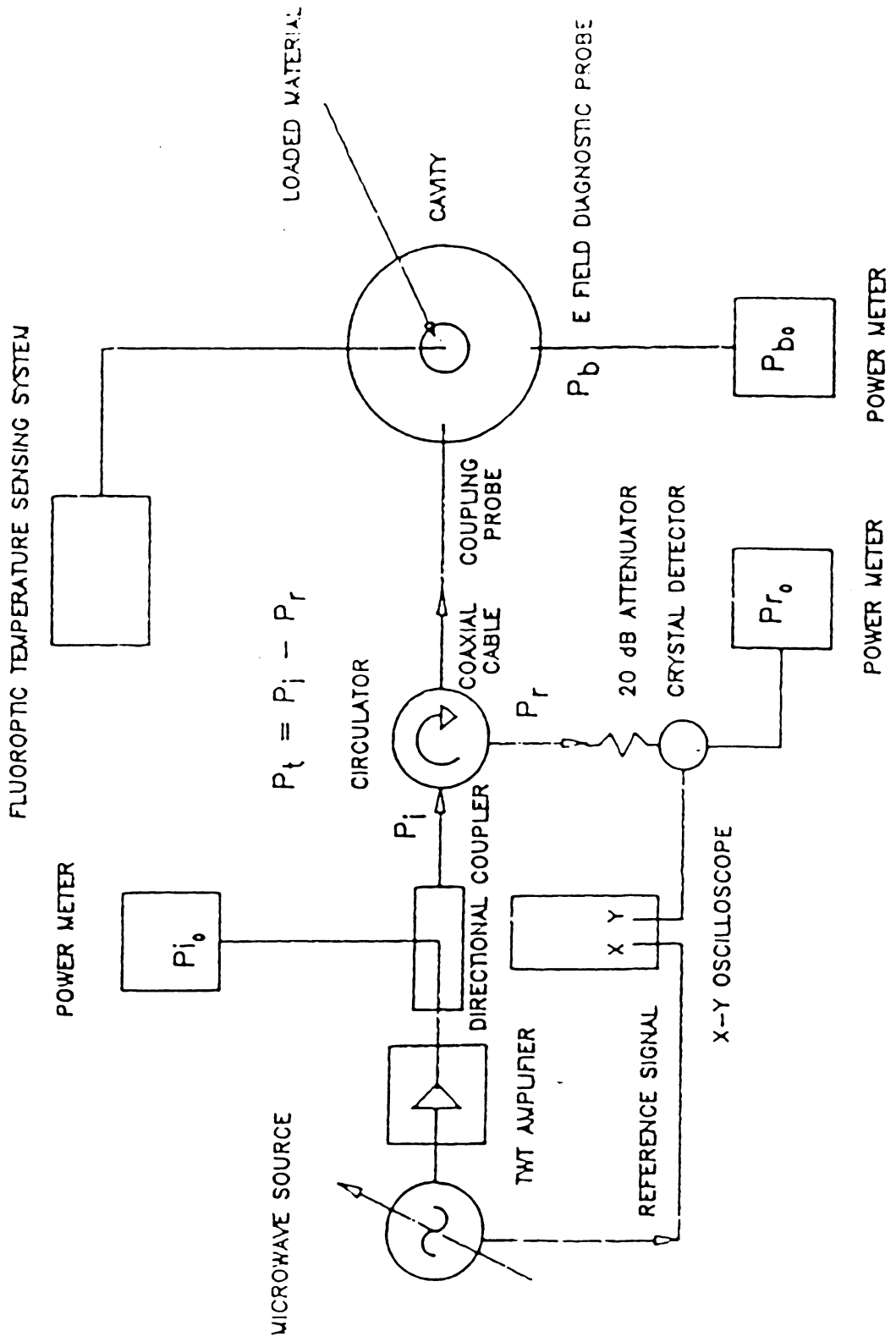

Figure 2.1: Microwave processing and diagnostic system circuit

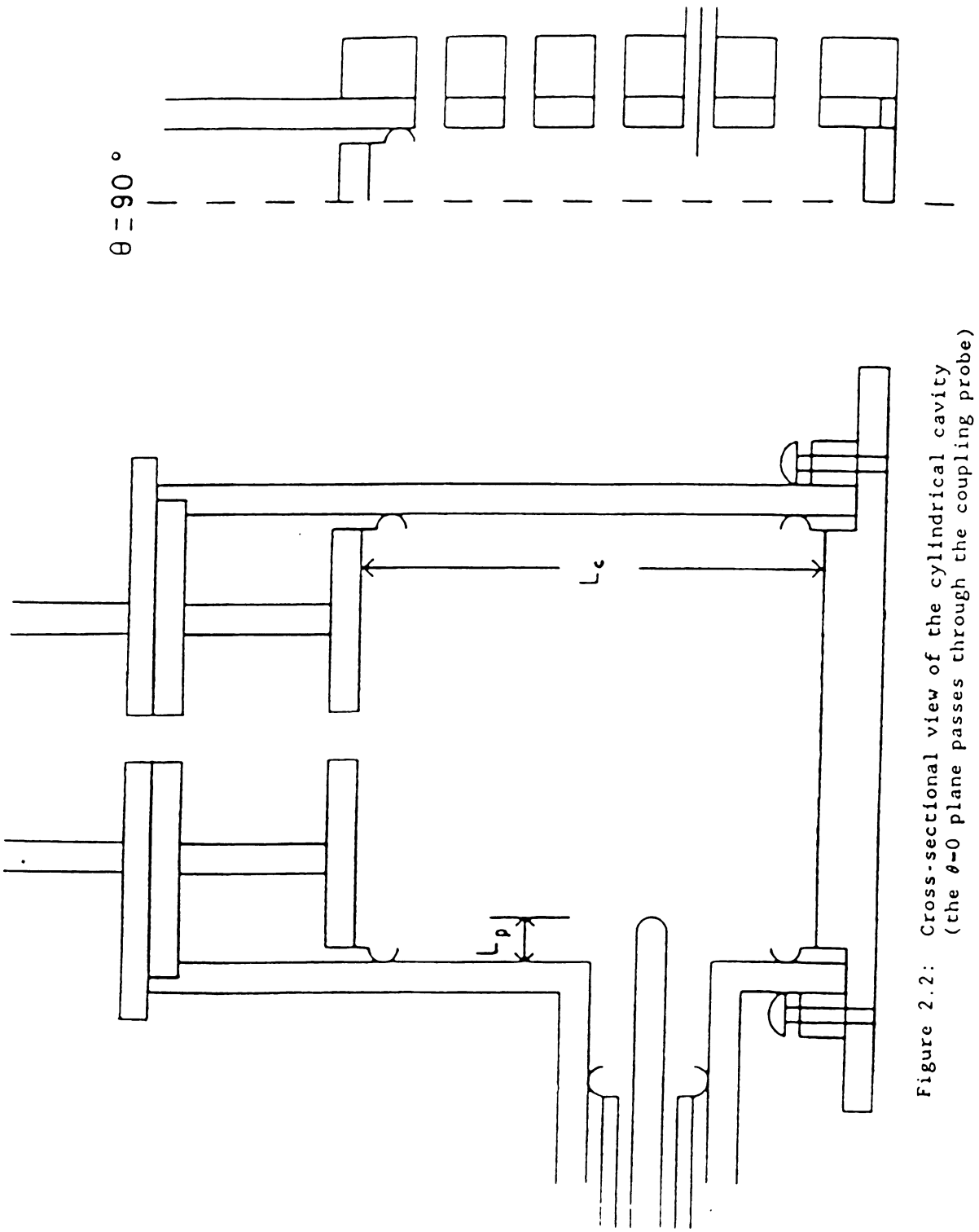

Figure 2.2: Cross-sectional view of the cylindrical cavity (the θ=0 plane passes through the coupling probe)

1.27 cm in radius is drilled through the center of the top and shorting plates. The sample with a cotton thread is loaded through this hole without removing the top plates of the cavity. The removable and shorting bottom plate is designed to easily place and process large disk materials. Silver fingers (Varian CF 300) are soldered around both internal shorting plates to provide good electrical contact with the cavity wall. Two cylindrical brass tubes (1.372 cm i.d. and 7.62 cm long) are perpendicular to each other and located 3.81 cm above the surface of the bottom plate. A semirigid 50 ohm impedance copper coaxial probe serving as a field excitation probe (a coupling probe) has an outer conductor of 1.27 cm diameter and an inner conductor of 0.44 cm diameter. The coupling probe through one brass tube provides a variable inner-conductor depth from 0.000 to 4.000 cm in order to couple microwave power into the cavity. Adjustments of the cavity length L_c and coupling probe depth L_p are made by manual rotation of the knobs and measured within 0.1 mm by the micrometer indicators.

A rectangular brass block (1.09 cm wide, 1.27 cm thick, and 17.145 cm long) is soldered on the outside of the cavity wall perpendicular to the direction of the coupling probe. Sixteen electric field diagnostic holes are equally spaced 0.922 cm apart, starting 0.635 cm above the surface of the bottom plate. These holes are drilled through this block and the cavity wall. A 2 mm copper microcoaxial probe is used as an E-field diagnostic probe. This diagnostic probe has only a very small inner-conductor depth of 0.15 cm into the cavity so that the electric field is detectable and essentially undisturbed. A diagram of this probe is shown in Figure 2.3 [12]. This E-field probe is inserted into the cavity applicator through the fifth diagnostic hole (4.32 cm above

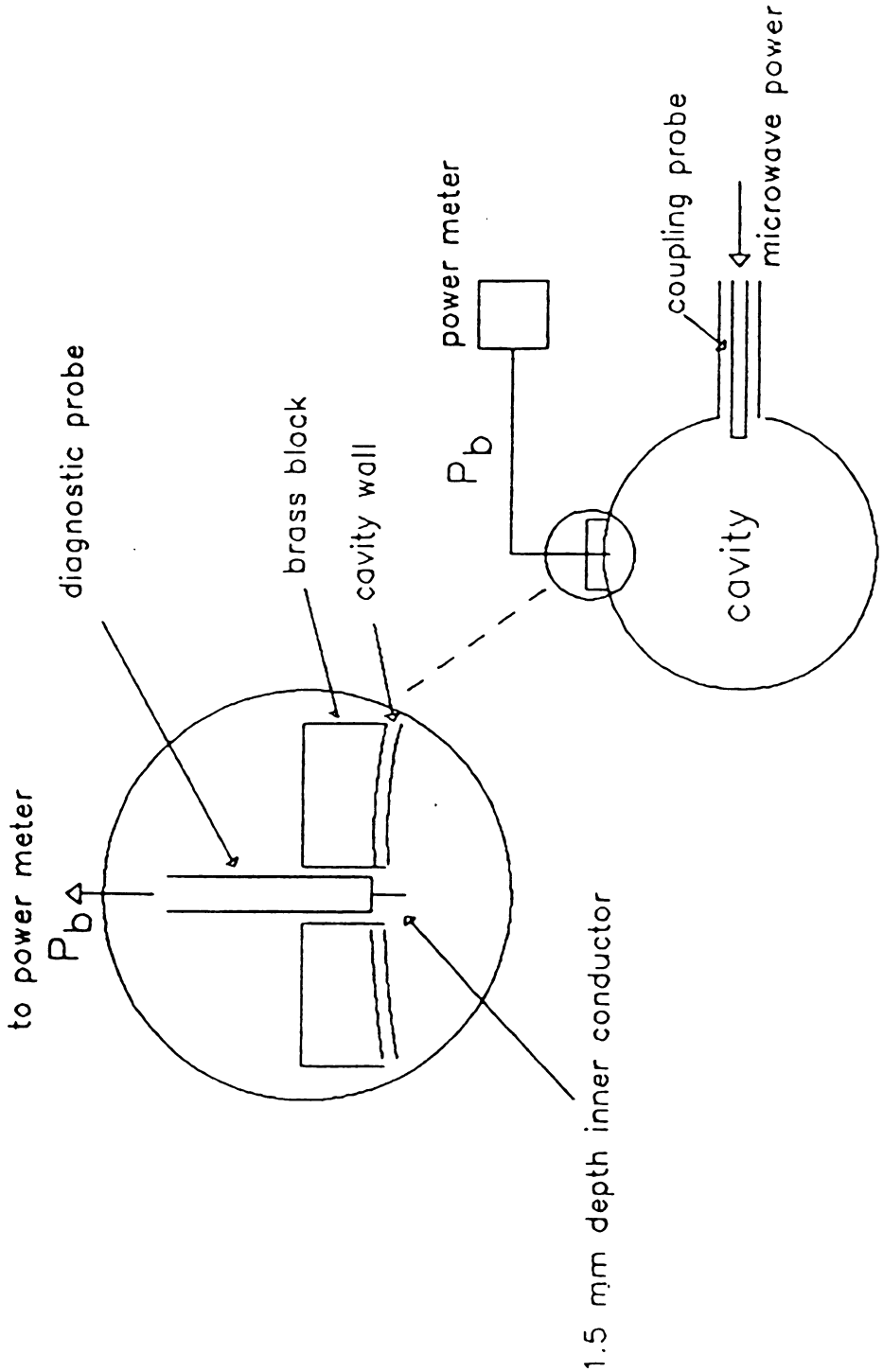

Figure 2.3: Top view of the diagnostic probe

the surface of the bottom plate), where the probe can diagnose almost the maximum magnitude of the TM_{012} standing radial wave at the cavity wall. The measured power by this diagnostic probe is proportional to the square of the radial electric field inside the cavity.

2.2.2 External microwave circuit

A microwave signal generator is a sweep oscillator (HP8350B) connected with an RF plug-in (HP86235A) via an adapter (HP11869A). The generator is protected by an isolator and incorporates a TWT amplifier (Varian 1356S) which can amplify the signal from 0 to 20 W. Another isolator (King KN-59-38) is used to protect the amplifier from power reflecting from the cavity. The incident input power P_{i0} from the source is decoupled by a 10 dB directional coupler (Narda 30010) and directly measured by a power meter (HP435B). The incident microwave energy is fed into the tunable cavity via the coupling probe. The reflected power P_{r0} from the cavity is guided by a circulator (Ferrite 2620), attenuated down by a 20 dB attenuator, and measured by another power meter (HP435B). The attenuated reflected signal is also rectified by a crystal detector so that a resonance curve can be displayed on an X-Y oscilloscope (Tektronix 485) whenever the swept frequency method is employed. The power P_b detected by the diagnostic probe and measured by a power meter (HP435B) is proportional to the square of the radial electric field inside the cavity ($P_b = K_b |E_r|^2$).

2.2.3 Temperature sensing system

The fluoroptic thermometry system is a Luxtron Model 750, manufactured by Luxtron Inc. The model is a four-channel fiber optic

temperature sensing system [13]. The system consists of a main system unit and optical fiber probes (one for each channel). The main system unit has a Xenon flash lamp, lenses, filter, four optical heads, and the processing electronics which manipulate signals and display temperature reading. Several types of probes can be used for different temperature ranges. These probes are electrically nonconductive and do not interfere with the electromagnetic fields. MIW fiber probes for the temperature range from -190 to 300 °C are used in this research. The probe consists of a sensing tip, a silica fiber with a jacket of teflon, and a connector connected to the optical head in the main system unit. The sensing tip (1.0 mm diameter) is designed to be immersed into the measured material for bulk temperature measurement or to be contacted with the material surface for surface temperature measurement. A temperature sensor in the sensing tip, located at one end of the fiber, is made of a small amount of magnesium fluorogermanate. Blue light is emitted from the Xenon flash lamp through the fiber and excites the sensor. The sensor exhibits a deep red fluorescence. The intensity of the red light decays exponentially with time. The decay time constant is inversely proportional to temperature. The response time of the optical probes is 0.25 second for stirred liquid and 0.5 second for still air. The measurement frequency can be set from once per 0.1 second to once every 999 hours. The accuracy of the temperature measurement is ±1.5 °C for one to three samples per measurement and ±1.0 °C for more than three samples per measurement.

2.2.4 Loaded materials

A nonreacting and microwave absorbing sample used in this study was Nylon 66, provided by Cadillac Plastic Co. The cylindrical shape of the

sample was selected in order to facilitate dielectric diagnosis in a cylindrical TM_{012}-mode cavity. The sample rod was always located at a position of the maximum TM_{012}-mode electric field (about the center of the cavity). Small sized Nylon rods (0.635 cm x 3.5 cm) were used so that the resonant frequency shift perturbed by the sample was less than one percent of the resonant frequency and dielectric measurement using material-cavity perturbation could be used during the entire microwave processing.

2.3 Material-cavity Perturbation Technique

A variety of dielectric measurements can be used to measure complex permittivity at microwave frequencies. Three widely used methods [14] are: (1) waveguide or transmission line methods, (2) cavity measurements, and (3) cavity perturbation techniques. However, only cavity perturbation techniques can be applied to samples with various shapes and do not require the cross section of the applicator to be filled with sample. Complex permittivity of the loaded material can be precisely measured using material-cavity perturbation, even though the material is heated and the material complex permittivity changes with temperature. Therefore, dielectric measurement using material-cavity perturbation is employed for this microwave resonant cavity technique.

2.3.1 Literature review

Theoretically, dielectric measurement using the material-cavity perturbation theory requires a criterion that the electromagnetic fields in the cavity with and without the sample are approximately equal. This means that changes of the stored energy between the sample-loaded and

unloaded cavity are very small. However, experiments usually violate this criterion. An essential criterion is that the resonant frequency shift due to introduction of the material must be much less than the resonant frequency [15]. Therefore, the mode field pattern remains the same but the changes of the stored energy in the cavity are not necessarily small due to perturbation of the sample. This idea has been used to precisely measure complex permittivity of materials from low loss to high loss (ϵ' up to 80 and ϵ'' up to 40) using different resonant modes [15-26].

Spencer et al. (1957) found that "small" samples were not required to be really small in all dimensions compared with the free space wavelength. But the sample should be located at a position of the maximum and nearly uniform field. This idea was demonstrated by measuring dielectric properties of spherical ferrite samples placed at a position of the maximum magnetic field in a cylindrical resonant cavity at 9.35 GHz. The ratio of frequency shift to resonant frequency was less than 0.1% and the volume ratio of the sample to the cavity was less than 2.0×10^{-4} in their experiments.

Labuda and LeCraw (1961) derived simple perturbation equations for a cylindrical TM_{012}-mode resonant cavity. An experimental cavity with a radius of 1.623 cm and a length of 4.836 cm at 9.4 GHz was used to determine complex permittivity of the sample. The dimension of the sample was 0.127 cm in diameter and half height of the cavity in length. The samples were suspended by a Nylon thread and always located at a position of maximum frequency shift along the axis of the cavity. The reproducible dielectric measurements were reported within 3% for ϵ' and 0.1% for ϵ''. The measurement accuracy of dielectric loss factor ϵ'' increased as the sample radius was increased. But too large samples

might violate approximation of perturbation.

Conger and Tung (1967) applied the Labuda perturbation equations to study the effects on the use of quartz holder, the sample size, and the sample form (either solid or powder) on dielectric measurement. A pure copper cylindrical cavity with a radius of 1.65 cm and a length of 5.08 cm was operated at 9.4 GHz. The samples were always placed at the center of the cavity. The Q factor of the empty cavity at room temperature was about 10,500. The presence of the quartz holder induced 2% error in dielectric measurement. Larger errors in dielectric measurement were also found for larger diameter solid samples but less for powder samples due to deviation on geometrical constants in perturbation equations.

Parkash et al. (1979) derived general perturbation equations for a cylindrical TM_{010}-mode cavity with the material rods smaller than the cavity length. Several materials (Teflon, ferrite, and lanthanum chromite) were used to study the effect of the sample length on dielectric measurement. The cavity with a radius of 3.1 cm and a length of 2.0 cm was operated at 3.6986 GHz. The Q factor of the empty cavity at room temperature was about 1,849. The ratio of resonant frequency shift to resonant frequency was less than 0.6 %. They found very good agreement in dielectric measurement using general perturbation equations for the sample length more than one-fourth of the cavity height. Measurements of dielectric constant ranged from 2.03 to 2.08 for Teflon, 13.7 to 14.40 for ferrite, and 9.40 to 9.50 for lanthanum chromite. Dielectric loss factor measurement of lanthanum chromite ranged from 4.86 to 5.24.

Li et al. (1981) used a TM_{010}-mode cylindrical cavity (5.131 cm in radius and 4 cm in length) to measure the complex permittivity of

several materials (Teflon, Quartz, Pyrex, Benzene, Acetone, Methanol, 1-Octanol, 1-Propanol, 2-Propanol, 1-Butanol, and water) at 2.23 GHz and 22 °C. The ratio of the resonant frequency shift to the resonant frequency was less than 1.2%. The radius of samples was less than one-twentieth of the free-space wavelength at the resonant frequency. The length of samples was equal to the height of the cavity. The volume ratio of the samples to the cavity was between 0.003% and 0.5%, depending on the magnitude of the sample dielectric loss factor. The smaller sample volume was used for the more lossy material. The measurement errors were reported less than 1% for ϵ' and 5% for ϵ'' when compared with the literature values. The measured values of dielectric constant ϵ' and dielectric loss factor ϵ'' at 2.23 GHz and 22 °C were 2.09 and less than 10^{-3} for Teflon, 3.80 and 0.002 for Quartz, 4.75 and 0.040 for Pyrex, 2.27 and 0.0038 for Benzene, 20.9 and 0.85 for Acetone, 22.6 and 13.1 for Methanol, 2.87 and 0.70 for 1-Octanol, 4.19 and 3.63 for 1-Propanol, 3.73 and 2.96 for 2-Propanol, 3.70 and 1.96 for Butanol, as well as 76.8 and 8.62 for water. Li et al. (1982) also studied the effect of the sample insertion hole on the complex permittivity measurement. The measured values using a cavity with a sample hole were smaller for dielectric constants but higher for dielectric loss factors than those without a sample hole. The cavity with a sample hole could have a lower resonant frequency and cavity Q factor than the cavity without a sample hole.

Chao (1985) derived an analytic formula to calculate measurement errors in dielectric constant and conductivity using perturbation for various radius samples in a TE_{103} rectangular cavity (1.02 x 2.29 x 6.46 cm) at 9.5928 GHz. Theoretical error analysis was also verified with experimental dielectric measurement of silicon (dielectric

constant: 11.85 and conductivity: 0.018/Ω·cm). The Q factor of this empty cavity was 2,630. The ratio of the resonant frequency shift to the resonant frequency was less than 0.45%. Since the Q factor change of highly conductive materials is small due to skin depth effects, he suggested that highly conductive samples should be placed at a position of the maximum magnetic field instead of the maximum electric field in order to produce a larger Q factor change. Chao concluded that the larger radius sample could reduce the measurement error in measuring the resonant frequency shifts and Q factor changes, but the smaller size sample could reduce the perturbation error due to assumptions on the uniform electric field over the sample.

Dielectric measurement using material-cavity perturbation has been applied to monitor chemical reaction at microwave frequencies [27,28]. Martinelli [27] used a cylindrical TE_{011} cavity at 9.5 GHz to on-line measure dielectric properties of thermo- and photo-initiated reactions of polymers heated by hot flowing nitrogen or UV light. The extent of reaction was related to the changes of dielectric properties. Terselius [28] used a TM_{010} cylindrical cavity with a thermostat controlled heating oven to make on-line measurements of the complex permittivity of rod-shaped vulcanizing rubber and polyethylene compounds at 2.8 GHz. TM_{010} cavity perturbation techniques were used to measure ϵ' (permittivity) from 2 to 10 and ϵ'' (loss) from 0.05 to 1.0. It was suggested that a TM_{012} cavity would be more suitable for higher lossy materials.

2.3.2 TM_{012}-mode material-cavity perturbation equations

A diagram of the field patterns in a TM_{012}-mode loaded cavity is shown in Figure 2.4. Using standard material-cavity perturbation

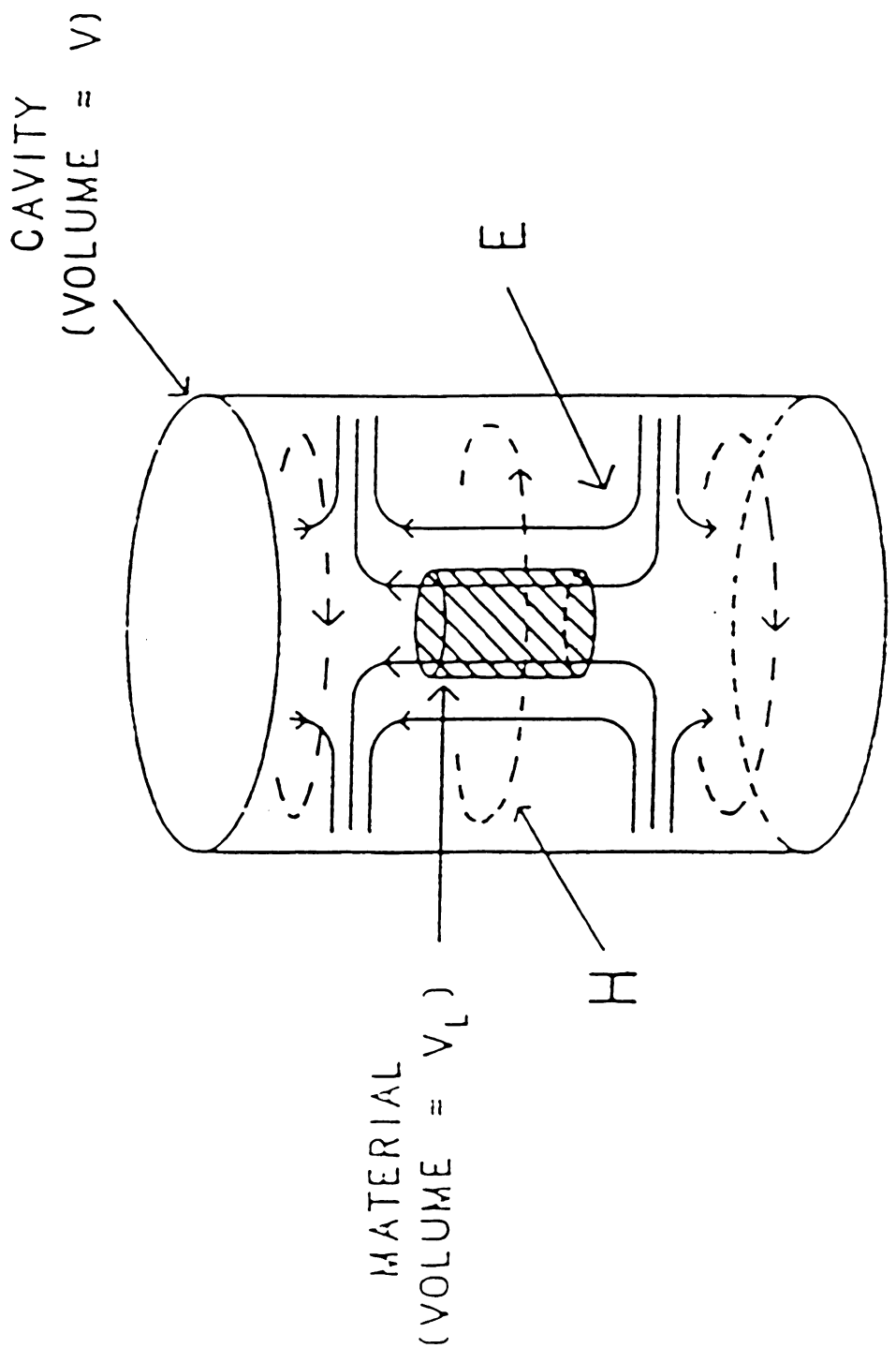

Figure 2.4: A diagram of the field pattern in the loaded TM_{012}-mode cavity

assumptions, the perturbation equations for a TM_{012}-mode resonant cavity with a small sample rod have been derived in Appendix A [4]. These equations are given below.

$$df/f_0 = (\epsilon' - 1)\ A\ B\ G\ V_s\ /\ V_c \tag{2.1}$$

$$(1/Q_s - 1/Q_0) = 2\ \epsilon''\ A\ B\ G\ V_s\ /\ V_c \tag{2.2}$$

where $A = J_0(2.405R_s/R_c)^2 + J_1(2.405R_s/R_c)^2$

$B = 1 + [L_c/(2\pi L_s)]\sin(2\pi L_s/L_c)\cos(4\pi H/L_c)$

$G = 0.2718[\upsilon_0/(f_0R_c)]^2$

$df = f_0 - f_s$

Permittivity and dielectric loss factor of the sample are ϵ' and ϵ''. The resonant frequency, Q factor, radius, length, and volume of the cavity without the sample (the unloaded cavity) are f_0, Q_0, R_c, L_c, and V_c. The radius, length, and volume of the sample are R_s, L_s, and V_s. The resonant frequency and Q factor of the cavity with the sample (the loaded cavity) are f_s and Q_s. The height from the center of the sample to the bottom of the cavity is H. The speed of light is υ_0. The zero- and first-order Bessel functions of the first kind are J_0 and J_1, respectively.

Assumptions used in deriving perturbation equations are (1) f_s is very close to f_0 (i.e. $df/f_0 < 1\%$), (2) $1 \ll Q_c$ and $1 < Q_s$, (3) the loaded sample must be cylindrical and placed along the longitudinal axis of the cavity, (4) the diameter of the sample is much less than the free space wavelength so that the quasi-static approximation for the electric fields is valid inside and outside the sample, and (5) integration of

radial electric fields over the entire sample is negligible compared with that of axial electric fields. Assumption (1) is a required criterion to use the material-cavity perturbation theory. Assumption (2) is an experimental condition to operate the cavity. Assumption (3) suggests that the sample length should be greater than the sample radius in order to obtain a cylindrical shape. From experimental experience, the volume ratio of the sample to the cavity is usually much less than 0.1% for $\epsilon'' > 1$ and much greater than 0.1% for $\epsilon'' < 0.001$. Assumption (4) suggests that the radius of the sample should be less than one-twentieth of the free space wavelength. Assumption (5) suggests that the sample is placed at a position of maximum axial electric fields and minimum radial fields, and has a length approximately one-quarter of the free space wavelength so that radial electric fields can be neglected compared with the axial electric fields integrated over the entire sample volume.

The accuracy of dielectric measurement using perturbation equations is directly related to the measurement accuracy of resonant frequency, Q factor, and sizes of the cavity and the loaded sample. The resonant frequency and Q factor can change due to thermal expansion of the cavity size and relative humidity in the microwave heating process. However, the resonant frequency shift (0.065 MHz) and the Q factor change (0.2%) for an empty cavity due to thermal expansion and relative humidity change [29,30] are negligible compared with the resolution of the frequency marker (0.1 MHz) and the measurement error of Q factor (5%). The dimensional changes of the cavity due to thermal expansion are also negligible (about 0.02% of the original cavity volume). But the sample dimensions at a higher temperature may significantly change due to thermal expansion. Therefore, the perturbation equations are required

to account for the sample size variation when material thermal expansion is not negligible during heating and cooling processes.

2.4 Single-mode Heating and Dielectric Diagnosis Methods

Material-cavity perturbation theory is used to relate the measured changes in mode resonant frequency and cavity Q factor to the permittivity and dielectric loss factor of the loaded material, respectively. The resonant frequency shift increases with increasing permittivity of the material but the cavity Q factor decreases as the dielectric loss factor of the material increases. When making the resonant frequency and cavity Q factor measurements, the cavity is required to critically couple with the external circuit. Two methods are used to measure the changes in the resonant frequency shift and cavity Q factor: (1) the swept frequency method, and (2) the single frequency. The swept frequency method directly measures the resonant frequency and the cavity Q factor from the critically-coupled resonance curve of a fixed-length cavity at swept frequencies. The single frequency method is used to measure the changes in the cavity length and power measurements for a critically-coupled cavity at a single frequency.

2.4.1 Swept frequency method

Swept-frequency power inputs from a microwave energy source are fed and coupled into the cavity via a coaxial coupling probe. The reflected swept power signals from the cavity are attenuated and rectified. These rectified power levels versus swept frequencies construct a resonance power absorption curve on an X-Y oscilloscope. This resonance curve can

explicitly represent the coupling condition between the cavity and the external circuit. Three coupling conditions are shown in Figure 2.5 [12]: (1) undercoupling, (2) critical coupling, and (3) overcoupling. These coupling structures are adjustable by the coupling probe depth L_p into the cavity. The critically coupled resonance curve is established when the reflected power at a point of the swept frequencies is zero on the resonance curve. The frequency with zero reflected power is the resonant frequency f_0. The cavity is resonated with the external microwave circuit at this frequency. By Fourier integration over the swept power spectrum at the resonant frequency f_0, the Q factor of the entire microwave system Q_m is determined by the ratio of the resonant frequency f_0 to the frequency bandwidth (Δf) between the half-power points on the critically-coupled resonance curve. The Q factor of the entire system Q_m is also equal to the Q factor of the cavity Q_c and the Q factor of the external circuit Q_{ext} as described in Equation 2.3. Since the cavity is critically coupled (resonated) with the external circuit, the Q factor of the cavity Q_c is equal to the Q factor of the external circuit Q_{ext}. The Q factor of the cavity is then equal to twice the measured Q factor Q_m.

$$1/Q_m = 1/Q_c + 1/Q_{ext} \tag{2.3}$$

The mode resonant frequency and cavity Q factor versus the cavity length for a given radius cavity can be theoretically calculated [31]. Several resonant modes as a function of frequency and cavity length for the cavity with 7.62 cm in radius are shown in Figure 2.6. Since the cavity is operated in the TM_{012} mode and resonated at 2.45 GHz, the resonant frequency and the cavity Q factor of this empty cavity are

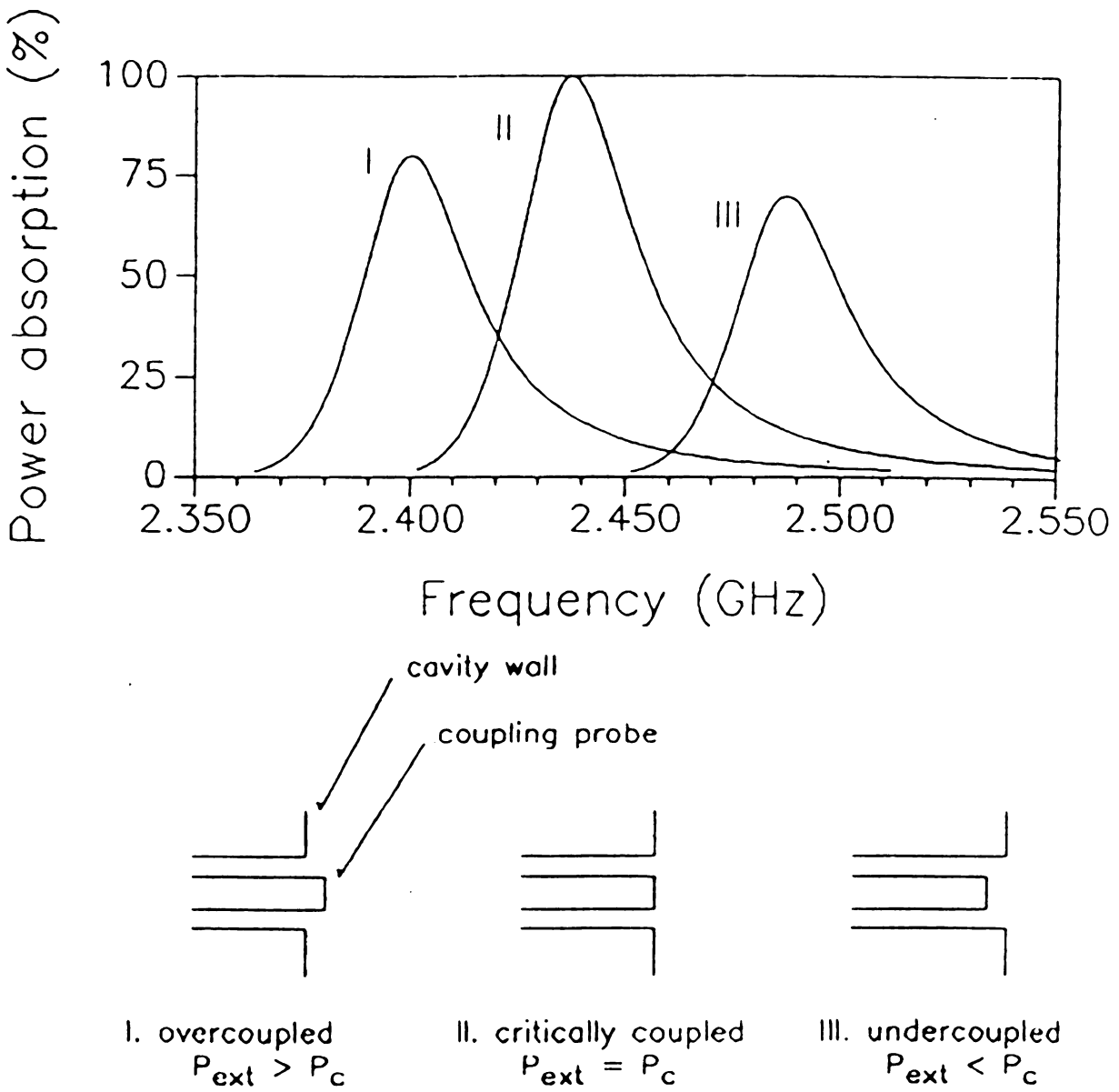

Figure 2.5: Typical resonance curves of a swept-frequency cavity

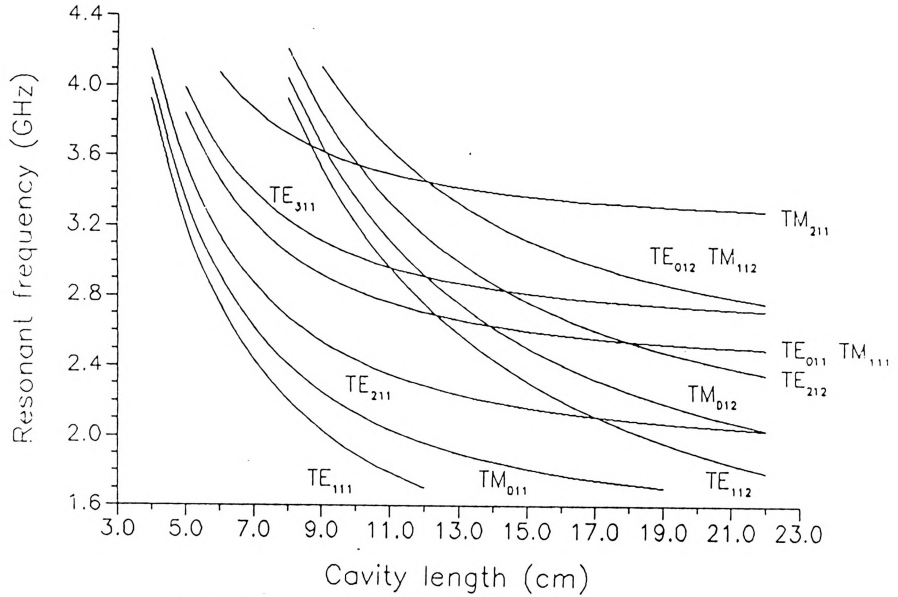

Figure 2.6: Theoretical mode resonant frequency versus the cavity length

calibrated as shown in Figures 2.7 and 2.8. The errors of the experimental results compared with the calculated values are less than 0.06% for the resonant frequency and 5% for the cavity Q factor.

When the sample rod is loaded and located at a position of the maximum resonant frequency shift (about the center of the cavity), the resonant frequency shifts down and the critically coupling structure changes to the undercoupling condition. The cavity is re-tuned to form a critically coupled resonance curve by adjusting the coupling probe depth. The new resonant frequency f_s and cavity Q factor Q_s are directly determined from this new critically-coupled resonance curve. The measured changes in the resonant frequency and cavity Q factor between the cavity with and without the sample are then related to the complex permittivity of the sample through material-cavity perturbation equations. The material complex permittivity during microwave heating and free convective cooling in a resonant swept-frequency cavity is also determined in the same manner.

2.4.2 Single frequency method

A continuous microwave power input at a selected frequency of 2.45 GHz is fed into the cavity. The cavity is tuned to a resonant TM_{012}-mode cavity length as shown in Figure 2.7 to minimize the reflected power at this selected frequency. This frequency is then called as the resonant frequency f_0. The coupling structure between the cavity and the external circuit is also determined by the depth of the coupling probe. A critically coupled structure is established when the reflected power P_r is negligible compared with the incident power P_i.

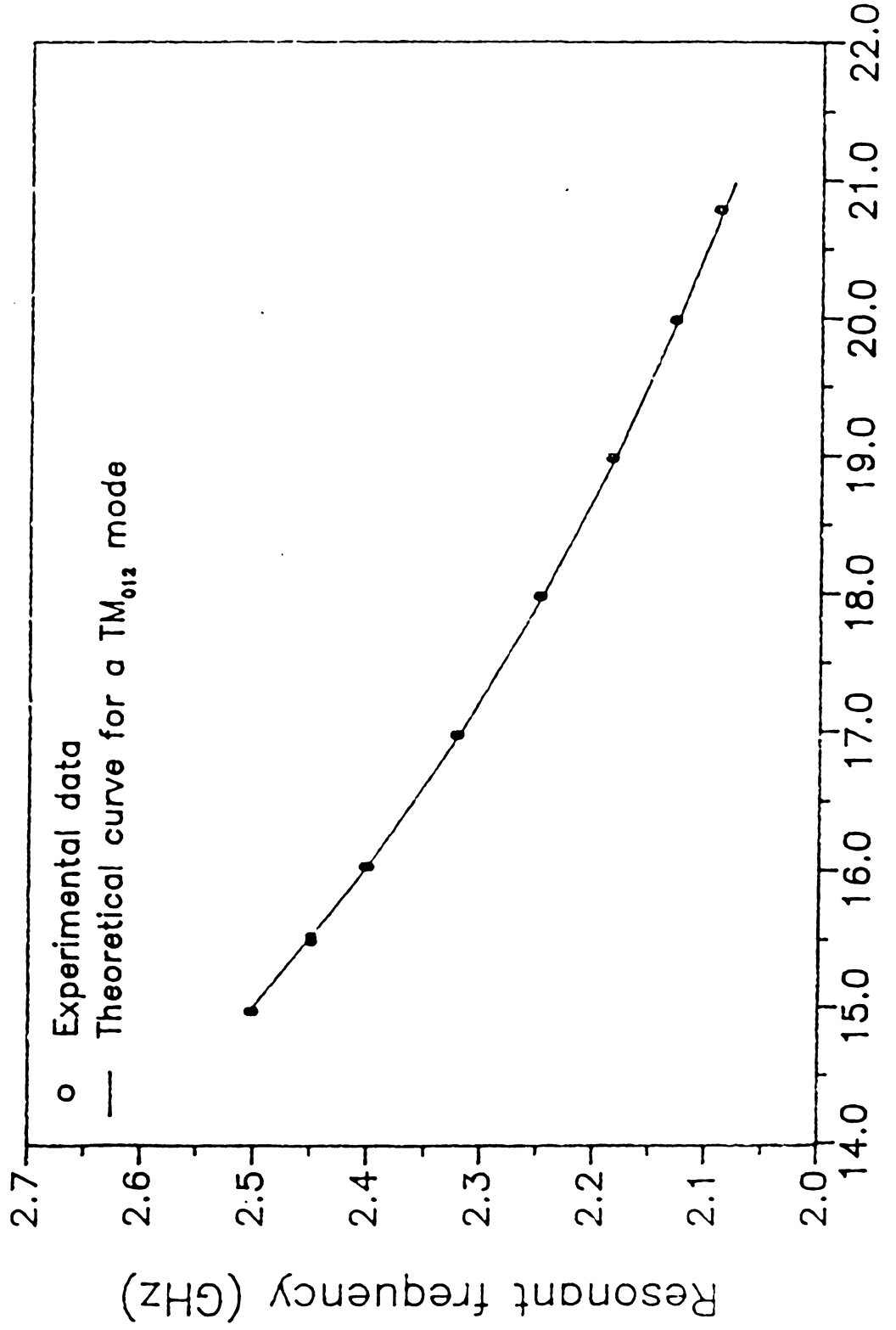

Figure 2.7: Calibration of the resonant frequency versus the cavity length for a resonant TM_{012}-mode cavity of 7.62 cm in radius

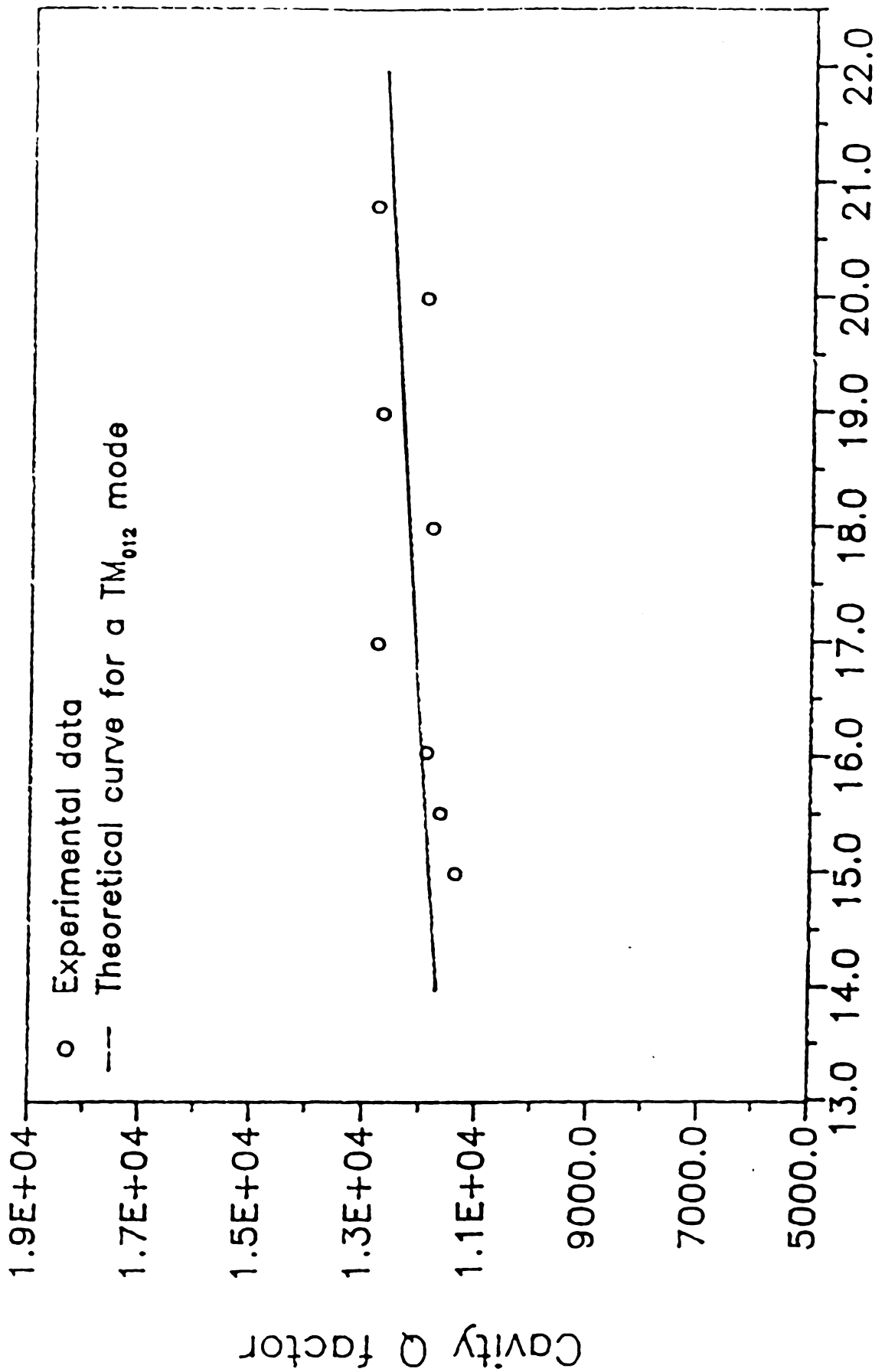

Figure 2.8: Calibration of the cavity Q factor versus the cavity length for a resonant TM_{012}-mode cavity with 7.62 cm in radius

The total dissipated power P_t in the microwave system is the difference between the measured incident and reflected powers. The total dissipated power is also equal to the power dissipated in the external circuit P_{ext} and in the cavity P_c as described in Equation 2.4.

$$P_t = P_i - P_r = P_{ext} + P_c \tag{2.4}$$

Since the cavity is critically coupled with the external circuit, a unique power coupling coefficient β between the cavity and the external microwave circuit can be defined. The relationship is described in Equation 2.5. Therefore, the power dissipated in this resonant cavity is determined using Equation 2.6.

$$\beta = P_{ext} / P_c \tag{2.5}$$

$$P_c = P_t / (1+\beta) \tag{2.6}$$

On the other hand, the power P_b measured by the diagnostic probe is proportional to the square of the radial electric field near the cavity wall ($P_b = K_b |E_r|^2$). An example of the diagnostic power measurements through the diagnostic holes with and without small nylon rods in this TM_{012}-mode resonant cavity at 2.45 GHz is shown in Figure 2.9. The axial variation of the diagnostic power shows a similar TM_{012}-mode standing wave. Therefore, the diagnostic power is directly proportional to the square of the radial electric field inside the cavity. From the Poynting theorem, the square of the radial electric field is proportional to the stored energy W inside the cavity. Therefore, the measured diagnostic power is proportional to the stored energy inside

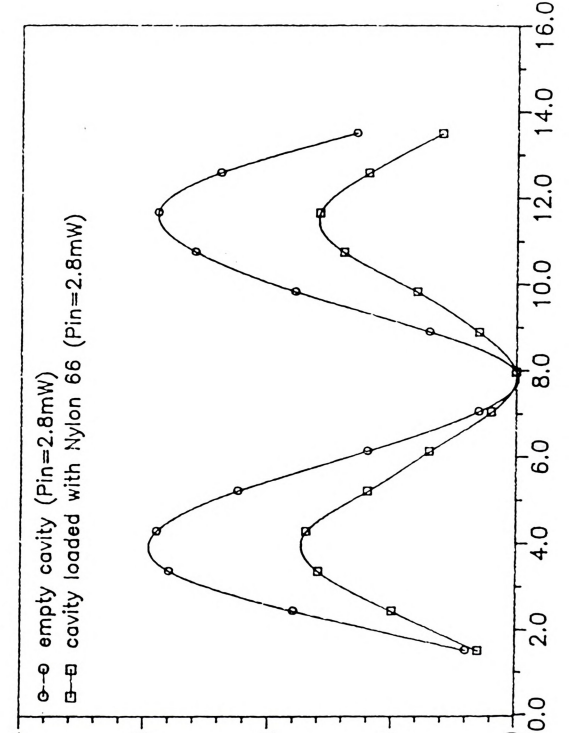

Figure 2.9: Axial variations of diagnostic power measurement near the cavity wall for a resonant TM_{012}-mode cavity at 2.45 GHz

the cavity as described in Equation 2.7.

$$P_b \propto |E_r|^2 \propto W \tag{2.7}$$

The cavity Q factor is defined as the ratio of the stored energy W to the dissipated power P_c in the cavity and multiplied by the angular resonant frequency ω_0 ($2\pi f_0$). Therefore, the Q factor of a resonant cavity is proportional to the power ratio P_e (P_b/P_t) at a given resonant frequency f_0 as described in Equation 2.8.

$$Q_c \propto W/P_c \propto P_b/P_t \tag{2.8}$$

The ratio of the cavity Q factor with and without the sample can be determined by the power ratio measurements as described in Equation 2.9. Only measurements of the cavity Q factor Q_0 and the power ratio P_{e0} of P_{b0} to P_{t0} for the unloaded resonant cavity, and the power ratio P_{es} of P_{bs} to P_{ts} for the loaded resonant cavity are required to determine the Q factor of the loaded resonant cavity [1,4].

$$Q_s/Q_0 = (W_s\omega_0/P_{cs})/(W_0\omega_0/P_{c0}) = (P_{bs}/P_{ts})/(P_{b0}/P_{t0}) \tag{2.9}$$

In the single frequency method, the unloaded cavity is first operated at low-power swept frequencies and resonated with the external circuit at a selected frequency f_0 in the TM_{012} mode. The Q factor of this unloaded cavity Q_0 is measured using the swept frequency method as described in the previous section. The swept-frequency input powers are then switched to a single-frequency power input at the resonant

frequency. The measurements of P_{b0}, P_{i0}, P_{r0}, and L_{c0} are made. The small material rod is loaded and located at a position of the maximum electric field (about the center of the cavity). The resonant frequency shifts down to a new resonant frequency f_s and the critically-coupled structure disappears due to introduction of the rod. The shift in the resonant frequency is compensated by re-tuning the cavity length. The cavity length L_{c0} is now tuned to a new cavity length L_{cs} where the reflected power is minimized. Critical coupling is then re-structured by adjusting the coupling probe depth to the point where the reflected power is negligible. Measurements of P_{bs}, P_{is}, P_{rs}, and L_{cs} are made. The loaded cavity Q factor is determined using Equation 2.9. The loaded material is then removed. The single-frequency system is switched into the swept-frequency system. Again, the unloaded cavity at this new cavity length L_{cs} is critically coupled with the external circuit by adjusting the coupling probe depth using the swept frequency method. The resonant frequency f_0' of the empty cavity with this new cavity length is determined. The resonant frequency shift due to introduction of the sample is then calculated by $df = f_0' - f_0$. Complex permittivity of the loaded sample is determined using Equations 2.1 and 2.2.

The measured changes in the cavity lengths and power ratios using the single frequency method are equivalent to the changes in the resonant frequency and cavity Q factor using the swept frequency method as previously described [4]. Typical calibration curves of the resonant frequency shift versus the new cavity length and the cavity Q factor versus the power ratio are shown in Figures 2.10 and 2.11, respectively. The measured values of the cavity length and the power ratio can be directly related to the resonant frequency shift and the cavity Q factor from these calibration curves. The cavity length and the power ratio

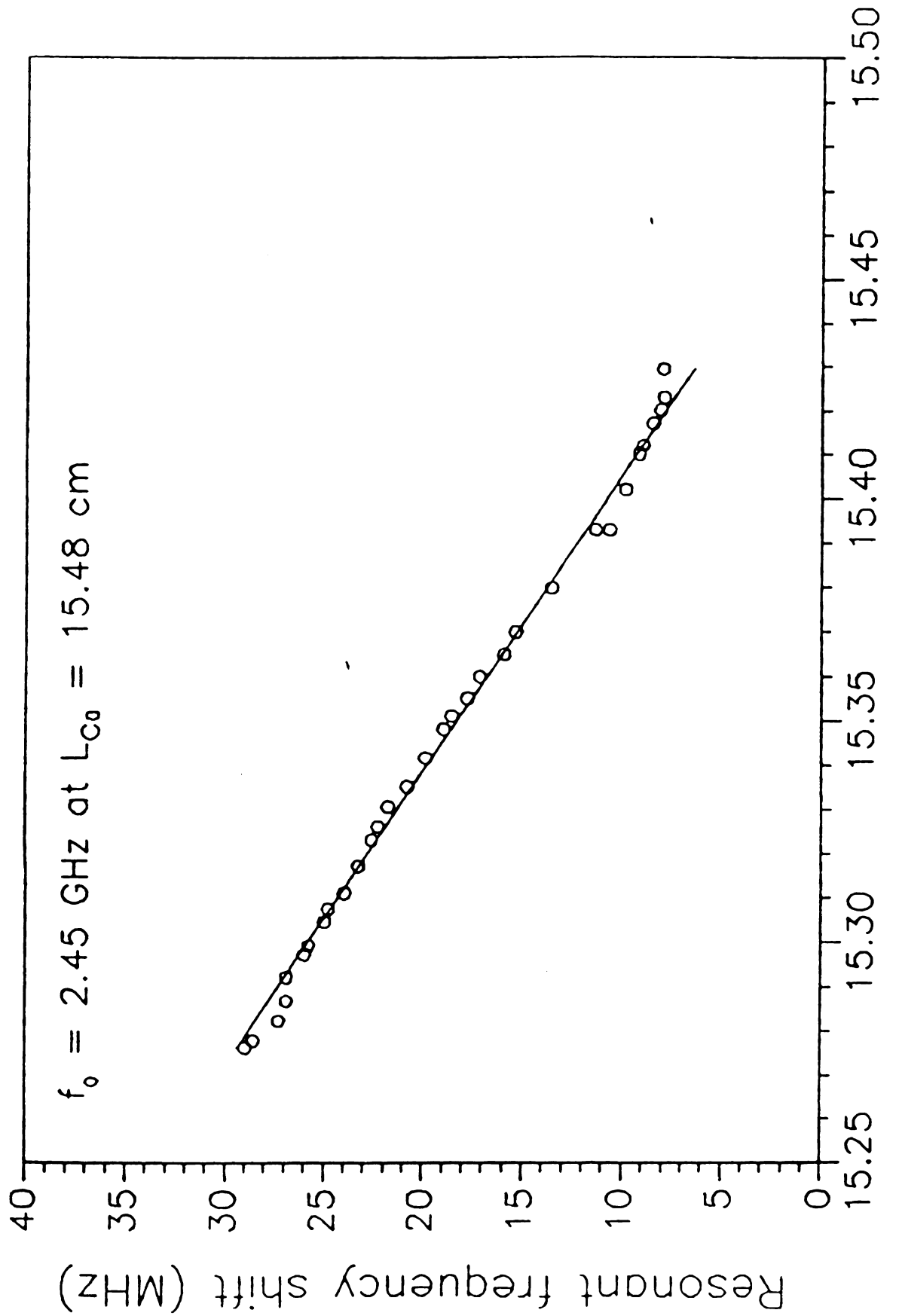

Figure 2.10: Calibration curve of the resonant frequency shift versus the cavity length for a TM_{012}-mode loaded cavity at 2.45 GHz

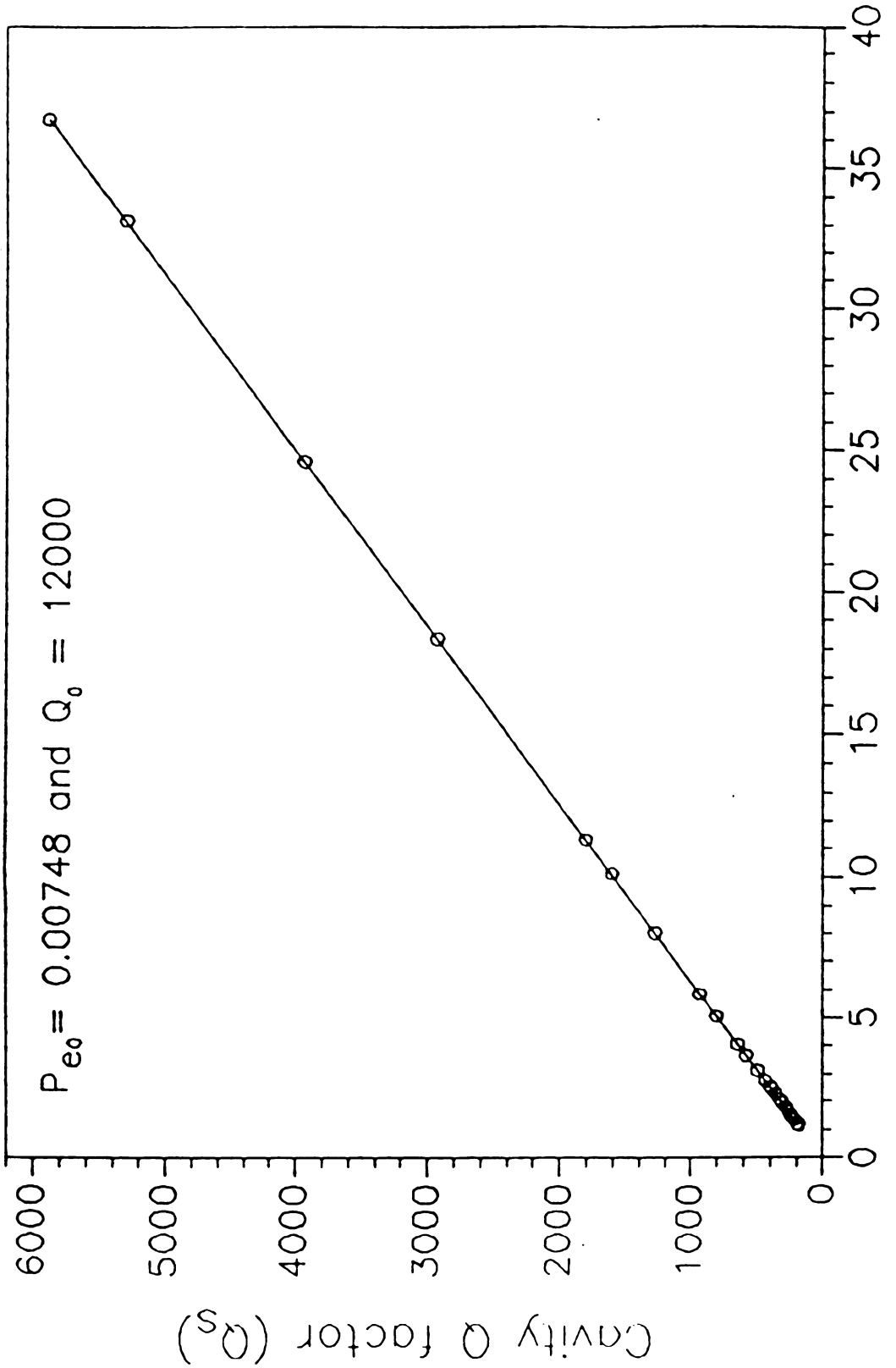

Figure 2.11: Calibration curve of cavity Q factor versus power ratio for a TM_{012}-mode loaded cavity at 2.45 GHz

decrease as permittivity and dielectric loss factor of the loaded material increase. Continuous measurements of the resonant cavity length and the power ratio during the single-frequency microwave heating of the sample are required to on-line calculate the resonant frequency shift and the cavity Q factor. Complex permittivity of the sample is then determined using material-cavity perturbation equations.

2.5 Results and Discussion

Nylon 66 rods were electromagnetically heated in a resonant TM_{012}-mode cavity at average input power levels of 4.2 and 5.0 W with the swept frequencies between 2.44 and 2.46 GHz. The rods were also heated at a single frequency of 2.45 GHz. Temperature and dielectric measurements were made during the single and swept frequency heating. The swept frequency method was used to determine the changes in the resonant frequency and the cavity Q factor during the swept frequency heating, while the single frequency method was used during the single frequency heating. Since a temperature gradient inside the rod could be built up during microwave heating [10], dielectric measurements were only made below 50 °C so that the temperature difference (less than 3 °C) between the center and the boundary of the rod could be neglected. Dielectric and temperature measurements were also made during free convective cooling. The swept frequency method at low power (milliwatts) levels in the same diagnostic mode was employed during cooling. The resonant frequency shifts upon introduction of the rods in these experiments were all less than 1% of the resonant frequency. The purpose of these experiments was intended to establish dielectric

measurements of materials during microwave heating using a newly developed single frequency method and compare with those using the conventional swept frequency method.

Complex permittivity throughout this thesis is relative to the free space permittivity. Temperature at the center of the rod with the measurement accuracy of ±1 °C is used here. Complex permittivity as a function of temperature during heating and cooling in a swept-frequency diagnostic mode is shown in Figure 2.12. Complex permittivity versus temperature of Nylon 66 in the single frequency heating and diagnostic mode is shown in Figure 2.13. Figure 2.12 shows that dielectric measurement using the swept frequency is independent of power levels. Permittivity of Nylon 66 below 50 °C at 2.45 GHz in Figures 2.12 and 2.13 is fairly constant but dielectric loss factor slightly increases with increasing temperature. The temperature-dependence and the values of complex permittivity of Nylon 66 are consistent with the literature [32]. The average values of permittivity of Nylon 66 at 2.45 GHz are 2.71 ± 0.13 for the swept frequency measurement and 2.82 ± 0.11 for the single frequency measurement. The literature values of permittivity of Nylon 66 at 3.0 GHz are 2.96 [32] and 3.03 [31]. The average values of dielectric loss factor at 2.45 GHz and 50 °C are 0.038± 0.006 for the swept frequency measurement and 0.042 ± 0.004 for the single frequency measurement. The literature value of dielectric loss factor of Nylon 66 at 3.0 GHz and 50 °C is 0.046 [32]. The measurement error using the swept frequency method is less than ±5% for ϵ' and ±15 % for ϵ''. However, The measurement error using the single frequency method is less than ±4% for ϵ' and ±10 % for ϵ''. In the swept frequency method, the measurement accuracy of the resonant frequency shift and the cavity Q factor is limited by the resolution of the cavity resonance curve on the

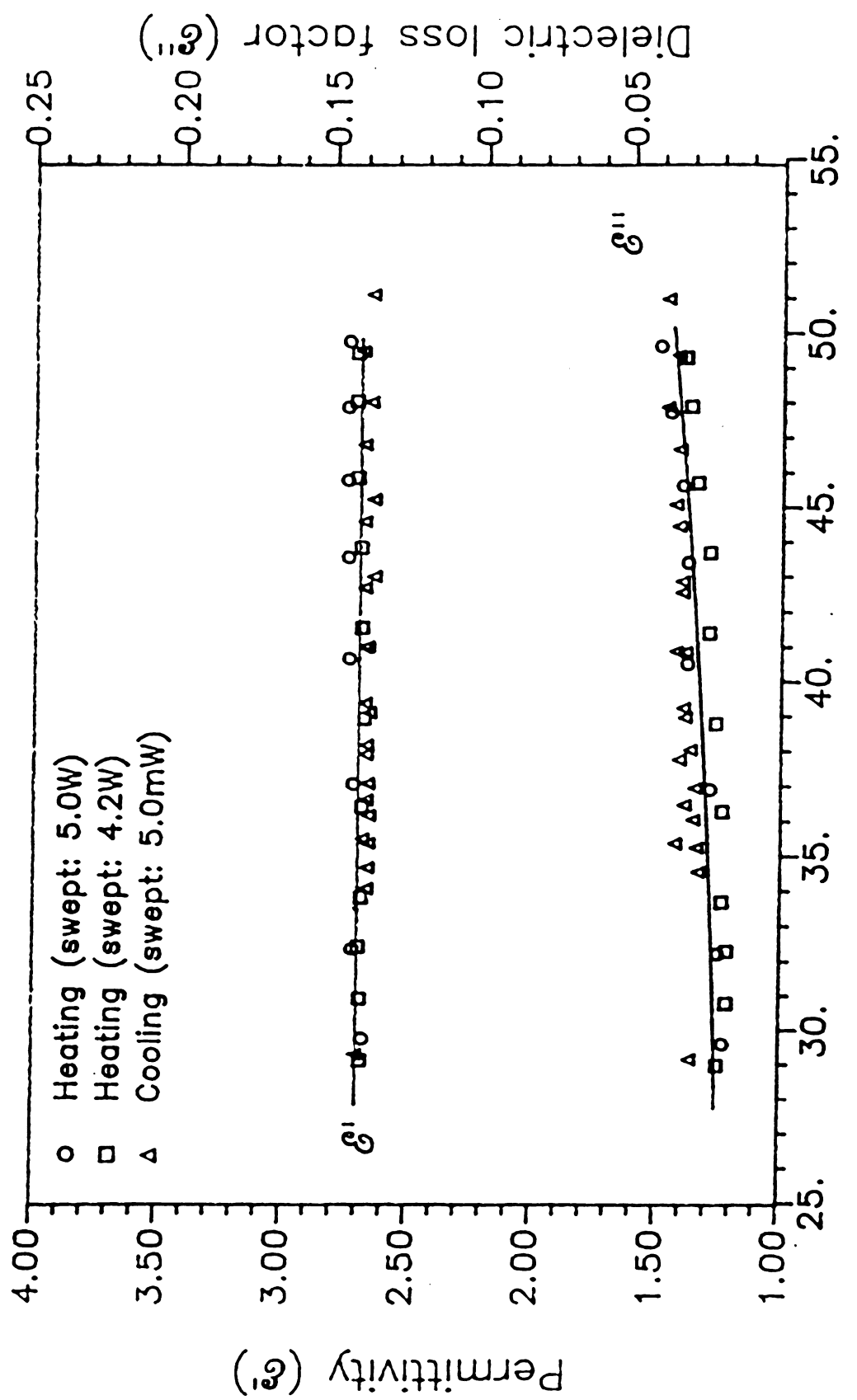

Figure 2.12: Complex permittivity of Nylon 66 versus temperature at 2.45 GHz in a swept frequency cavity

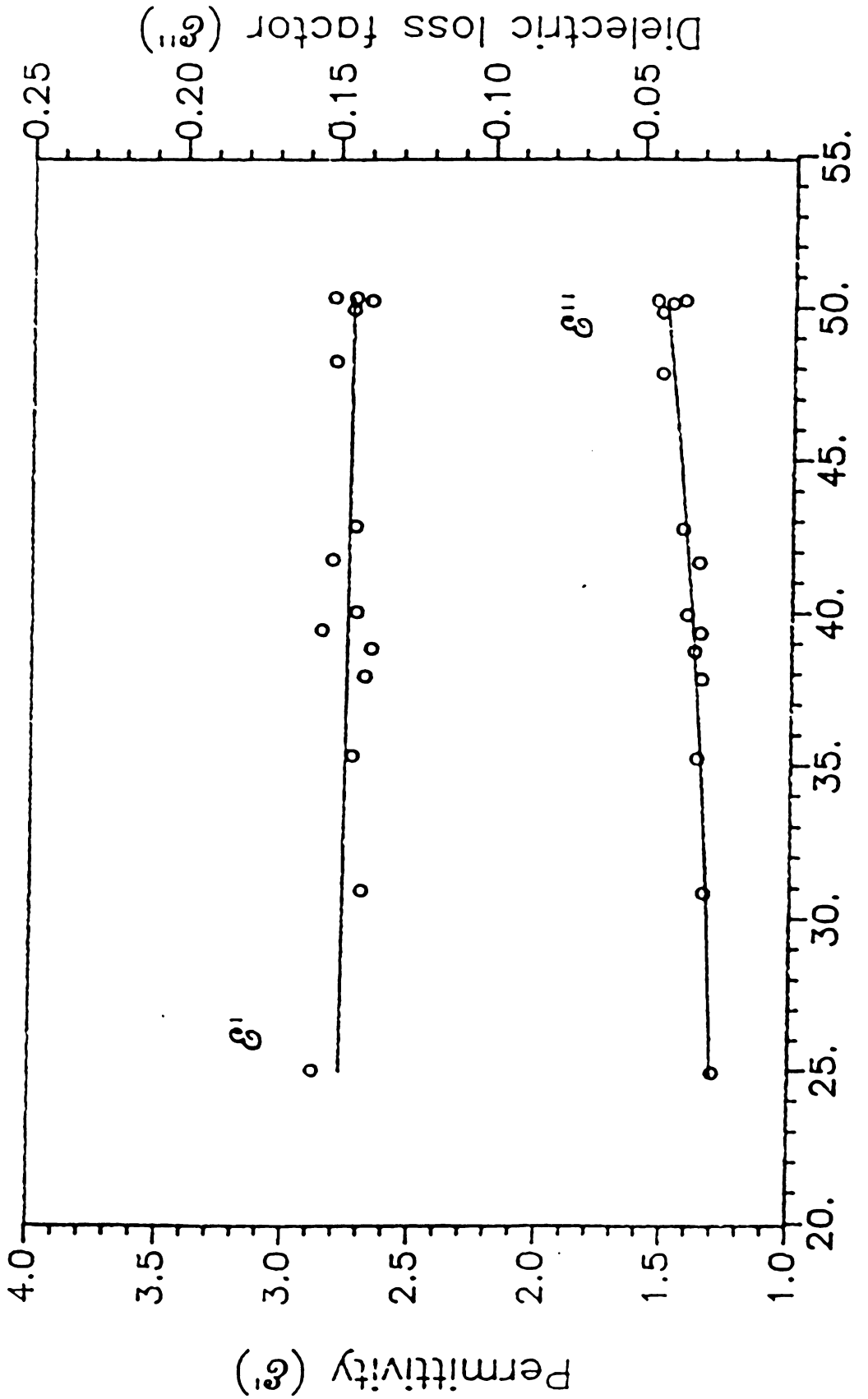

Figure 2.13: Complex permittivity of Nylon 66 versus temperature at 2.45 GHz in a single frequency cavity

X-Y oscilloscope and frequency marker. Power ratio and cavity length measurements during dynamic heating of materials are usually more accurate in the single frequency method.

2.6 Conclusion

This work shows that dielectric measurements using the single frequency method are repeatable and consistent with those using the conventional swept frequency method. However, the single frequency method is faster, more accurate, and more efficient and adaptable for control of power coupled into the loaded material. The single frequency method is therefore a very useful method to simultaneously heat and diagnose materials in a dynamic microwave heating process.

CHAPTER THREE

CONTINUOUS MICROWAVE PROCESSING AND DIAGNOSIS OF EPOXY

3.1 Introduction

An alternative method of promoting reactions of polymers which require heat is to use microwave heating instead of conventional thermal heating. Molecules contain polar groups which undergo molecular rotation due to thermal Brownian motion. Incident microwave radiation interacts with the polar groups in the molecules so that the normal random orientation of the dipoles becomes ordered. The molecules then relax to their normal random orientation. Since energy is required to hold the dipoles in place, the relaxation of the dipole is accompanied by transfer of energy to the material. The relaxation is described by an exponential decay function with a characteristic relaxation time (τ_o). When the angular frequency of the incident radiation (ω) is equal to the reciprocal of the relaxation time, the rotation of the polar molecule is in resonance with the oscillation of the electric field and energy is significantly absorbed. This frequency is defined as the molecular relaxation frequency (ω_o). If the radiation frequency is much lower than the molecular relaxation frequency (i.e. $\omega << \omega_o$), the motion of the dipoles is much faster than the oscillation of the electric field and the transfer of energy is negligible. If the radiation frequency is much higher than the molecular relaxation frequency (i.e. $\omega >> \omega_o$), the dipoles are static and no energy will be absorbed. Molecular rotations of polar polymers tend to have relaxation times such that they resonate

and absorb energy at microwave frequencies.

Microwave processing (heating) can be combined with dielectric measurement techniques to simultaneously heat materials and monitor the heating process. Conventional dielectric measurements using cavity perturbation at microwave frequencies usually employ sweeping frequencies along with a resonant cavity of fixed cavity dimensions to measure the changes in the resonant frequency and the Q-factor of the cavity with and without a loaded material. Application of on-line dielectric diagnosis during microwave curing of epoxy in a swept resonant cavity has been previously described [3]. However, most of the incident power supplied from the swept energy source is reflected and cannot be coupled to the material. Therefore, a single-frequency heating and dielectric measurement technique is developed to improve the power efficiency during microwave processing of materials in the same heating and diagnostic mode. This single-frequency technique has also been previously described [1,4].

The objective of this chapter is to illustrate on-line processing and dielectric diagnosis of chemically reacting polymers using the single frequency method in a single-mode microwave resonant cavity. An early example of this heating and measurement technique using small nylon has been reported in Chapter 2 [1,2]. Here a thermosetting resin (epoxy/amine) is cured and diagnosed in a TM_{012}-mode at 2.45 GHz. Since the relaxation time for an epoxy/amine mixture changes with temperature and extent of cure, it is not possible to identify a single molecular relaxation frequency for the system. This chapter is instead focused on demonstrating how complex permittivity is determined during microwave curing of epoxy/amine mixtures at a single frequency of 2.45 GHz. A data base of complex permittivity versus temperature and extent of cure

at 2.45 GHz is to be generated in the next chapter.

3.2 Literature Review on Microwave Curing of Epoxy

Microwave curing of epoxy has been investigated in wave guides [33,34] and multi-mode microwave ovens [35,36]. Temperature and power level during microwave curing of epoxy have been measured in these experiments. A typical temperature-time profile during continuous microwave curing of epoxy/amine resins is shown in Figure 3.1.

Gourdenne et al. [33] used a TE_{01} wave guide operated at 2.45 GHz to study temperature-time profiles of DGEBA type epoxy cured with DDM (diaminodiphenyl-methane) at different input power levels of 40, 60, 80, and 100 W. Three microwave heating stages were classified: (1) heating before polymerization, (2) heating with polymerization, and (3) heating with convective heat loss after polymerization. They demonstrated that higher microwave power caused faster polymerization and sharper exothermic temperature peaks. Karmazsin et al. [34] studied thermomechanical properties of an epoxy resin (AY103) with a hardener (HY 991) using a 2.45 GHz TE_{10} wave guide operated at a 75 W continuous wave and an equivalent 75 W (150 W with 50 % cyclic ratio) pulsed power level. Young modulus and Tg (determined using Mettler TMA 40) of the microwave cured samples were found to be at least as good as those of the thermally cured samples. Wilson et al. [35] investigated the temperature/time profiles of epoxy during microwave curing in a conventional microwave oven at two power levels of 245 and 700 W. Two epoxy/curing agent systems were used: 100 parts of Epon 828 to 49 parts of T-403 and 100 parts of Epon 828 to 20 parts of Z. Experimental data indicated that the temperature slope increased rapidly at the lower

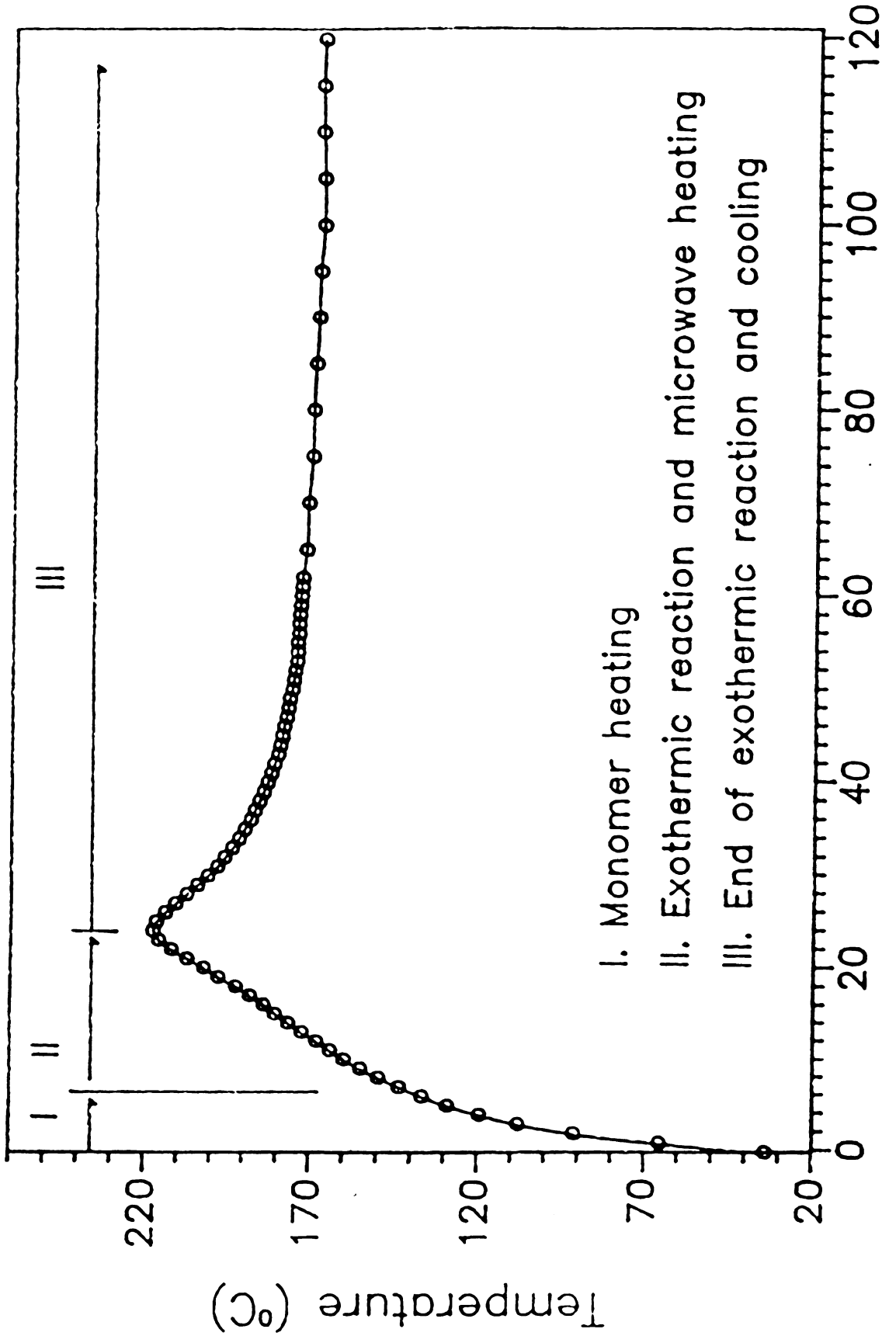

Figure 3.1: Typical temperature-time profile during continuous microwave curing of epoxy

temperature due to microwave heating. But the increase in the temperature slope after microwave power turned off was due to heat produced by the exothermic reaction. Strand [36] compared the temperature-time profiles of the thermal cure at oven temperatures of 66, 93, 121, 149, and 177 °C with the conventional 2.45 GHz microwave cure at various power levels of 0.75, 1.5, 2.25, and 6 KW for epoxy. He concluded that cure times could be reduced 30 times using microwave heating than thermal heating. The heat transfer mechanism was also different between microwave and thermal curing. The microwave energy directly heated the polymer; however, for the conventional thermal case, the mold was first heated and heat was subsequently transferred into the polymers via conduction.

A microwave single-mode resonant cavity technique is developed here to efficiently transfer microwave energy into the loaded epoxy and to measure dielectric properties, power levels and temperatures during microwave curing of epoxy [4]. A summary of research on microwave curing of epoxy is listed in Table 3.1. On-line measurements of dielectric property and temperature can be related to the extent of cure in order to monitor the cure process. However, heat produced by the epoxy curing reaction can significantly increase the temperature gradient. The intelligent control of microwave power cycles is required to eliminate the exothermic temperature gradient and to maintain constant cure temperature. Controlled pulsed microwave processing of epoxy, which can control power input by feedback of material temperature measurements, will be studied in Chapter 5.

Table 3.1: Summary of review on microwave cure of epoxy at 2.45 GHz

Author	Year	Methods	Power levels	Epoxy
Wilson	1977	multimode oven	245 and 700 W	Epon 828/T-403
				Epon 828/Z
Gourdenne	1979	TE_{01} waveguide	40, 60, 80, 100 W	DGEBA/DDM
Strand	1980	multimode oven	0.75, 1.5, 2.25, 6 kW	casting epoxies
Springer	1984	multimode oven	700 W	AS/3501-6
				S2/9134B
Karmazsin	1985	TE_{10} waveguide	75 W continuous	AY103/HY991
			150 W continuous pulsed	
Jow	1987	TM_{012} cavity	5 W continuous	DER 332/DDS
Jow	1988	TM_{012} cavity	15 W controlled pulsed	DER 332/DDS

3.3 Experimental

3.3.1 Materials

The conversion of thermosetting resins to rigid solid is brought about by small chain polymer molecules reacting with curing agents or each other to form a crosslinked molecular network. Epoxy resins are one example of thermosetting resins. Other thermosetting resins, such as phenolics, amino resins, polyesters, polyurethanes, polyisocyanurates, silicones, and polyimides, react in a similar fashion. However, epoxy resins have great versatility, low shrinkage, good chemical resistance, high mechanical properties, outstanding adhesion, and reaction without the evolution of by-product. Epoxy curing may be accomplished at room temperature or may require the addition of external heat, depending on the type of the curing agent. High T_g epoxy/amine resins used in this study are a difunctional liquid DGEBA resin (DER 332; manufactured by Dow Chemical Co.) and a tetrafunctional aromatic amine (diaminodiphenyl sulfone; DDS), which require heat to initiate reaction [37]. The chemical structures of these materials are shown in Figure 3.2. Epoxide groups react with amine via a ring-opening mechanism. Functionality of epoxy or curing agent is determined by the number of reactive groups per molecule. The crosslinking occurs through reaction of terminal (chain ending) epoxy groups with amine groups, and subsequent reaction of epoxy groups with hydroxyl groups formed during the reaction. The progress of the reaction is defined in terms of extent of cure or percentage of available epoxide groups reacted.

Epoxy

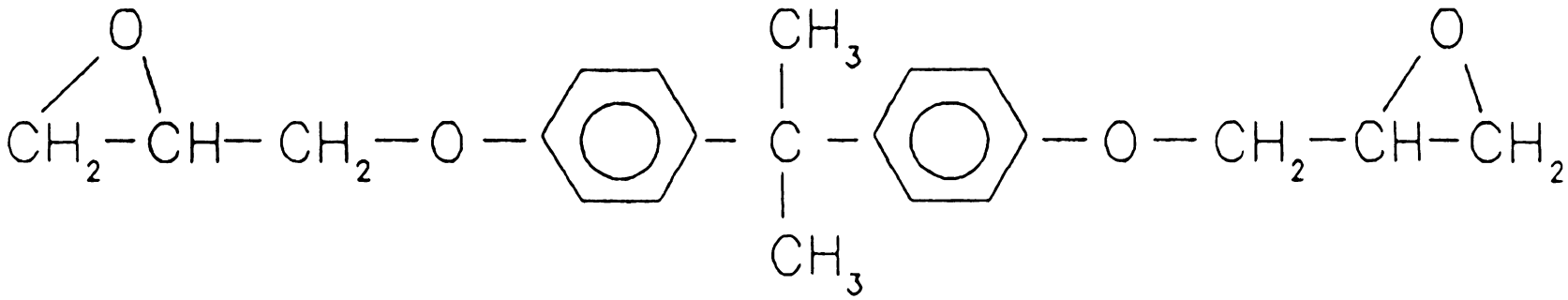

Diglycidyl Ether of Bisphenol A (DER 332)

Primary Amine

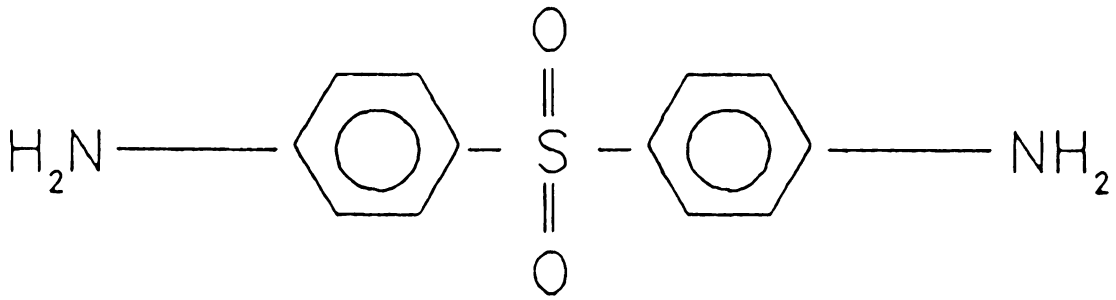

4,4'-Diaminodiphenyl Sulfone (DDS)

Figure 3.2: Chemical Structures of DER 332 and DDS

An equivalent molar mixture of DER 332 (mol. wt. 346 g/mole) and DDS (mol. wt. 248 g/mole) was prepared by mixing 100 parts resin with 36 parts curing agent by weight. DER 332 was heated up to 130 °C and white amine powder was then added. The mixture was well stirred until amine was completely dissolved (usually less than 5 minutes). However, in this study, the solution was overheated for 15 minutes. The residual heat of this epoxy/amine solution using differential scanning calorimetry at a heating rate of 5 °C/min was determined to be 308 J/g. The extent of cure for this epoxy (23%) was calculated by the difference between the measured residual heat and the total heat of reaction (400 J/g) and divided by the total heat of reaction. Dielectric measurements of epoxy samples with different length and radius were made using material-cavity perturbation. The suitable sample volumes for precise complex permittivity measurement ranged from 2.0 to 3.0 cm^3. The volumes of samples used in this study were 2.00 and 2.35 cm^3. The resonant frequency shifts were less than 1% of the resonant frequency during the course of microwave processing for these epoxy-amine volumes.

3.3.2 Experimental system

The experimental system for microwave processing and diagnosis has been described and shown earlier. A cylindrical brass cavity applicator was designed as reported earlier for processing of rod shaped material loads. This cavity was operated in a TM_{012} mode at 2.45 GHz. The frequency of 2.45 GHz was selected due to commercial availability of low cost energy sources operating at this frequency for future industrial application. A teflon holder was required to contain the liquid epoxy-amine mixture. Several advantages for using teflon as a sample holder

are very low dielectric loss factor ($\epsilon'' = 0.0003$), temperature-independent dielectric properties, high temperature resistance (up to 260 °C), and chemical inertness to reactants and products [3]. A cylindrical teflon sample holder of 0.476 cm in radius was found to be suitable for this application. The teflon holder was 3.5 cm long with 0.476 cm inner radius and 0.635 cm outer radius. The similarity in shapes of the cavity and loaded material was selected in order to facilitate diagnosis.

A fluoroptic fiber temperature sensing device (Luxtron Model 750) was used to on-line measure material temperature. A fluoroptic fiber probe was protected by a 3 mm o.d. pyrex capillary tube and placed in the center of the teflon holder. The temperature at the center of the sample was measured. It should be pointed out that this temperature could be significantly greater than the temperature at other parts within the sample during microwave heating.

The cavity with the empty teflon holder and a fluoroptic probe was considered as an unloaded cavity, while the cavity with the epoxy-filled teflon holder was loaded. The Q-value of this unloaded cavity was about 11000 at 2.45 GHz. The Q-value of the loaded cavity varied from 100 to 3000 at the same frequency during processing. The cavity with or without the sample was always tuned to critically couple with the external circuit by manual adjustments of the cavity length and the probe depth. The cavity length and the coupling probe depth for the entire microwave processing in the TM_{012} mode at a selected frequency of 2.45 GHz ranged from 15.336 to 15.400 cm and from 10.52 to 17.06 cm, respectively.

3.3.3 Single-frequency heating and dielectric measurement method

The experimental heating and dielectric diagnostic technique is a single frequency method which is to critically couple the cavity with the external microwave circuit in the TM_{012} mode at a selected microwave frequency by adjusting the cavity length L_c and the excitation probe depth L_p to obtain a zero reflected power P_r compared with the input power P_i. The changes in the mode resonant frequency and cavity Q factor measured by single-frequency method are related to material complex permittivity using material-cavity perturbation equations [2,4].

The complex permittivity of the material itself is a function of material temperature, pressure, excitation frequency, and material composition and structure. The accuracy of complex permittivity measurement using material-cavity perturbation is dependent on the dimension of the sample. In this study, the sample volume due to thermal expansion can be increased by 6% at the temperature of 170 °C. Therefore, continuous monitoring of sample temperature is required to account for the volume change of the sample. Since thermal expansion occurs after solidification, volume change is considered in dielectric measurement at the end of the exothermic reaction (after passing through the maximum temperature during microwave heating). The general perturbation equations for chemically reacting materials then can be expressed as follows.

$$(f_0 - f_s)/f_0 = [\epsilon'(X,T,P,f_0) - 1]\ A\ B\ G\ V_s(T) / V_c \qquad (3.1)$$

$$(1/Q_s - 1/Q_c) = 2\ \epsilon''(X,T,P,f_0)\ A\ B\ G\ V_s(T) / V_c \qquad (3.2)$$

where $A = J_0(2.405R_s/R_c)^2 + J_1(2.405R_s/R_c)^2$

$B = 1 + [L_c/(2\pi L_s)]\sin(2\pi L_s/L_c)\cos(4\pi H/L_c)$

$G = 0.2718[v_0/(f_0 R_c)]^2$

$$V_s(T) = V_s(T_0)\ [1 + \alpha\ (T - T_0)]^3$$

$$L_s(T) = L_s(T_0)\ [1 + \alpha\ (T - T_0)]$$

$$R_s(T) = R_s(T_0)\ [1 + \alpha\ (T - T_0)]$$

The permittivity of the sample is ϵ' and the loss of the sample is ϵ''. The resonant frequencies of the unloaded cavity and the loaded cavity are f_0 and f_s, respectively. The quality factors of the unloaded cavity and the loaded cavity are Q_c and Q_s, respectively. The speed of light is v_0. The height from the center of the sample to the cavity bottom is H. The radius, length, and volume of the cavity are R_c, L_c, and V_c, respectively. The thermal expansion coefficient of the material is α. The original radius, length, and volume of the material at a temperature of T_0 are $R_s(T_0)$, $L_s(T_0)$, and $V_s(T_0)$. The material temperature is T. The extent of cure is X. The working frequency and pressure are f_0 and P.

In this single-frequency technique of monitoring a chemically reacting material, initial measurements of the powers dissipated on the diagnostic probe P_{b0} and the empty cavity P_{t0} were made when this empty cavity was tuned to critically couple with the external circuit at a specific cavity length (at a selected frequency of 2.45 GHz and TM_{012} mode). The critical coupling of the cavity was accomplished by adjusting the excitation probe depth L_p so that the reflected power P_{r0} was close to zero compared with the incident power P_{i0}. The quality factor Q_0 of this critically-coupling empty cavity at the same position of L_c and L_p was then measured from the cavity resonance curve on the X-Y oscilloscope using a conventional swept frequency method.

After these initial measurements, a teflon sample holder with a fluoroptic probe was suspended at the center of the cavity by a cotton

thread. This cavity was called an unloaded cavity. The critically-coupled tuning of this unloaded cavity was done by manually adjusting L_c and L_p at the same frequency and mode to minimize the reflected power. The measurements of P_b, P_t, L_p, and L_c were then made. The value of the quality factor Q_c of this unloaded cavity was calculated by Equation 2.9. The holder was removed and the resonant frequency f_0 of the empty cavity was measured using the swept frequency method. The holder was then filled with the epoxy/amine resin to be processed and placed at a position of the maximum axial electric fields (around the center of the cavity). This cavity containing the sample is called as the loaded cavity. The loaded cavity length L_c and the coupling probe depth L_p were manually readjusted to critically couple at the same selected frequency and low input power level (10 to 14 mW) in the same mode. Input power was then raised to the desired level and the loaded material was heated electromagnetically. As the material was heated, its complex permittivity changed so that the loaded cavity tended to become untuned. Therefore, the loaded cavity was continuously tuned to a critically coupled condition by manually adjusting L_c and L_p to maintain a zero reflected power during the microwave heating process. At selected time intervals (such as every minute), the power levels (P_b, P_i, and P_r), the cavity length, and the coupling probe depth were measured. The value of the quality factor Q_s of the loaded cavity was determined for each measurement using Equation 2.9. After completing the heating process, the loaded material was removed and the resonant frequency f_s for each set of L_c and L_p measured during the processing was determined using the swept frequency method. The resonant frequency shift (df) was then calculated. On-line temperature measurement of the sample was made during the entire microwave heating process. The complex permittivity

of the material was then determined for each data point using Equations 3.1 and 3.2.

3.4 Results and Discussion

The temperature, permittivity, and loss are plotted versus time during microwave diagnosis and processing of epoxy in Figures 3.3 and 3.4. The permittivity and loss as functions of temperature are shown in Figures 3.5 and 3.6. The purpose of these reported experimental results is to document the methodology of simultaneous measurement of the complex permittivity and temperature profiles during a reaction in which the complex permittivity of the products differs from that of the reactants. Therefore, these results do not represent an optimal cure cycle.

The dielectric properties increased with increasing temperature until a temperature of about 160 °C was reached. The dielectric properties subsequently decreased after this point due to the curing reaction. After the reaction was completed, it was shown that the dielectric properties of the cured epoxy decreased with decreasing temperature. This once again demonstrates [3] that the dielectric properties increase with increasing temperature and decrease with increasing extent of cure. The dielectric measurements during the heating cycle were carried out using a single frequency method while the dielectric measurements during the cooling cycle were conducted using a swept frequency method. Results of both techniques are presented in Figure 3.6. The continuity between the heating and cooling curves is apparent. The error associated with dielectric measurements for both single and swept frequency methods is less than ±5% for permittivity and

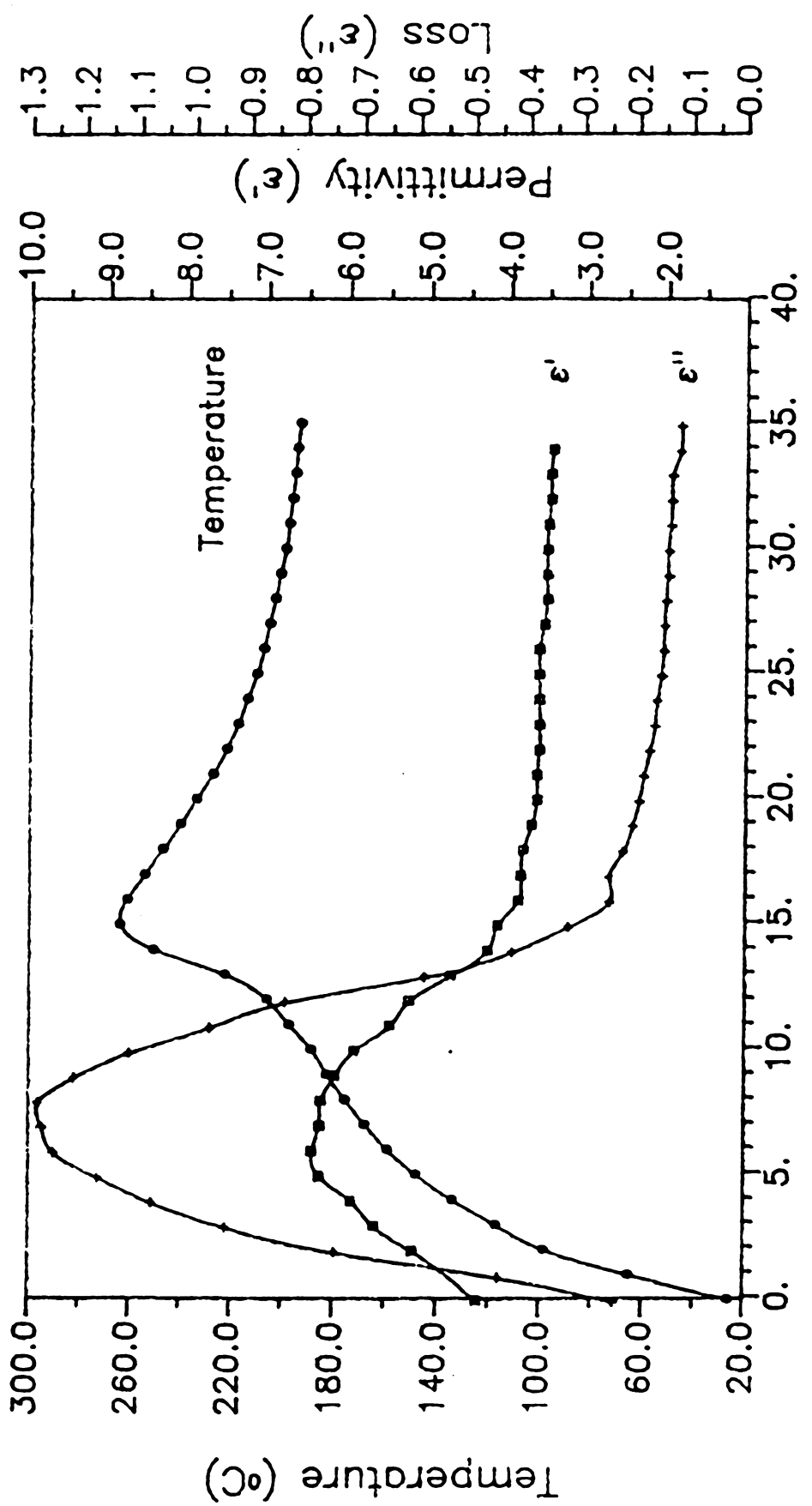

Figure 3.3: Temperature and complex permittivity versus microwave cure time (average P_1:5.7 W, sample volume: 2.35 cm^3, f_0: 2.458 GHz)

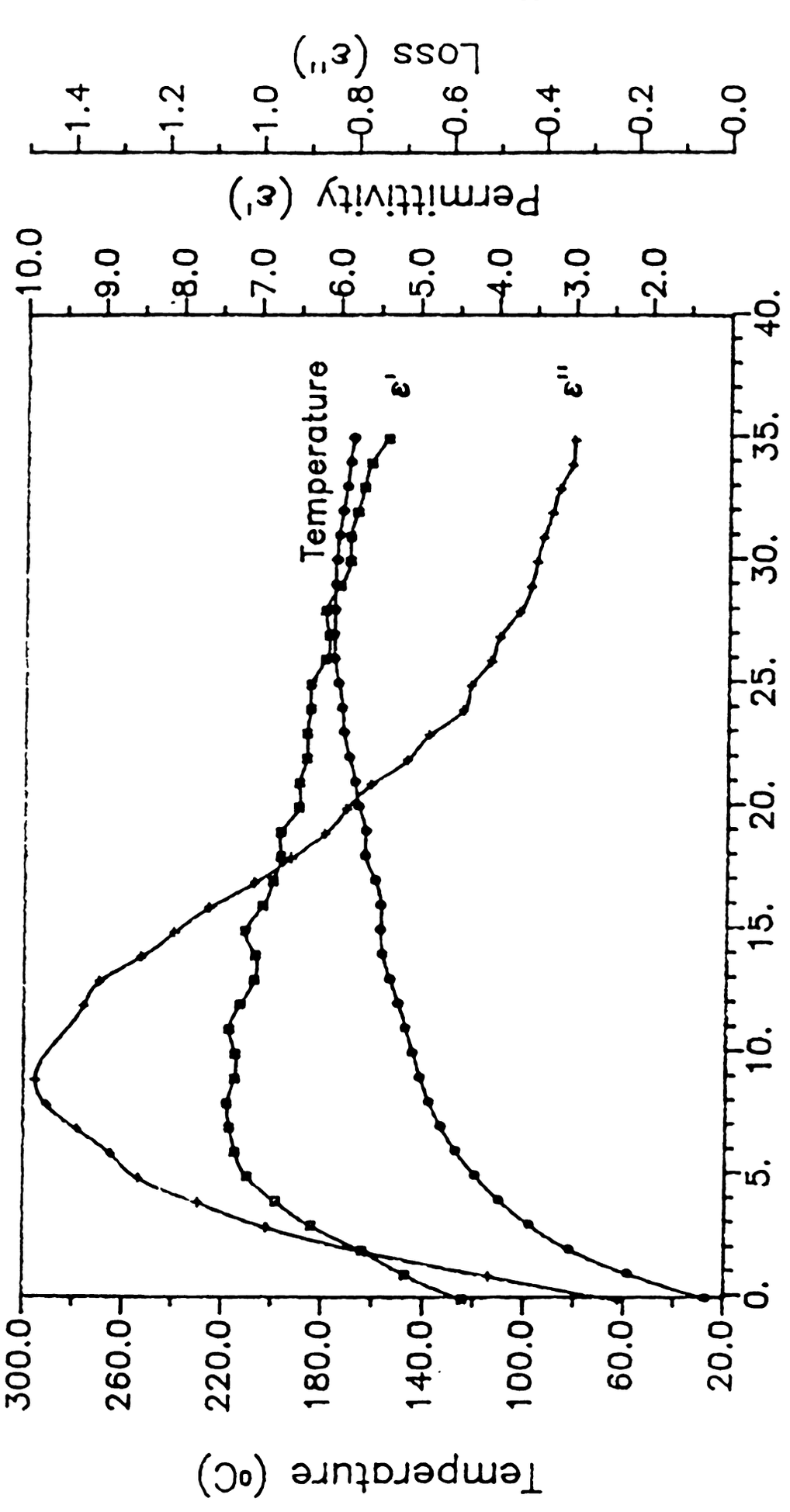

Figure 3.4: Temperature and complex permittivity versus microwave cure time (average P_i: 4.3 W, sample volume: 2.00 cm^3, f_0: 2.450 GHz)

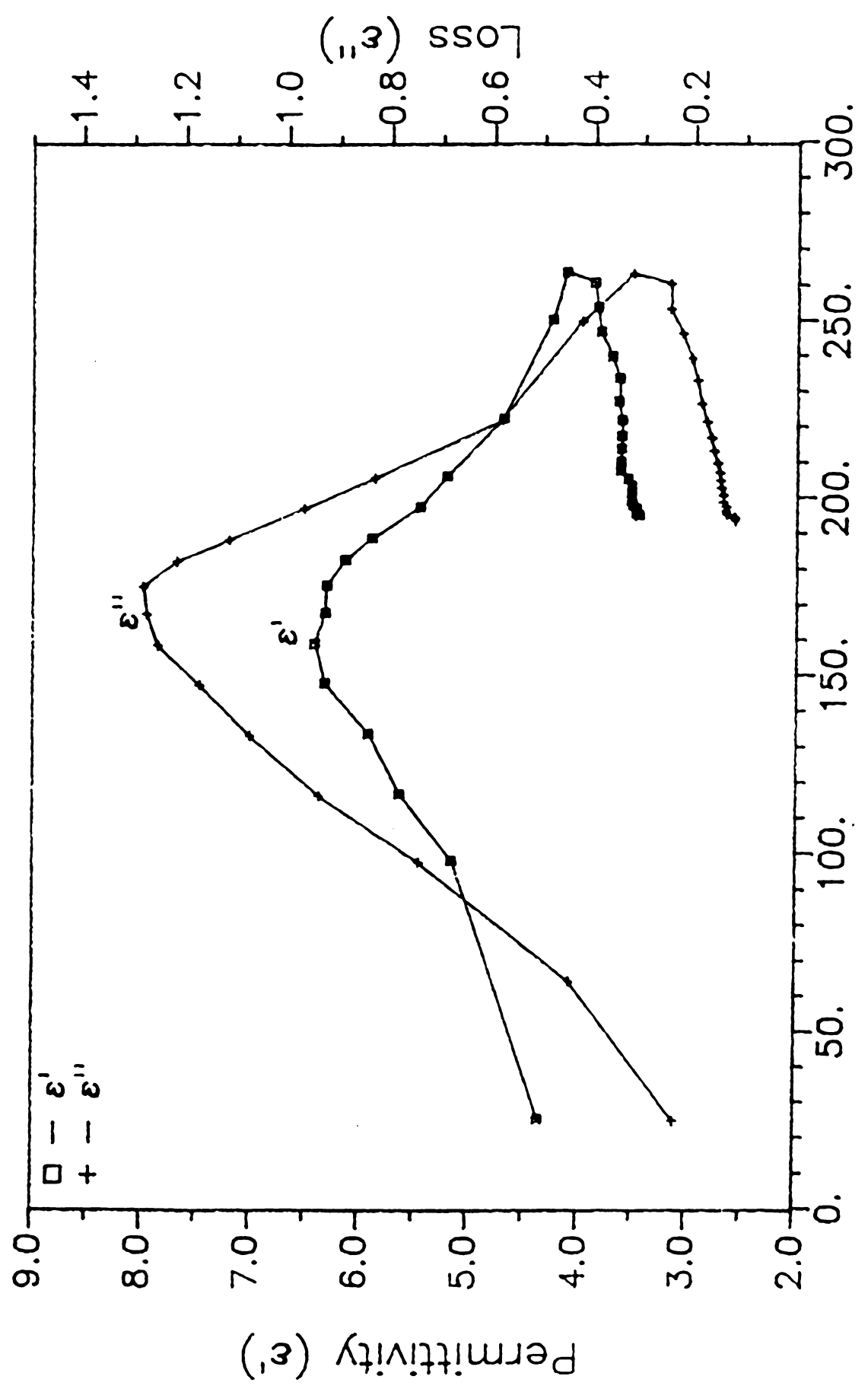

Figure 3.5: Complex permittivity versus temperature during microwave heating (average P_i: 5.7 W, sample volume: 2.35 cm^3, f_o: 2.458 GHz).

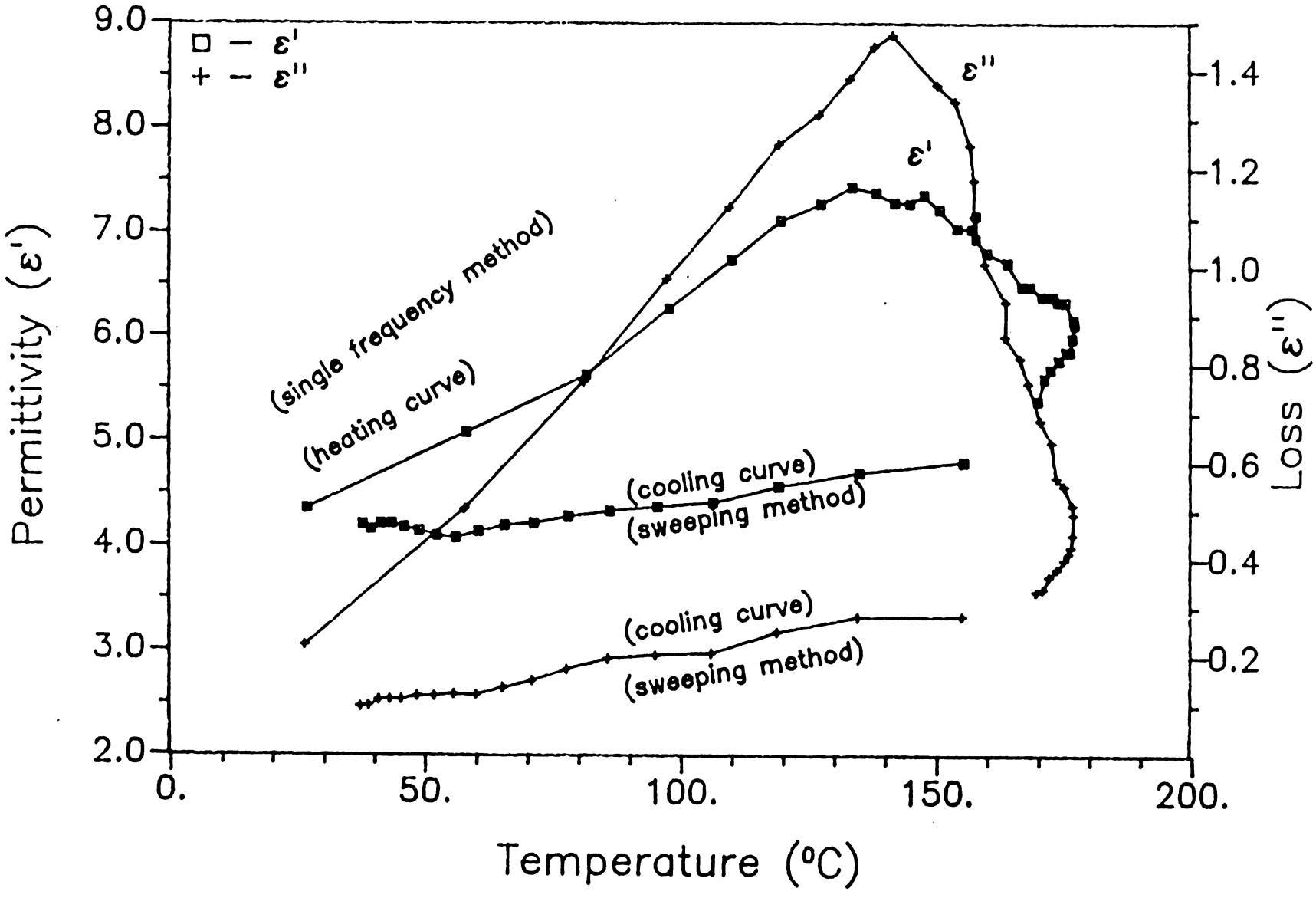

Figure 3.6: Complex permittivity versus temperature for microwave heating and convective cooling (average P_i: 4.3 W, sample volume: 2.00 cm^3, f_0: 2.450 GHz)

less than ±15% for loss. This clearly demonstrates the consistency of the two methods.

Epoxy systems approach molecular resonance as they are heated so that absorption tends to increase with temperature. However, once the reaction has progressed to a significant extent, the dipoles can no longer rotate freely due to the formation of a crosslinked molecular network. This moves the molecular resonant frequency of the absorbing material away from the microwave region with a consequent loss of microwave absorption. The net result is that epoxy/amine systems tend to absorb increasing amounts of microwave power initially as the system heats followed by decreased absorption as the system crosslinks. These systems would therefore be expected to have complex permittivity which increases during the initial heating and which decreases as the reaction progresses.

Comparison of Figures 3.3 and 3.4 shows that this is indeed the case for the epoxy/amine systems. The parameter (ϵ'') which governs the energy absorption increases initially and then decreases as the reaction progresses. Quantitative knowledge of how the complex permittivity changes with temperature and reaction extent is necessary so that absorption phenomena can be predicted. This in turn would allow optimal cure cycles to be properly selected. Constant temperature/time profile inside the sample could be achieved by controlling the input power level during the course of the reaction. Critical coupling of the TM_{012}-mode loaded cavity at a selected resonant frequency of 2.45 GHz is always accomplished by adjusting the cavity length and the coupling probe depth so that the reflected power is negligible compared with the incident power. An example of on-line measurements of P_b, P_i, P_r, L_c, and L_p

during microwave curing of epoxy in a TM_{012}-mode cavity at a single frequency of 2.450 GHz is shown in Figures 3.7 and 3.8. These results indicate that this microwave processing and diagnostic technique can efficiently transfer most of the input power into the loaded cavity and can be used to diagnose the complex permittivity of the loaded material. Also, this technique can be adaptable to intelligent, automatic processing during microwave heating in a single-mode resonant cavity at a single frequency.

3.5 Conclusion

This work successfully demonstrates the use of a microwave single mode resonant cavity applicator at a single frequency in conjunction with fluoroptic temperature measurement to process and to on-line diagnose curing of epoxy resin. Consistent results were obtained for both single frequency and conventional swept methods as previously reported [2,4].

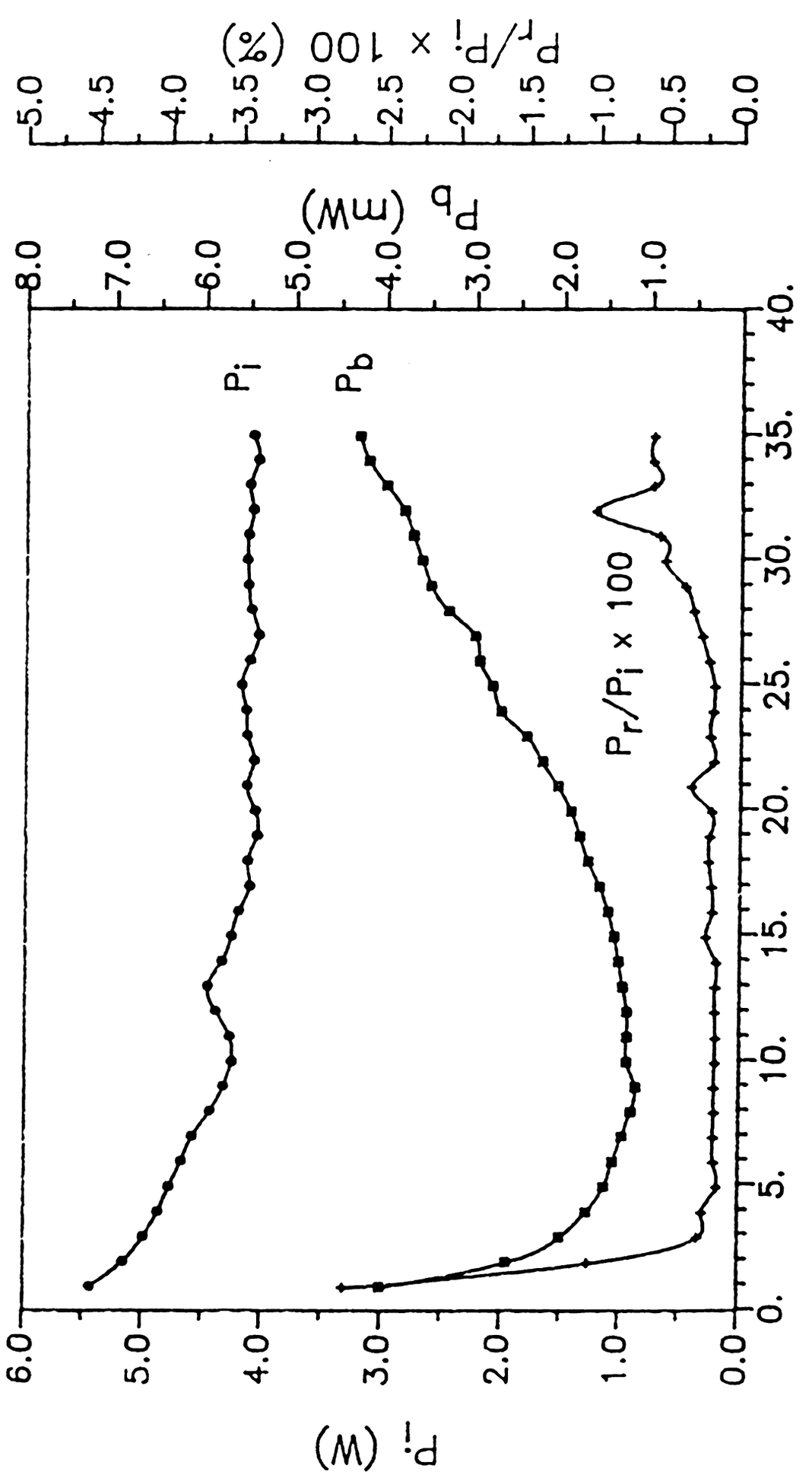

Figure 3.7: Power measurements versus microwave cure time at 2.450 GHz

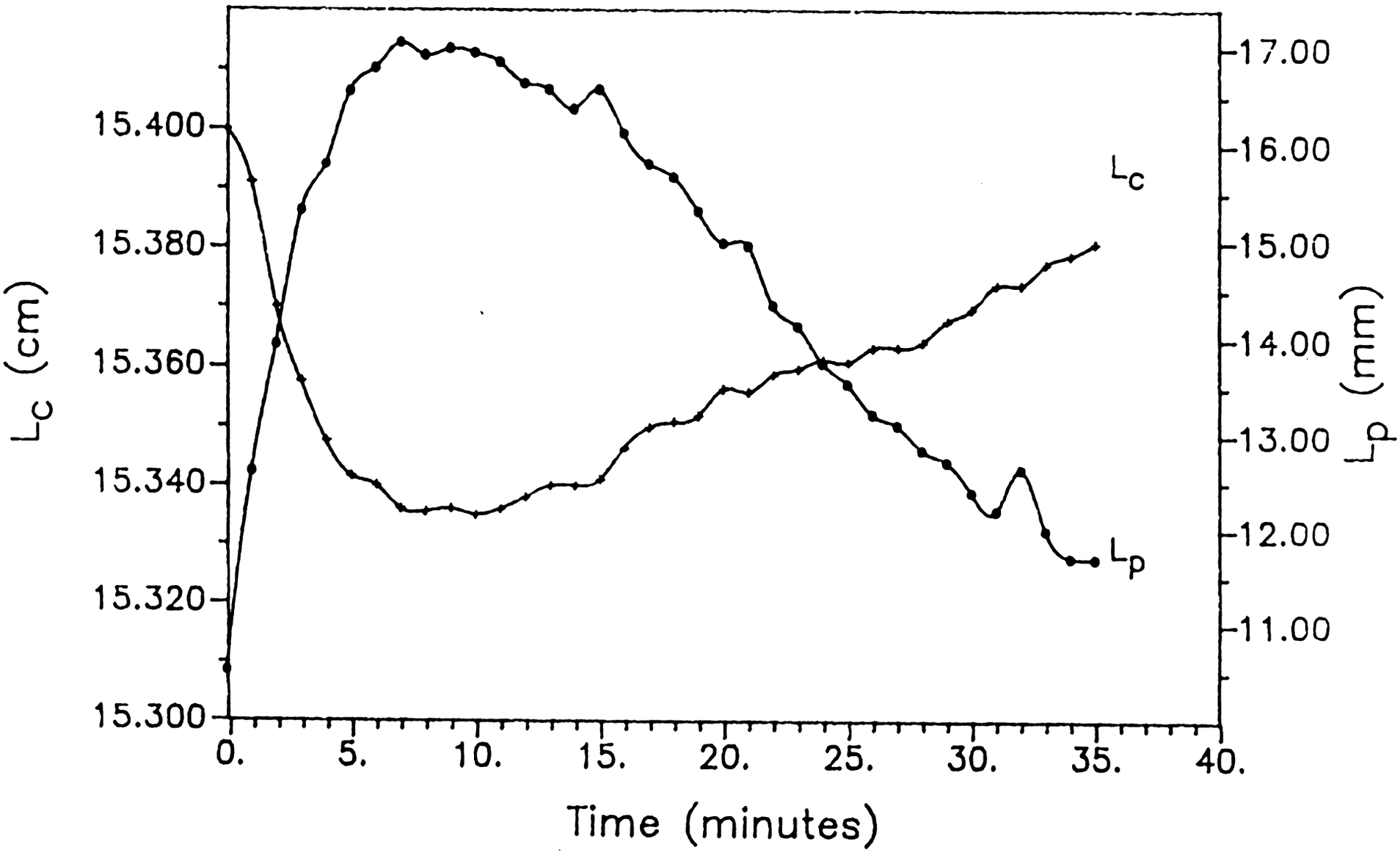

Figure 3.8: Cavity length and excitation probe depth versus microwave cure time at 2.450 GHz

CHAPTER FOUR

DIELECTRIC ANALYSIS OF EPOXY/AMINE CURE

4.1 Introduction

Dielectric techniques (dielectrometry or dielectric analysis) below microwave frequencies have been applied extensively to monitor thermal curing of thermosetting resins and composites by several investigators [38-48]. These dielectric measurements are usually performed by measuring an admittance of the materials placed between two conducting electrodes below microwave frequencies (less than 10 MHz). Significant data variations in dielectric measurement due to the interference of electrode polarization at low frequency or glass transition at high cure temperatures have been reported in the literature [47,48].

Instead of using conventional thermal heating, microwave energy has been applied to processing of thermosetting resins in wave guides [33,34] and multi-mode microwave ovens [35,36]. These experiments indicate that fast and direct heating can be obtained using microwave heating when compared with thermal heating.

A microwave cavity technique is used here to obtain dielectric data and to diagnose the microwave curing of the epoxy/amine matrix resin at a frequency of 2.45 GHz. Dielectric properties of epoxy/amine resins at microwave frequencies are not due to the ionic contribution but due to the presence of polar groups in the molecules. Microwave energy can be directly absorbed by these polar groups to cause localized heating which initiates the curing process. Absorption of microwave radiation occurs

primarily at epoxide and amine groups during the early stages of heating. These polar groups are consumed during cure via chemical reaction while hydroxyl groups are formed, which also absorb microwave radiation and subsequently react with epoxide groups. The mobility of polar chains decreases as the crosslinking proceeds. The effect of changing mobility and population of these polar groups on the dielectric properties of the system can be determined by dielectric loss factor measurement. The rate of absorption of microwave energy is determined by dielectric loss factor and electric field strength at a constant frequency. The crosslinked molecules (low dielectric loss) do not absorb microwave energy as readily as the uncrosslinked molecules (high dielectric loss). Therefore, dielectric loss factor can be an index of energy dissipation in the resins and an index of extents of reaction in the microwave curing process. The advantages of using microwave heating and dielectric diagnostics to initiate and monitor the curing process are: (1) selective and controlled direct heating due to absorption of microwave energy by polar groups, and (2) increased control of material temperature-time profile and input power to decrease thermal degradation and to optimize the cure cycle. These advantages may cause microwave cured materials to have superior mechanical characteristics by chemically modifying the polar groups or by intelligently selecting the microwave power cycle conditions.

The objectives of this chapter are to survey fundamental dielectric models and experimental methods, to review dielectric analysis of epoxy/amine resins below microwave frequencies, and to obtain dielectric data of epoxy/amine resins as a function of temperature and extent of cure at a microwave frequency of 2.45 GHz. On-line measurements of temperature and dielectric loss factor are also made in order to monitor

the cure process during microwave curing of epoxy/amine resins. Dielectric loss data between thermally and microwave cured samples at a constant temperature and frequency are also investigated.

4.2 Background on Dielectric Analysis

4.2.1 Fundamental models for dielectric response

The response of a material to an external mechanical or electrical force field is a non-equilibrium statistical thermodynamic effect. The equilibrium-state material under an external force field is changed to a non-equilibrium state which tends to reach a new equilibrium by a time-dependent relaxation process. If the external force field is not too strong and the response is linear, the non-equilibrium state can be described in terms of a perturbed equilibrium distribution function through the statistical thermodynamics [49]. Since it is very difficult to use the statistical thermodynamic approach for practical illustration, a corresponding approach based on the phenomenological model is commonly used [49-52]. A comparison of the phenomenological model between mechanical and electrical approaches is listed in Table 4.1. The charge is the electrical analogue of the strain, as the voltage is the electrical analogue of the stress. Since voltages add in series while stresses add in parallel, a series electrical model is equivalent to a parallel mechanical model. If the material is under a dynamic electric field, the linear material response to this force field is defined as complex permittivity (complex dielectric compliance), which is an analogue of the complex mechanical compliance.

Complex permittivity ϵ_t^* of the material has dipolar ϵ^* and ionic ϵ_i^* contribution. Ionic contribution due to the motion of ions or

Table 4.1: Comparison of phenomenological models

Property	Mechanical	Electrical
External force	Stress (σ)	Voltage (V)
Response	Strain (ε)	Charge (Q)
Flow	Velocity (v)	Current (I)
Linear elastic	Spring (K)	Capacitor (C)
Linear viscous	Dashpot (η)	Resistor (R)
Kelvin Model	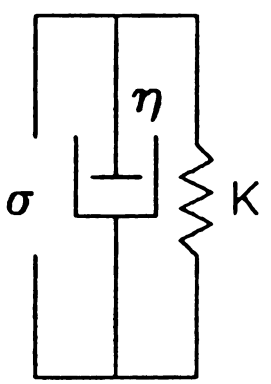	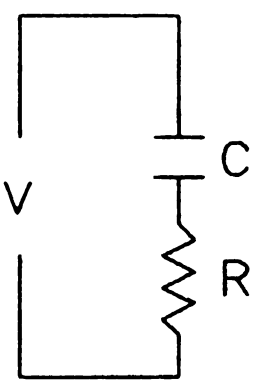
Maxwell Model	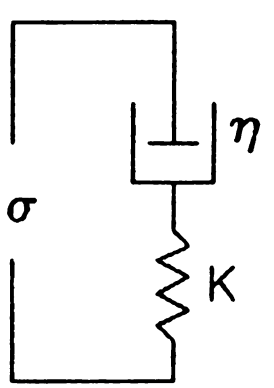	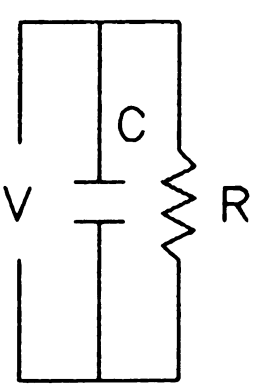
Compliance	$J^*=J'-J''j$	$\mathscr{E}^*=\mathscr{E}'-\mathscr{E}''j$
Modulus	$G^*=G'+G''j=1/J^*$	$G_e^*=1/\mathscr{E}^*$

electrons can be very important for conductive materials. However, for non-conducting materials, complex permittivity is mainly contributed by the presence of the dipoles.

$$\epsilon_t^* = \epsilon^* + \epsilon_i^* \approx \epsilon^* = \epsilon' - \epsilon''j \tag{4.1}$$

The simple dielectric relaxation model for a non-conductive material under a sinusoidal force field has been proposed by Debye [49]. The Debye dielectric model assumes an overall relaxation time for all molecular species. An average value of dielectric response is usually obtained in all dielectric measurement techniques. The Debye model can not fit all types of materials. Therefore, Cole and Cole (1941) proposed an empirical equation for a distribution of the relaxation time process which considered that each dipole had its own relaxation. This distribution of dielectric relaxation time process can be represented and derived using a generalized Maxwell relaxation model. Later, Davidson and Cole (1951) proposed another empirical equation from the experimental observation of the asymmetric dielectric dispersion curve due to interaction of neighboring dipoles. Finally, Scaife (1963) combined the Davidson-Cole and Cole-Cole models and proposed a general empirical model. These four models are given below.

Debye model

$$\epsilon^*(\omega) = \epsilon'(\omega) - \epsilon''(\omega)j = \epsilon_u + \frac{(\epsilon_r - \epsilon_u)}{1 + \omega\tau\, j} \tag{4.2}$$

where $\epsilon'(\omega) = \epsilon_u + \dfrac{(\epsilon_r - \epsilon_u)}{(1 + \omega^2 \tau^2)}$ and $\epsilon''(\omega) = \dfrac{(\epsilon_r - \epsilon_u)\,\omega\tau}{(1 + \omega^2 \tau^2)}$

Cole-Cole model: $0 \leq n \leq 1$

$$\epsilon^*(\omega) = \epsilon_u + \frac{(\epsilon_r - \epsilon_u)}{1 + (\omega\tau\, j)^{1-n}} \qquad (4.3)$$

Davidson-Cole model: $0 \leq m \leq 1$

$$\epsilon^*(\omega) = \epsilon_u + \frac{(\epsilon_r - \epsilon_u)}{(1 + \omega\tau\, j)^{m}} \qquad (4.4)$$

Scaife model: $0 \leq n, m \leq 1$

$$\epsilon^*(\omega) = \epsilon_u + \frac{(\epsilon_r - \epsilon_u)}{(1 + (\omega\tau\, j)^{1-n})^{m}} \qquad (4.5)$$

	Debye (1929)	Cole-Cole (1941)	Davidson-Cole (1951)	Scaife (1963)
n	0	$0 \leq n \leq 1$	0	$0 \leq n \leq 1$
m	1	1	$0 \leq m \leq 1$	$0 \leq m \leq 1$

The unrelaxed and relaxed permittivities are ϵ_u (ϵ_∞ at very high frequency) and ϵ_r (static dielectric constant; ϵ_o at very low frequency), respectively. The relaxation time is τ and the angular frequency is ω ($2\pi f$). The parameters for the width and the asymmetry of the dielectric dispersion curve are n and m, respectively. Using the complex identity ($j^p = e^{jp\pi/2}$), the Scaife's empirical expression can be separated into the real (permittivity; dielectric constant) and the imaginary part (dielectric loss factor), and described as follows.

$$\epsilon' = \epsilon_u + \frac{(\epsilon_r - \epsilon_u)\cos m\phi}{[\,1 + 2(\omega\tau)^{1-n}\cos((1-n)\pi/2) + (\omega\tau)^{2(1-n)}\,]^{m/2}} \quad (4.6)$$

$$\epsilon'' = \frac{(\epsilon_r - \epsilon_u)\sin m\phi}{[\,1 + 2(\omega\tau)^{1-n}\cos((1-n)\pi/2) + (\omega\tau)^{2(1-n)}\,]^{m/2}} \quad (4.7)$$

$$\text{where } \tan\phi = \frac{(\omega\tau)^{(1-n)}\sin((1-n)\pi/2)}{1 + (\omega\tau)^{(1-n)}\cos((1-n)\pi/2)}$$

Complex permittivity is a function of frequency, temperature, pressure, and material structure and composition. Two most important variables in the dielectric spectrum are temperature and frequency. Four types of graphs based on these two variables are usually used to present dielectric data: (1) arc diagram (Cole-Cole plot), (2) complex permittivity versus frequency, (3) the relaxation time at maximum loss versus the reciprocal of temperature, and (4) complex permittivity versus temperature.

The arc diagram is obtained by plotting the imaginary part versus the real part of complex permittivity at constant temperature, each point corresponding to one frequency. The Debye model is a semicircle in the Cole-Cole plot. This arc diagram is usually used to verify one of the above dielectric models. Plotting complex permittivity versus frequency at constant temperature is used to illustrate the time-temperature superposition. The third type of dielectric graph is used to identify the type of the molecular relaxation motions and to calculate activation energy for the relaxation transition. In practice,

frequency is mostly used as a parameter and temperature as a variable. Complex permittivity versus temperature is plotted at a fixed frequency. Therefore, the dielectric spectra can be easily compared with mechanical relaxation spectra, and thermomechanical, dilatometric and differential scanning calorimetric curves which are also measured as a function of temperature.

Since the relaxation time is determined by the minimum energy configuration of the dipole, the molecular motion is temperature-dependent. Two types of molecular transitions can be easily identified by plotting the relaxation time at maximum loss versus the reciprocal of temperature: (1) Arrhenius relation for local molecular transitions, and (2) WLF (William-Landel-Ferry) relation for structural transitions.

Arrhenius relation

$$\tau = \tau_o \, e^{(-E/RT)} \tag{4.8}$$

WLF relation

$$\tau = \tau_o \, e^{(-A(T-T_g)/(B+T-T_g))} \tag{4.9}$$

Two constants are A and B. The activation energy of transition E is usually from 1.5 to 25 Kcal/mole. Temperature and glass transition temperature are T and T_g, respectively. Typical methods to characterize these two transitions are summarized in Table 4.2. Three types of molecular motions are classified in the structural transition region: (1) α": the motion of larger crystallite on the melting phase, (2) α': the motion of macromolecules in crystalline region at the

Table 4.2: Characterization of structural and local molecular transition

Method	Structural transition	Local molecular motion
Thermal Dilatation	abruptly change	not significantly change
DSC	abruptly change	not significantly change
Mechanical Relaxation	not Arrhenius equation	Arrhenius equation
Dielectric Relaxation	not Arrhenius equation	Arrhenius equation

beginning of the melting process, and (3) α: the segmental motion (principal relaxation process; glass-rubber transition). Several types of molecular motions below the principal relaxation process are defined in the local molecular transition regions, such as β (motion of side groups), γ (motion of individual groups of atom in the backbone chains), and γ' (motion of groups of atom in branches or at the ends).

4.2.2 Experimental techniques for dielectric analysis

Dielectric analysis is based on the interaction of electromagnetic radiation with the electric dipole moments of the material. In the infrared optical and ultraviolet region (above 100 GHz), the changes in the induced dipole moment are due to the polarization of the atoms but not due to the motion of molecules. At very low frequencies (below 0.0001 Hz), the induced dipole moments are negligible when compared with the permanent (static) dipole moments of the material. Therefore, the frequency range of interest for dielectric spectroscopy is usually between 0.0001 Hz and 100 GHz.

However, there is no single experimental method which can cover the entire frequency range from 0.0001 Hz to 100 GHz. Each method has its own applicable frequency range and equation to determine the material complex permittivity. Experimental methods and related publications are summarized in Table 4.3. Five commercial dielectric instruments are listed in Table 4.4. For the DC transient current method, a step voltage is applied to the sample and the current-time response is measured by an electrometer. The time response is transformed into frequency through Fourier Transformation. For the bridge method, the resistance and the capacitance of the sample are balanced by the

Table 4.3: Summary of experimental dielectric measurements and work

Frequency range	Applicators	Research Work
Low frequency	DC transition	Hamon (1952), Hedvig (1973)
(0.0001 Hz - 10 KHz)		
Medium Frequency	(1) Electrode	Delmonte (1959), Senturia (1986)
(0.1 Hz - 10 MHz)	(2) Bridge	Yalof (1972), Kranbuehl (1986)
High Frequency	Resonant Circuit	--------
(100 KHz - 100 MHz)		
Microwave Frequency	(1) Waveguide	Wilson (1978), Springer (1984)
(100 MHz - 100 GHz)	(2) Cavity	Labuda (1961), Jow (1987)

Table 4.4: List of commercial dielectric analyzers

Operation method	Analyzer	Frequency range
Admittance Bridge	GenRad 1689 Digibridge	11 Hz - 0.1 MHz
	HP 4192A LF Impedance Analyzer	5 Hz - 13 MHz
Electrode Method	Micromet (Microdielectrometer)	0.1 Hz - 10 KHz
	Polymer Laboratories PL-DETA	20 Hz - 100 KHz
	(with temperature and environment control)	
Waveguide	HP 8510 Network Analyzer	1 GHz - 26.5 GHz

reference resistance and capacitance of the circuit by changing the circuit voltages. For the electrode method, the sample is placed between two conducting electrodes. A time-varying voltage is applied between the electrode and the time-varying current is measured. For a resonant circuit, a signal generator provides an inductance, resistance, and variable capacitance in a series RLC resonant circuit, and is coupled with the parallel capacitance and resistance of the sample. This series RLC circuit is always resonated with and without the sample. For a waveguide method, the null shift, voltage standing wave ratio, and the wavelength need to be measured first. The magnitude and phase of the transmitted and reflected signal is then measured in order to determine complex permittivity of the sample. For the resonant cavity (resonator) method, material-cavity perturbation is usually employed to relate measured changes in mode resonant frequency and cavity Q factor to complex permittivity of the material.

4.2.3 Literature review on dielectric study of epoxy/amine resins

Nondestructive dielectric measurement techniques have been applied below microwave frequencies to monitor the epoxy reaction by several investigators [38-48]. A summary of dielectric study on epoxy resins is listed in Table 4.5. Delmonte [38] used aluminum foil electrodes to measure complex permittivity as a function of time for three epoxy resins (DER 332, Epon 828, and Ciba Araldite 6020) with a curing agent (diethylenetriamine; DETA) at a frequency of 0.01 MHz and temperatures of 23.9 to 29.4 °C. Uncured epoxy resins of lower molecular weight were found to have higher permittivity (ϵ') and loss (ϵ'') than those of higher molecular weight. These experiments also indicated that the loss

Table 4.5: Summary of review on dielectric measurement of epoxy

Author	year	methods	frequency	epoxy
Delmonte	1959	electrodes	60Hz, 1KHz, 10KHz, 1MHz	DER 332/DETA
				Epon 828/DETA
Haran	1965	electrodes	30 Hz - 10 MHz	Epon 826/DETA
Wilson	1977	transmission lines	1.0 - 2.5 GHz	Epon 828/T-403
				Epon 828/Z
Springer	1984	waveguide	2.45 GHz	S2/9134B
				AS/3501-6
Sheppard	1985	microdielectrometer	0.1 Hz - 10 MHz	Epon 825/DDS
Day	1986	microdielectrometer	1 and 10 Hz, 1 and 10 KHz	Epon 828/DDS
Lane	1986	electrodes	240 Hz - 10 KHz	Epon 828/Versamide 140
Kranbuehl	1986	LF Impedance Analyzer	5 Hz - 5 MHz	Epon 828/U
Jow	1987	Resonant Cavity	2.45 GHz	DER 332/DDS

decreased before epoxy molecules approached an irreversible gel structure, abruptly increased around gelation, and then decreased due to continuous curing after gelation. However, the permittivity slightly decreased before the gel structure formed and rapidly decreased during reaction. He defined the time of maximum loss as the time of gelation. Haran et al. [39] investigated the isothermal polymerization of DGEBA epoxy (Epon 828) with amine (DETA) as a curing agent. Complex permittivity measurements as a function of time were made using a specially designed electrode within the frequency interval from 330 Hz to 1 MHz and at constant temperatures of 30, 45, and 60 °C. The permittivity and loss showed the similar frequency dependence as described by Delmonte. The minima of the loss disappeared and the maxima became flatter as frequency was increased. They found that the time of gelation and magnitude of the complex permittivity decreased with increasing temperature and frequency, which the authors concluded was due to molecular absorption phenomena.

Kranbuehl et al. [40] used a low frequency impedance analyzer to monitor the polymerization of the epoxy resin (Epon 828) with an unidentified curing agent at a cure temperature of 30 °C between heating plates. Dielectric measurements were made at three frequencies of 0.125 KHz, 5.0 KHz, and 0.5 MHz. Complex permittivity-time graphs had the same profiles as those obtained by other investigators. However, minima in the loss curve decrease as the frequency is decreased and disappear at 0.125 KHz. Day [41] studied effects of stoichiometric mixing ratio on isothermal epoxy (Epon 828/DDS) during the 177 °C thermal cure on complex permittivity used the dielectric sensor (microdielectrometry). Dielectric measurements were made over the

sweeping frequencies from 0.1 Hz to 0.01 MHz Again, the complex permittivity profiles were the same as before and minima in the loss curve disappear when the frequency is decreased down to 10 Hz. The tendency of the minima in the loss curve as the frequency changes was completely different between Haran's and Day's experiments. These phenomena have not been fully understood, but might be due to interaction of complicated molecular relaxations at low frequencies.

Lane et al. [42] studied dielectric data during isothermal cure of two epoxy resin systems (50 phr DGEBA/polyamide and 25 phr TGDDM/DDS) using a cell electrode. The admittances of the sample cell were measured at a temperature range of 22 to 70 °C and three selected frequencies (1, 5, and 10 KHz) for DGEBA-polyamide and at a temperature range of 140 to 190 °C and three frequencies (0.1, 0.4, and 1 KHz). The overall activation energy determined from dielectric data increased as the cure temperature increased. The authors concluded that the reaction mechanism was temperature-dependent. The values of activation energy of epoxy/amine reaction were 12 to 13 from these dielectric measurements, 13.5 from Sanjana's dielectric data, and 16 to 17 Kcal/mole from DSC measurement. A Cole-Cole dielectric relaxation model was proposed to analyze DGEBA-polyamide from 0.24 KHz to 2 MHz. The best parameters for ϵ_r, ϵ_u, and n were 12.4, 4.4, and 0.67, respectively. The average relaxation time at maximum dielectric loss increases as the cure proceeds.

Lane et al. [43] also intended to combine the dielectric relaxation time model with nth-order reaction kinetics. A six-parameter model similar to a viscosity-relaxation time model was proposed and described below.

$$\ln \tau = \ln \tau_\infty + E_{n'}/RT + \Phi/(n'-1)\ln[1 + (n'-1)K_\infty \exp(-E_k/RT)t] \qquad (4.10)$$

Relaxation times at time t and at infinite temperature are τ and τ_∞. Relaxation and kinetic activation energy are $E_{n'}$ and E_k. The entanglement parameter and kinetic frequency factor are Φ and K_∞. The order of reaction is n'.

Bidstrup et al. [46] related the ionic conductivity measurement of the stoichiometric mixture of DER 332 and DDS to the cure temperature and conversion by combining the Williams-Landel-Ferry and empirical DiBenedetto equations. A seven-parameter model was proposed and given by Equations 4.11 and 4.12. The best estimated values of these seven parameter (C_1, C_2, C_3, C_4, C_5, C_6, and C_7) were 9.0, -194, 0.73, -18.0, 0.013, 0.3 and 0.18 for the stoichiometric mixture of DER 332 and DDS.

$$\sigma(T, T_g) = \sigma_0 \, e^{[C_1(T-T_g)/(C_2 + C_3 T_g + (T-T_g)) + C_4 + C_5 T_g]} \qquad (4.11)$$

$$T_g = T_{g0} + T_{g0} \frac{(C_6 - C_7) X}{(1 - (1-C_7) X)} \qquad (4.12)$$

Glass transition temperatures are T_{g0} for the unreacted resin and Tg for the reacted resin at extent of cure X.

Zukas [48] indicated inconsistent data on dielectric measurement due to ionic effect in the isothermal cure of Fiberite (FX123L) at lower frequency or higher cure temperature using microdielectrometry. Ionic contribution at the higher cure temperature could be increased when the material temperature approached the onset of the ultimate glass transition temperature. Ionic conductivity could be interfered with electrode polarization at the lower frequencies. This variation could

be reduced to cure materials at a higher frequency or a low cure temperature.

4.3 Experimental

4.3.1 Experimental materials and system

The epoxy resin is DER 332 and the curing agent is diaminodiphenyl sulfone. The microwave diagnostic and processing system consists of a microwave external circuit (an energy source, transmission lines, and the coupling probe), diagnostic elements (an X-Y oscilloscope, power meters, the E-field diagnostic probe, and a temperature sensor device) and the loaded cavity (the cavity and the loaded material) as shown in Figure 2.1. The use of this circuit for microwave processing and diagnosis is reported in the literature [1,4]. A cylindrical TM_{012}-mode cavity is used to process epoxy/amine resins at a frequency of 2.45 GHz. A fluoroptic temperature sensing device (Luxtron 750) which does not absorb electromagnetic energy or interfere with electromagnetic fields is used to on-line monitor the epoxy temperature. The fluoroptic probe is protected by a 3 mm O.D. pyrex capillary tube. A cylindrical teflon sample holder is also required to contain the liquid epoxy/amine mixture [3]. The cylindrical geometry of both the cavity and loaded materials is selected in order to facilitate diagnosis, modeling, and theoretical analysis. A differential scanning calorimeter (Du Pont DSC 9300) is used to determine extent of cure after the epoxy/amine resin is thermally or electromagnetically heated. Samples are scanned in DSC pans at a heating rate of 2 °C/min from 30 to 330 °C and the residual heat of reaction is measured. The extent of cure is calculated by the difference in heat of reaction between the uncured and cured sample and

divided by the heat of reaction (434 J/g) for the uncured sample.

4.3.2 Experimental methods

Dielectric measurements at microwave frequencies usually employ the material-cavity perturbation technique in a single mode. A practical experimental criterion for this perturbation technique is that the resonant frequency shift due to introduction of the material must be much less than the resonant frequency. Dielectric measurements using perturbation can be made by (1) measuring conventional frequency shift and Q-factor change in a resonant cavity at a fixed cavity length (swept frequency method) and (2) measuring changes in the cavity length and the power ratios at a selected resonant frequency (single frequency method). Measured changes in the mode resonant frequency and cavity Q factor between the cavity with and without the materials can be related to permittivity and dielectric loss factor of the materials through material-cavity perturbation. The resonant frequency shift increases with increasing permittivity of the materials but the cavity Q factor decreases as the dielectric loss factor of the materials increases.

In the swept frequency method, the reflected signal from the cavity is rectified by a crystal detector and forms a cavity resonance absorption curve on an X-Y oscilloscope. The cavity resonance absorption curve displays the resonant frequency and the cavity Q factor while the cavity is critically coupled with the external microwave circuit by continually adjusting the coupling probe penetration depth into the cavity. The changes in the resonant frequency and cavity Q factor are directly measured from the changes in the critically-coupled cavity resonance curve shown on the X-Y oscilloscope.

In the single frequency method, the length of the resonant cavity

corresponds to the resonant frequency. The shift in the resonant frequency due to the change in material permittivity needs to be compensated by tuning the cavity length. Critical coupling structure is then accomplished by continually adjusting the coupling probe depth so that the reflected power P_r is close to zero when compared with the incident power P_i. The ratio of the power P_b on the diagnostic probe to the incident power P_i is proportional to the cavity Q factor. The changes of the resonant cavity length and power ratio in the single frequency method are similar to the resonant frequency shifts and cavity Q factor changes in the swept frequency method as previously described [2-4]. Therefore, in the single frequency method, the cavity length and the power ratio decrease as permittivity and dielectric loss factor of the loaded material increase, and vice versa.

Consistent dielectric measurements of epoxy/amine resins using swept and single frequency methods have been reported earlier [4]. The swept frequency method is usually employed to make precise dielectric measurements in a very low power microwave circuit. Application of the swept frequency method to electromagnetic processing of epoxy/amine resins in a TM_{012}-mode resonant cavity has been previously studied at input power levels between 3 and 6 W [3]. Most of the incident power supplied from the sweeping energy source is reflected and cannot be efficiently coupled into the processed materials. Therefore, the single frequency method is used here to efficiently focus and match microwave energy into the processed materials during microwave heating while the swept frequency method is used for ease and precision of diagnosis during free convective cooling.

DER 332 was heated up to 130 °C and well mixed with equivalent moles of DDS and degassed in a vacuum oven at 80 °C for an hour. The

sample volumes (about 2.00 cm^3) of epoxy/amine resins were experimentally determined so that the resonant frequency shift was much less than the resonant frequency throughout the entire process. A teflon holder with a fluoroptic probe was located at the position of the strongest electric field in the TM_{012}-mode cavity by a cotton thread. This cavity was critically coupled with a microwave external circuit and initial measurements were made by single and swept frequency methods at 2.45 GHz [4]. The teflon holder was removed, filled with the sample, and relocated in the strongest electric field region of the cavity. The sample was then heated in this cylindrical single-mode resonant cavity at a power level of 5 W for selected cure times between 5 and 120 minutes. The cavity with the sample was continually tuned to critically couple with the microwave external circuit at the same frequency of 2.45 GHz. On-line measurements of temperature and dielectric loss factor by the single frequency method were made during the microwave curing process as shown in Figure 4.1. The temperature profile shown in Figure 4.1 was common to all samples, although all samples were not heated for the same period of time. Sample heating times, maximum sample temperature, and final extents of cure are shown in Table 4.6. After the completion of each selected heating time, the single-frequency microwave curing and diagnostic system was switched to a low-power swept-frequency diagnostic system by removing the traveling-wave-tube (TWT) amplifier. Measurements of temperature and dielectric properties using the swept frequency method were made continually during free convective cooling. Measurements were made at temperatures below 150 °C so that the extent of cure remained constant and temperature differences (less than 5 °C) inside the resins could be neglected during the course

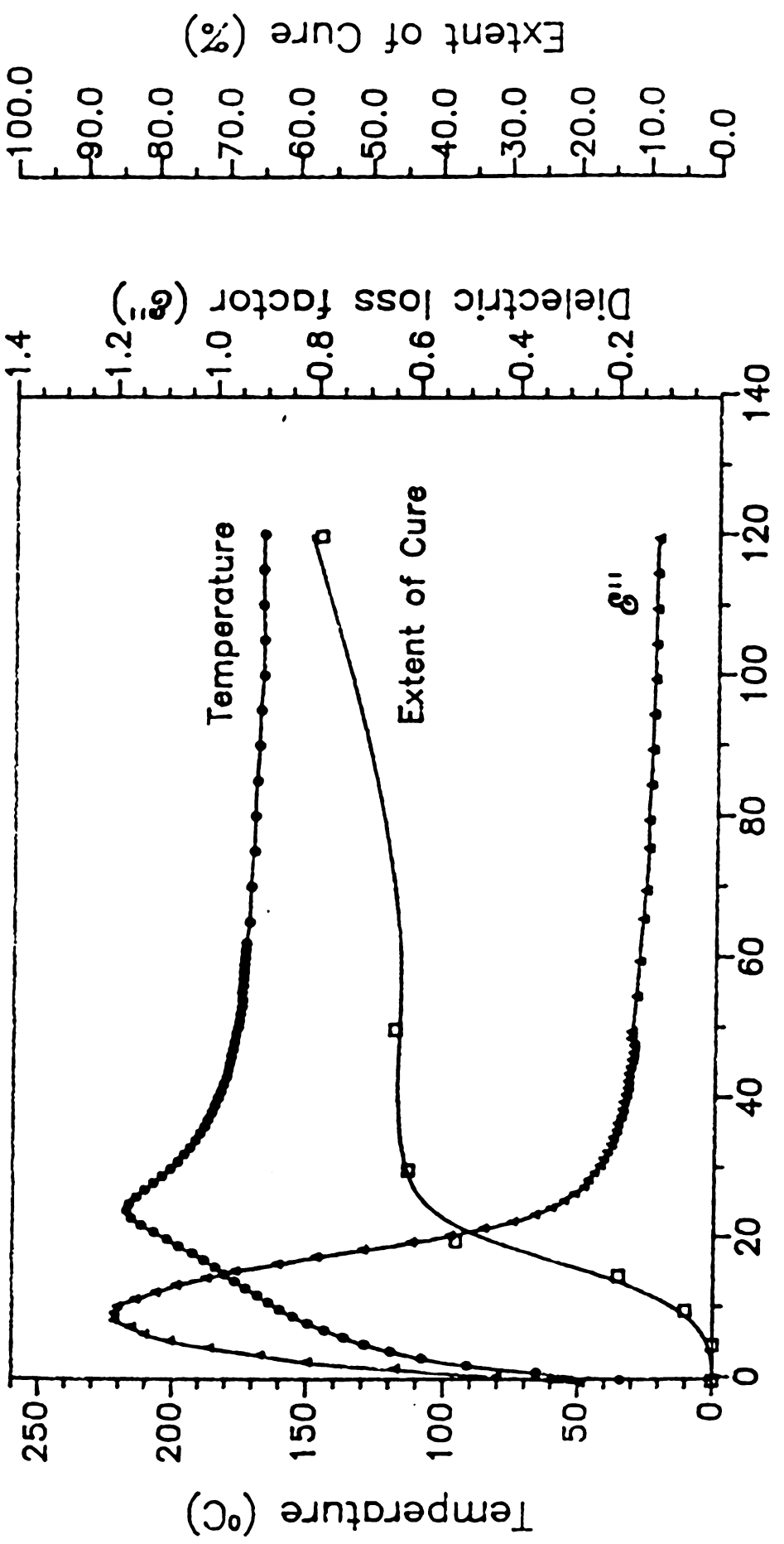

Figure 4.1: Temperature, dielectric loss factor, and extent of cure versus microwave cure time for the stoichiometric mixture of DER 332 and DDS at an input power level of 5 W and 2.45 GHz

Table 4.6: Sample heating time, maximum temperature, and extent of cure

Heating time (min)	Maximum temperature (°C)	Extent of cure (%)
5	128.9	0
10	159.8	4
15	180.5	14
20	202.2	37
30	220.0	44
50	220.0	46
120	220.0	57

of sample cooling. The extent of cure of the epoxy/amine resin was then determined by differential scanning calorimetry. These swept-frequency dielectric measurements as shown in Figures 4.2 and 4.3 provided information regarding the dependence of dielectric properties on temperature and extent of cure at 2.45 GHz. However, the reaction at the temperatures reached in this experiment occurred so rapidly between extents of 14% and 37% that samples of intermediate extent could not be produced with consistency. Therefore, data between 14% and 37% extent are not reported in Figures 4.2 and 4.3.

Five epoxy/amine samples were thermally cured in a conventional oven at a temperature of 170 °C for selected heating times between 10 and 120 minutes. Extents of cure for these thermally cured samples were also determined using DSC. Dielectric measurements of all these thermally and microwave cured samples were made using the low-power swept frequency diagnostic system at 33 °C and 2.45 GHz. Dielectric loss factor as a function of extent of cure at 33 °C and 2.45 GHz was compared for both thermally and microwave cured samples in Figure 4.4.

4.4 Results and Discussion

Permittivity and dielectric loss factor are expressed relative to the permittivity of free space. On-line measurements of temperature and dielectric loss factor during the microwave curing and off-line measurement of extent of cure of the samples for selected microwave cure time at an input power level of 5 W at 2.45 GHz are shown in Figure 4.1. Dielectric loss factor increases with increasing temperature up to the temperature of 140 °C in the early stages of heating. Dielectric loss

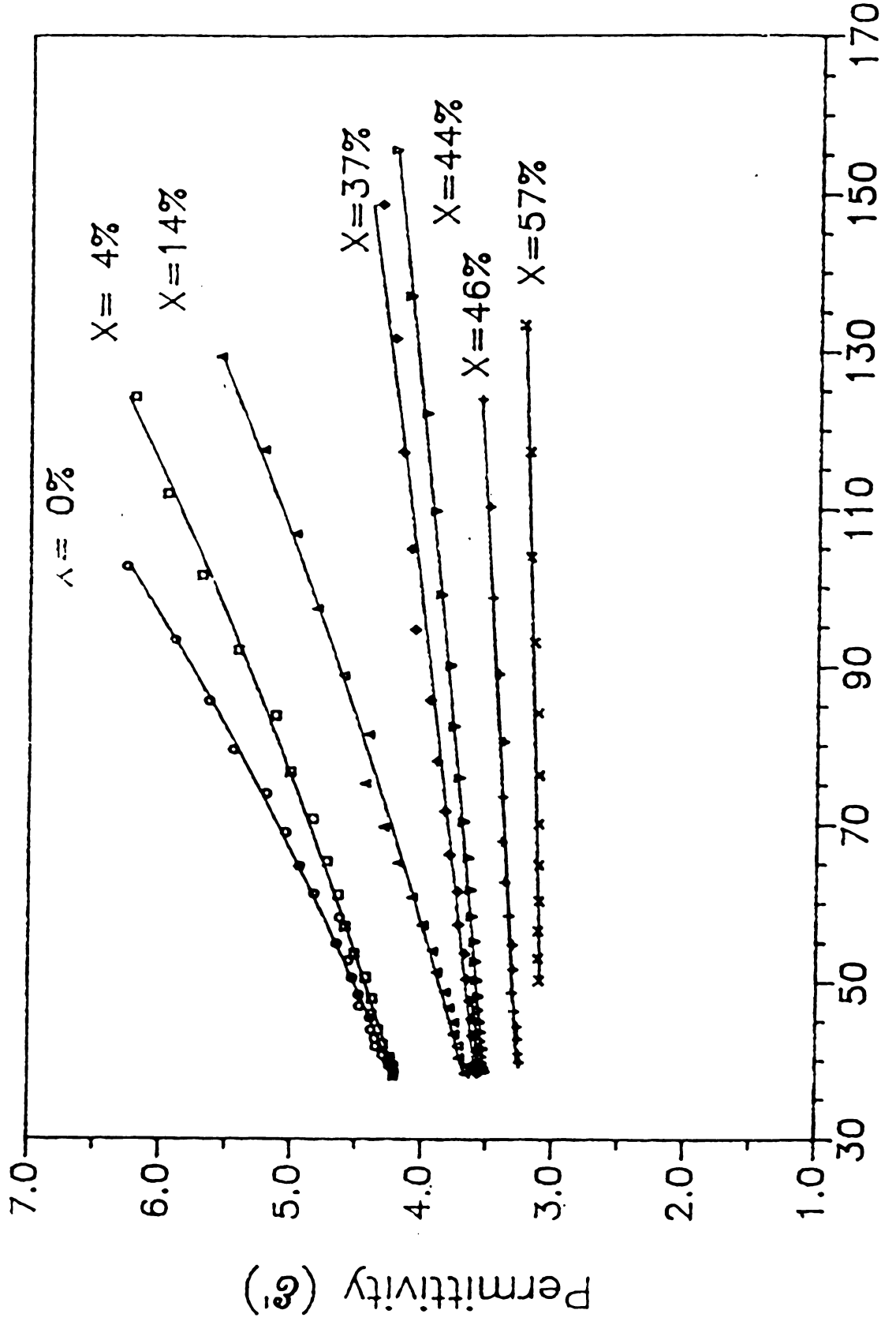

Figure 4.2: Permittivity versus temperature and extent of cure for the stoichiometric mixture of DER 332 and DDS at 2.45 GHz

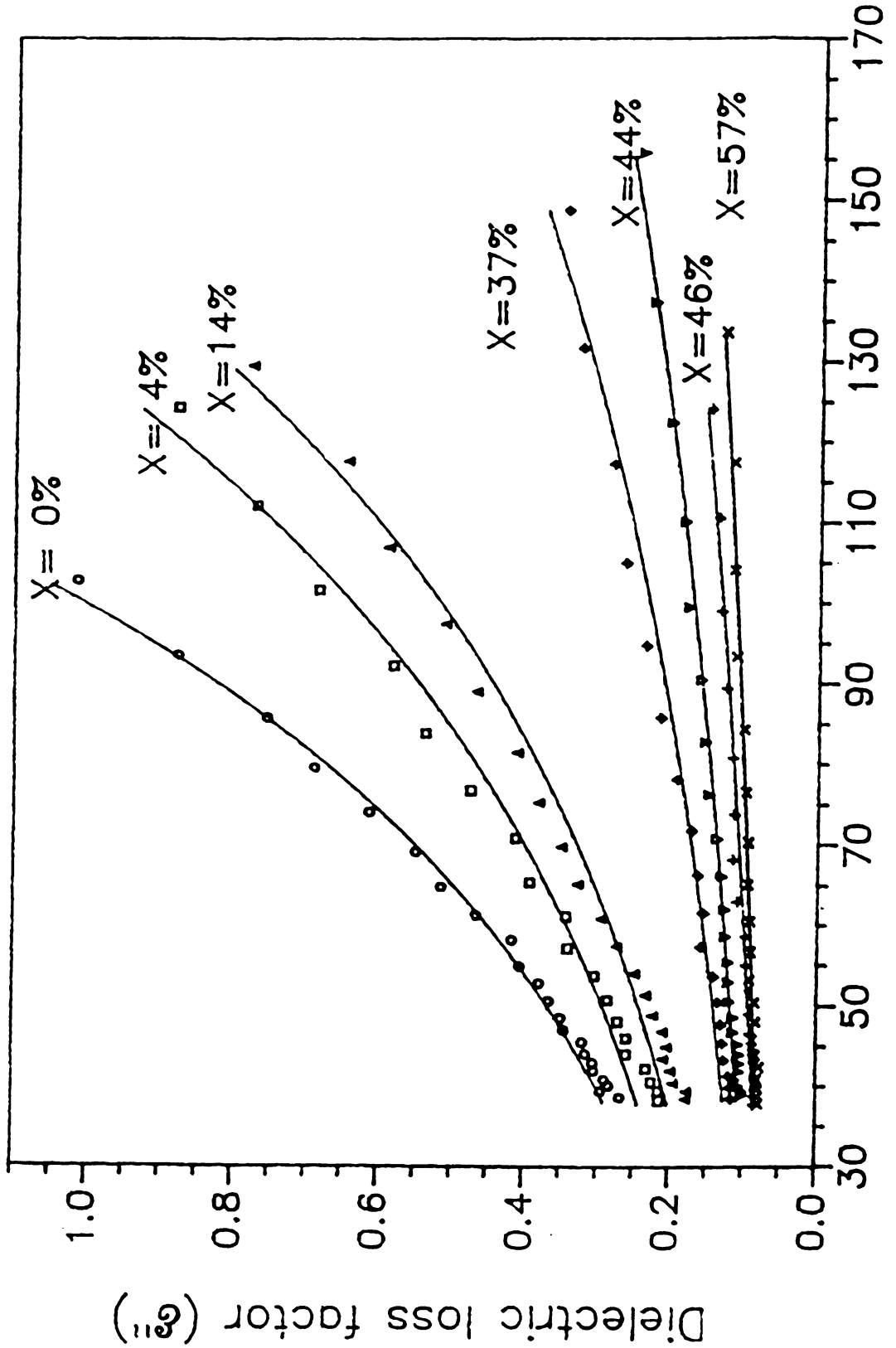

Figure 4.3: Dielectric loss factor versus temperature and extent of cure for the stoichiometric mixture of DER 332 and DDS at 2.45 GHz

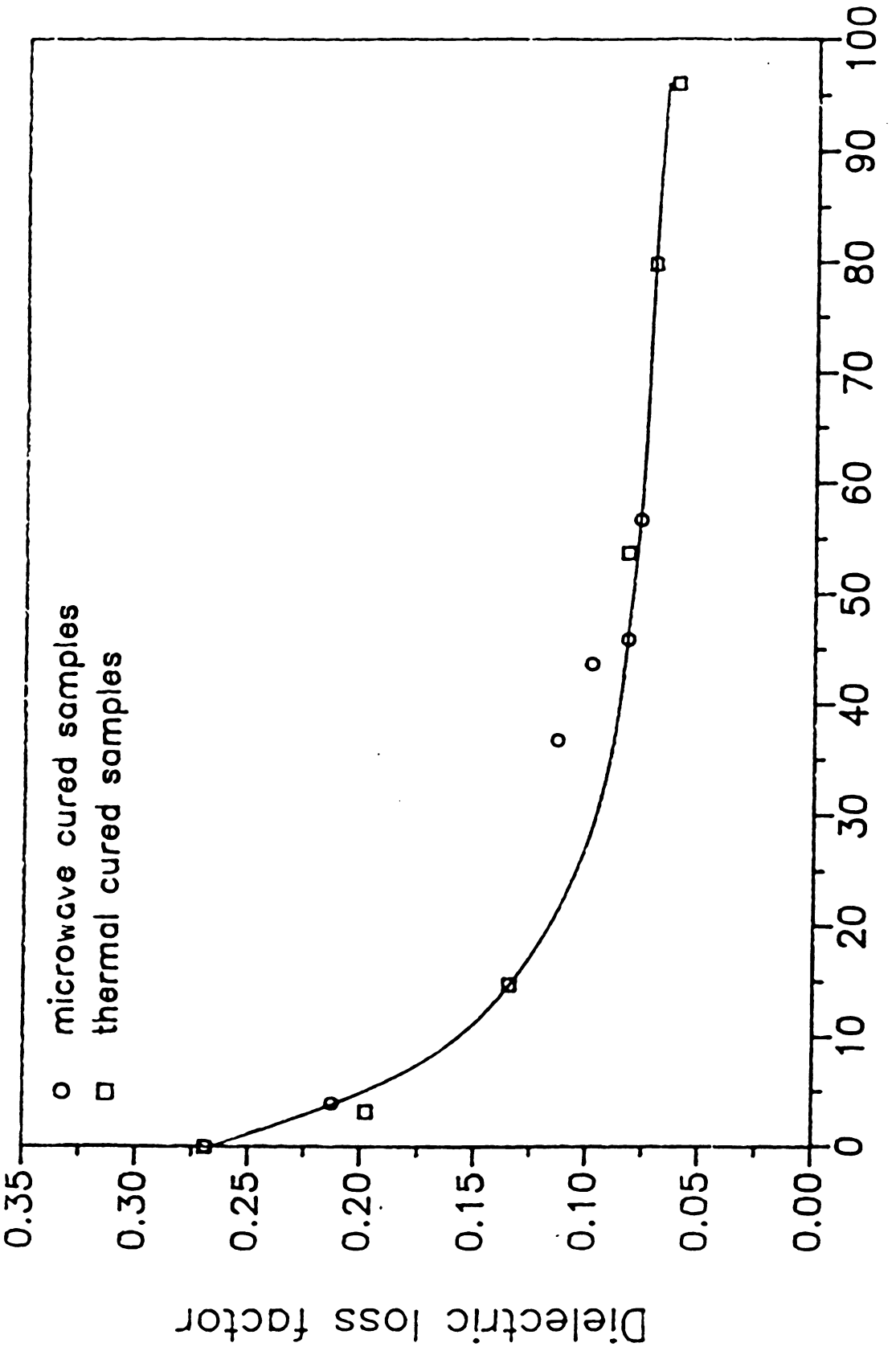

Figure 4.4: Comparison of dielectric loss factor versus extent of cure between thermally and microwave cured samples at 33 °C and 2.45 GHz

factor then abruptly decreases as the cure proceeds, even though temperature continues to rise due to the exothermic cure reaction. After an extent of 40% is reached, dielectric loss factor slightly decreases with increasing extent of cure. It implies that there are three different material structure stages in the cure process. The first stage is liquid monomer heating. Significant decreases in dielectric loss factor are the characteristic of the second stage where linear and branch chain formation and gelation are likely to occur. The third stage leads to three-dimensional network formation and a fully cured structure.

Permittivity and dielectric loss factor of epoxy/amine resins increase with increasing temperature and decrease with increasing extent of cure as shown in Figures 4.2 and 4.3. This is due to increased mobility of dipoles during heating and subsequently decreased mobility of dipoles during crosslinking. Figure 4.3 shows that dielectric loss factor is more dependent on temperature before 40% cure but less dependent on temperature after 40% cure.

Dielectric loss factor as a function of extent of cure for thermally and microwave cured samples at 33 °C and 2.45 GHz is shown in Figure 4.4. Again, dielectric loss factor decreases with increasing extent of cure at constant temperature and frequency, and is indistinguishable between thermally and microwave cured samples.

4.5 Conclusion

Material-cavity perturbation technique is shown to be a useful technique to obtain dielectric data of chemically reacting materials at

microwave frequencies. Dielectric properties (permittivity and dielectric loss factor) of stoichiometric mixtures of DGEBA epoxy (DER 332) and amine (diaminodiphenyl sulfone; DDS) as a function of temperature and extent of cure have been measured at a microwave frequency of 2.45 GHz. Permittivity and dielectric loss factor of this resin increase with increasing temperature and decrease with increasing extent of cure. Dielectric loss factor is more dependent on temperature in the early stages of cure but becomes less dependent on temperature as the cure proceeds. Temperature- and cure-dependent dielectric loss factor at microwave frequencies can be used to monitor the cure process. On-line measurements of temperature- and cure-dependent dielectric loss factor show three material structure stages and significant changes in dielectric loss factor during the microwave cure process. A significant transformation in the dielectric loss factor/cure time/temperature profile is also found at an extent of reaction of about 40% in this epoxy/amine matrix resin. The relationship between dielectric loss factor and extent of cure for thermally and microwave cured samples is the same at constant temperature and frequency.

CHAPTER FIVE

COMPUTER-CONTROLLED PULSED MICROWAVE PROCESSING OF EPOXY

5.1 Introduction

Microwave energy using single-mode cavities [53-56], conventional multi-mode microwave ovens [33,34] or waveguides [35,36] has been used to cure epoxy/amine resins. These experiments indicate that direct and fast heating can be accomplished using microwave energy. Continuous power inputs were used in these experiments. Three typical temperature-time stages in this continuous microwave heating of thermosetting resins are: (1) initial rapid temperature rise by directly heating the monomers, (2) a significant temperature peak due to the exothermic curing reaction, and (3) free convective cooling at the end of reaction. Fast exothermic reaction heating usually accelerates the temperature rise and gradient inside the samples during the curing. Neither continuous microwave nor thermal processing can be effectively controlled in order to maintain constant temperature-time profiles through the entire process. However, pulsed microwave heating can be used to control temperature/time profiles for the exothermic reaction system.

A microwave processing and diagnostic system aided with a computer data acquisition and control is developed here to intelligently pulse the power input, to regulate the temperature-time profile, and to measure dielectric loss factor and temperature during the microwave curing of epoxy/amine resins. Dielectric measurements are made using

the single-frequency material-cavity perturbation technique [4]. Temperature measurements are made using fluoroptic thermometry. The pulsed power quickly heats the resins to the cure temperature, eliminates the exothermic temperature peak, and retains the same temperature even at the end of reaction. This controlled pulsed system has a unique feature of processing epoxy/amine resins at a higher cure temperature below the thermal degradation temperature and without the exothermic temperature peak which always occurs in thermal or continuous microwave processing. The temperature-time profiles during thermal, continuous microwave, and controlled pulsed microwave curing of epoxy are compared in this study. Higher temperature cure than conventional thermal cure and dielectric loss factor measurements during the pulsed microwave processing of epoxy are illustrated. The differences in glass transition temperature and cure kinetics between thermally and pulsed microwave cured samples are also investigated.

5.2 Experimental

5.2.1 Experimental system

A computer-aided microwave processing and diagnostic system was used in these experiments as shown in Figure 5.1. A fluoroptic temperature sensing system (Luxtron 750 four channel system) was used to measure temperature. Temperature measurement data from the Luxtron system were transferred through a standard RS-232C communication port to a Zenith 159-13 personal computer. A sampling time for temperature measurements of 0.1 sec is possible with an accuracy of 1 °C. An analog pin diode switch (Narda S213D-04) was used to control microwave power input from the microwave energy source to the cavity. Three power

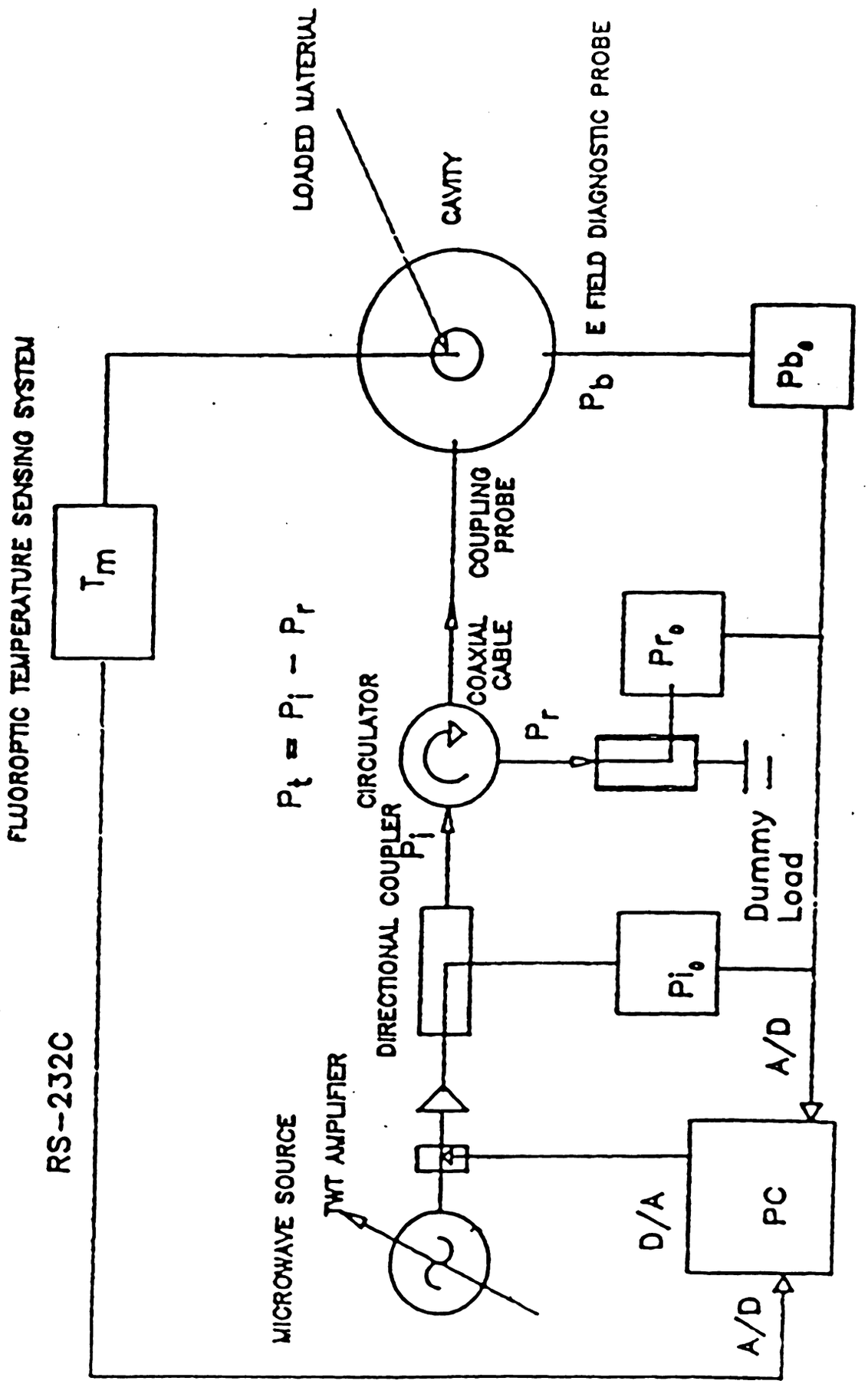

Figure 5.1: Computer-aided microwave processing and diagnostic system

levels (incident, reflected, and diagnostic power) were directly measured using three analog power meters (HP 435A) and related to the dielectric loss factor of the sample loaded in the cavity [2]. A high speed I/O interface board (Omega DAS-16) was used to control the pin switch and to transfer the power measurements into the personal computer. The rest of the microwave processing and diagnostic system has been described [1,2,4]. A block diagram of this computer-controlled microwave processing and diagnostic system is shown in Figure 5.2. A data acquisition and control program written in BASIC language was used to store temperature and power measurements, to calculate dielectric loss factors, and to turn the power switch on or off. A cure temperature was selected and set using this program. The temperature measurements at the sample center were used in a feedback loop to control the power input. The power input was turned on or off depending on the sample temperature below or above the selected cure temperature. A conventional thermal oven (Precision Thelco Model 29) with an accuracy of 5 °C was also used to perform thermal cure experiments. A differential scanning calorimeter (Du Pont DSC 9300) was used to determine extent of cure and glass transition temperature of the cured samples.

5.2.2 Materials

A clear liquid DGEBA epoxy resin, DER 332 (mol. wt. 346, Dow Chemical Co.), was used in this study. A white aromatic primary amine powder (4,4'-diaminodiphenyl sulfone; mol. wt. 228, Aldrich Chemical Co.) was used as a curing agent. The stoichiometric mixtures of DER 332 and DDS were prepared by mixing 100 parts resin with 36 parts curing

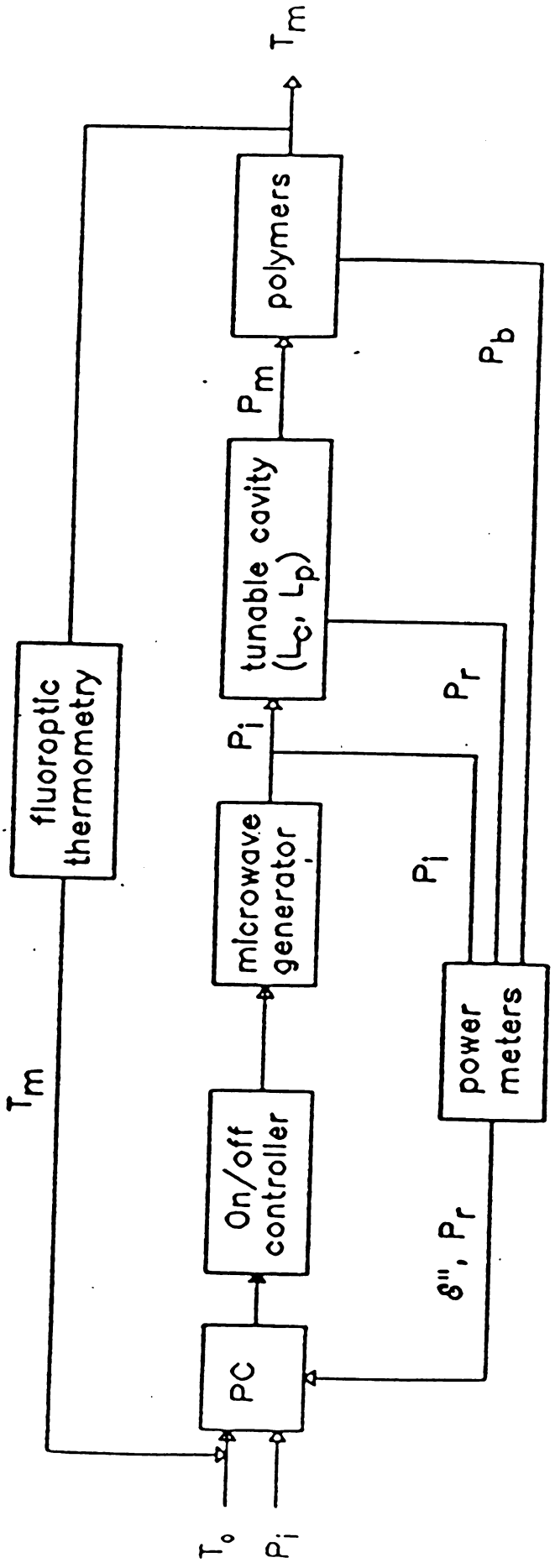

Figure 5.2: Block diagram of computer-controlled pulsed microwave processing and diagnostic system

agent by weight. Epoxy was heated up to 130 °C. Amine was then added and the mixture was well stirred until amine was completely dissolved (less than 5 minutes). The clear pale yellow mixture was then cooled down and degassed in a vacuum oven at 80 °C for about an hour.

5.2.3 Experimental procedures

The fresh sample was poured into a cylindrical teflon sample mold (3/8" i.d., 1/2" o.d., and 4.0 cm long). Several advantages for using teflon as a sample holder have been mentioned previously [3]. Two fluoroptic fiber probes were protected by 3 mm o.d. pyrex capillary tubes and located at the center and boundary of the sample. Temperatures at the sample center and boundary were measured using the fluoroptic thermometer. The epoxy-filled mold with two temperature sensing probes was loaded into the thermal oven or the microwave cavity. The cavity was always operated in a TM_{012} mode at 2.45 GHz and resonated with the external microwave circuit. The temperature-time profiles during thermal, continuous microwave, and controlled pulsed microwave curing of epoxy/amine samples were measured and compared. A higher temperature cure experiment using this controlled pulsed processing technique was performed at a temperature of 280 °C. Measurements of dielectric loss factor and temperature during the pulsed microwave processing of epoxy/amine and pure epoxy samples were also made. The differences in glass transition temperature and cure kinetics between thermally and pulsed microwave cured samples were studied.

Temperature measurements of epoxy/amine resins were made during thermal, continuous microwave, and controlled pulsed microwave curing. A fresh sample was thermally cured in the thermal oven at a temperature

of 190 °C. The air temperature in the oven, and the center and boundary temperatures of the sample were measured. For microwave experiments, one sample was electromagnetically cured without feedback temperature control at a continuous input power density of 2.5 W/cm^3. The other sample was cured using the computer-controlled pulsed microwave power at the selected cure temperature of 190 °C. The temperature measurement at the sample center during pulsed microwave curing was used in a feedback loop to control the power input. The power input was turned off when the center temperature was above the selected cure temperature, and vice versa. Temperature/time profiles at the center and the boundary of the samples for thermal, continuous microwave, controlled pulsed microwave curing were compared.

Another computer-controlled pulsed microwave curing of the epoxy/amine resin at a cure temperature of 280 °C was performed in order to illustrate the ability of processing thermosets at a higher cure temperature. Temperature/time profiles at the sample center and boundary were made.

Epoxy/amine and pure epoxy samples were diagnosed during computer-controlled pulsed microwave processing at 2.45 GHz. Measurements of the sample temperatures and the power levels (input, reflected, and diagnostic power) were made during the microwave processing. Dielectric loss factors were determined using the single-frequency material-cavity perturbation technique [2]. These experiments were intended to show the ability of measuring dielectric loss factor during pulsed microwave curing of epoxy/amine resins and to illustrate the temperature-dependence of the dielectric loss factor of pure epoxy at 2.45 GHz.

The next cure experiments were performed in order to study the differences in glass transition temperature and cure kinetics between

thermally and pulsed microwave cured samples. For computer-controlled pulsed microwave experiments, three cure temperatures of 190, 240, and 280 °C were selected. Fresh epoxy/amine samples were cured with processing times of 15, 30, 45, 60, 90, and 120 minutes at the cure temperatures of 190 and 240 °C, and with processing times of 10, 15, 20, 30, and 60 minutes at 280 °C. Another six samples were cured in the thermal oven at a temperature of 190 °C. They were cured with heating times of 15, 30, 45, 60, 90, and 120 minutes. Temperatures at the sample center and boundary during curing were measured. After the completion of each selected processing time, extents of cure and glass transition at the boundary parts of these cured samples were determined using DSC. The samples were scanned in the DSC pans at a heating rate of 20 °C/min from 30 to 400 °C. The total heat of reaction for the fresh mixture was 369.3 J/g. The extent of cure for the cured sample was calculated as the ratio of the total heat of reaction minus the residual heat of reaction of the cured sample to the total heat of reaction. Glass transition temperature was defined as the inflection temperature of a step transition change on the DSC thermograph close to the residual exothermic peak.

5.3 Results and Discussion

5.3.1 Effect on temperature-time profiles

Epoxy/amine resins were cured using thermal, continuous microwave, and controlled-pulsed microwave energy. The temperature-time profiles at the center and the boundary of the sample during thermal curing are shown in Figure 5.3. Temperatures at the sample boundary are higher than those at the center due to surface driven heating in the early

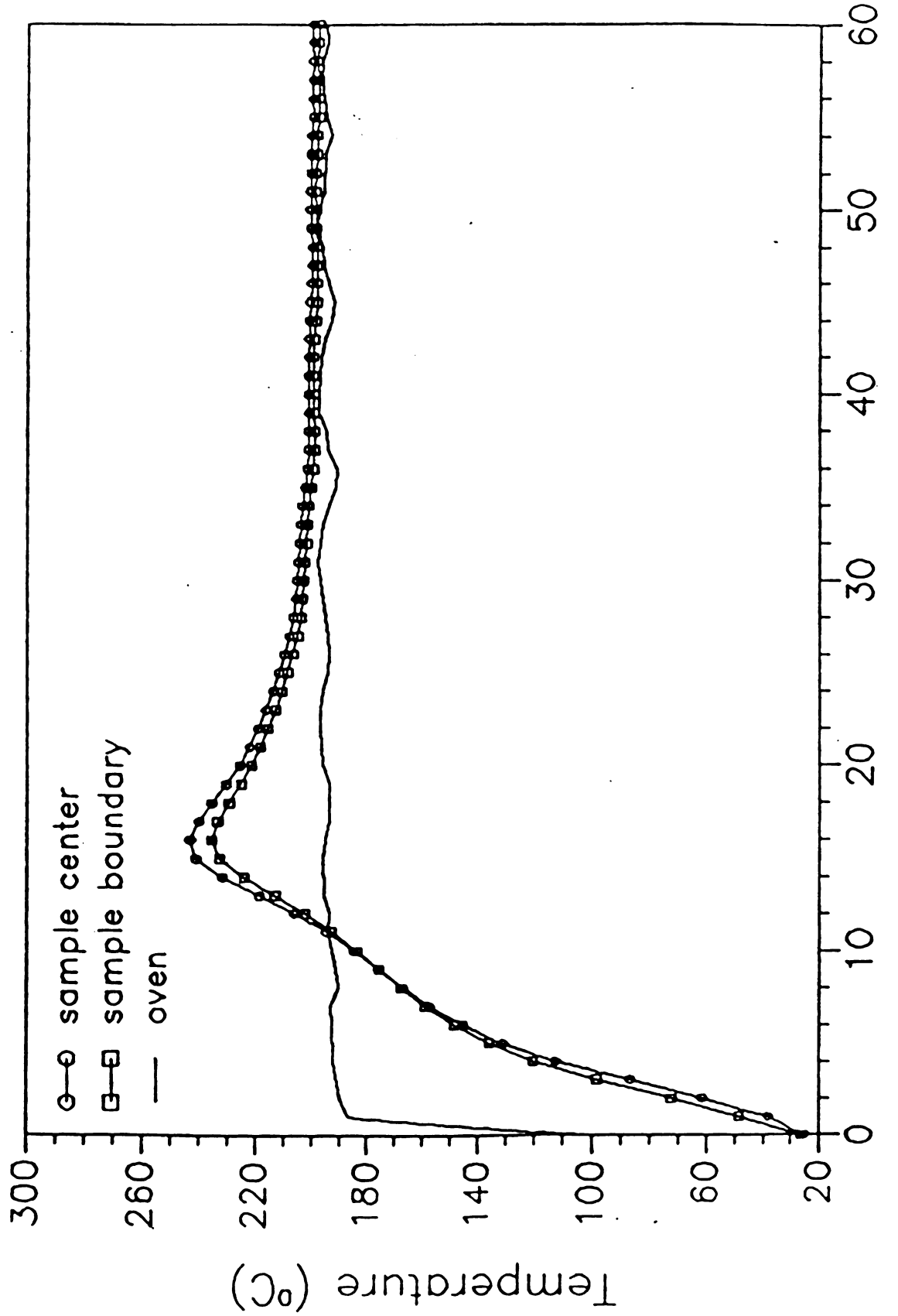

Figure 5.3: Temperature-time profiles during thermal curing of DER 332/DDS resins

stages of thermal heating. Later, temperatures at the center are higher due to exothermic heat and low thermal conductivity characteristic of epoxy. The temperature-time profiles at the sample center and boundary during slow continuous microwave curing are shown in Figure 5.4. Temperatures at the sample center are higher than those at the sample boundary due to preferential microwave energy absorption of dipoles of epoxy/amine resins interacting with the electric field, slow heat conduction inside the sample, and heat transfer across the cold material boundary. However, a significant exothermic temperature peak and a short uniform temperature period before the exothermic peak are always found in either thermal or continuous microwave processing. The temperature-time profiles during controlled pulsed microwave curing are shown in Figure 5.5. Figure 5.5 shows that computer-controlled microwave heating can quickly heat the resins, fully utilize the exothermic heat of reaction, and eliminate the exothermic temperature peak which may cause the thermal stress build-up during the exothermic cure reaction. Cure temperatures at a given position in the material are constant throughout the pulsed-power cure process. However, a temperature gradient inside the resin is always built up during the microwave processing due to the surface heat transfer and the low material thermal conductivity [10]. Improvement of microwave heating to obtain a uniform temperature distribution inside the materials has been discussed elsewhere [10].

Temperature/time/position profiles during the pulsed power curing of the epoxy/amine resins at 190 and 280 °C for 60 minutes are shown in Figure 5.6. Figure 5.6 shows that the temperature gradient inside the sample increases as the set-point temperature is increased. Again, this

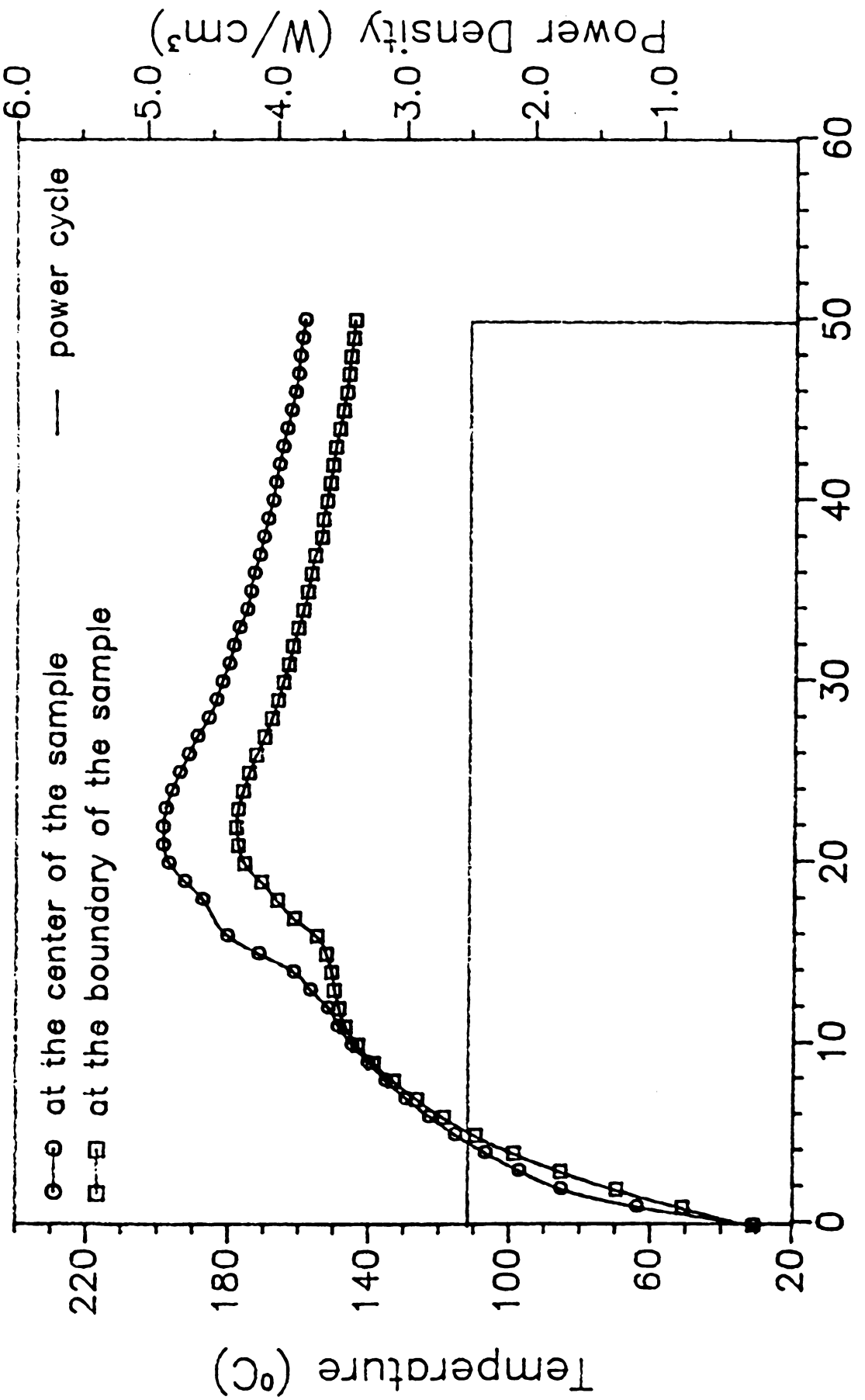

Figure 5.4: Temperature-time profiles during continuous microwave curing of DER 332/DDS resins

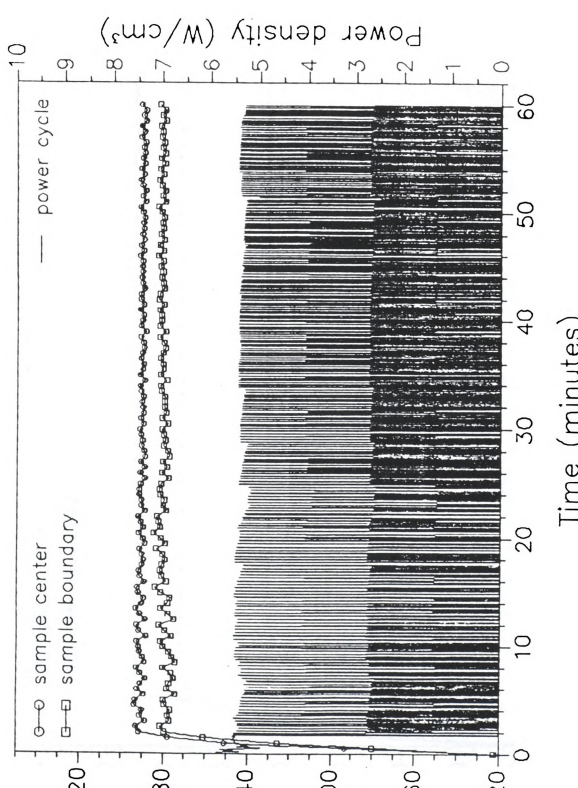

Figure 5.5: Temperature-time profiles during controlled pulsed microwave curing of DER 332/DDS resins

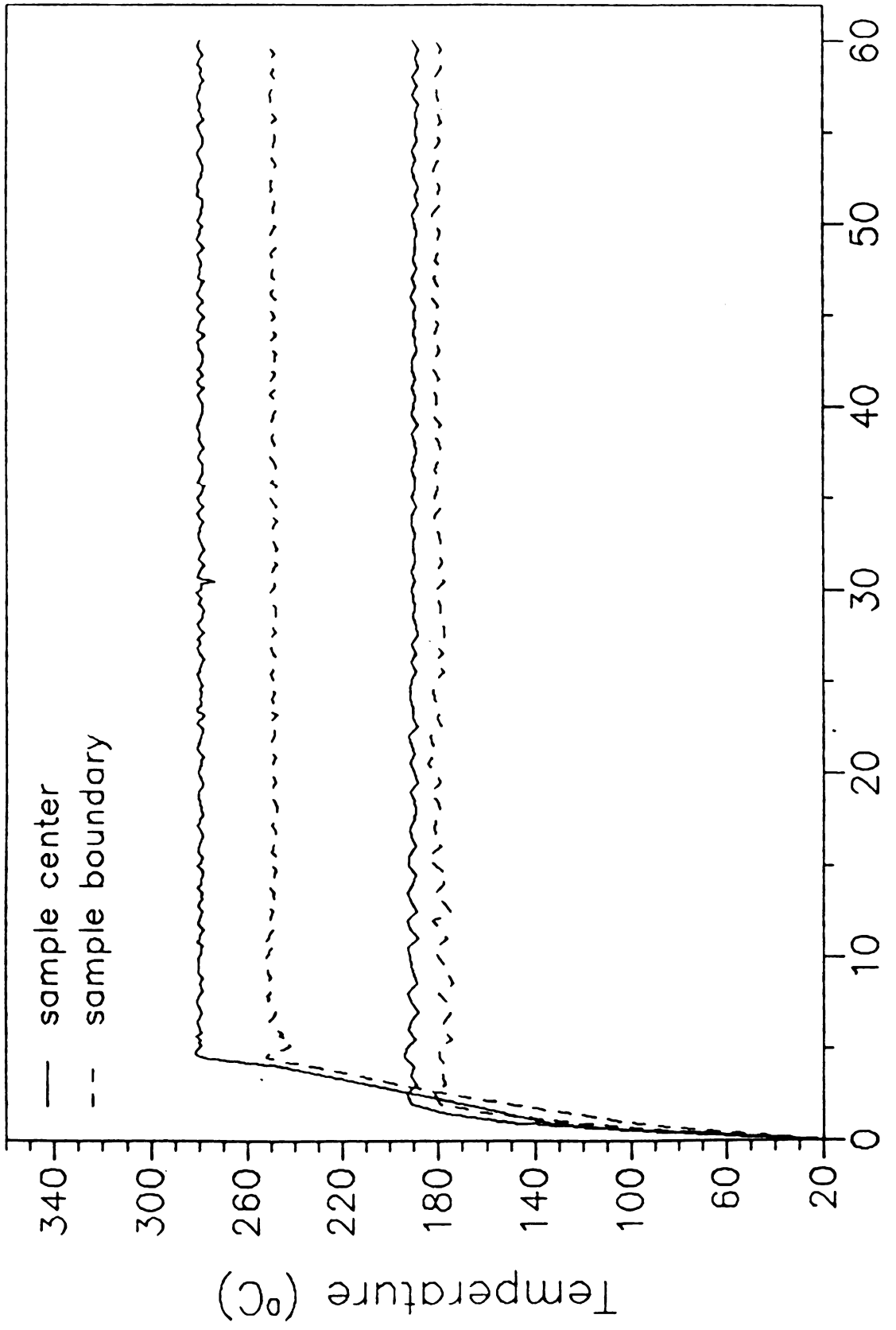

Figure 5.6: Temperature-time profiles during controlled pulsed curing of DER 332/DDS resins at 190 and 280 °C cure

is due to the greater boundary heat transfer at a higher cure temperature for the microwave processing. The controlled pulsed microwave cure experiment at the temperature of 280 °C was successfully performed without thermal degradation of the cured samples. On the other hand, an epoxy/amine sample was thermally cured at an oven temperature of 240 °C for 60 minutes. Thermal degradation occurred in this thermally cured sample due to occurrence of the maximum exothermic temperature greater than 300 °C during the cure process.

5.3.2 On-line diagnostic measurements

Temperature and dielectric loss factor measurements of the stoichiometric mixture of DER 332 and DDS were made using this computer-controlled pulsed processing and diagnostic cavity at 2.45 GHz. Measurements of sample temperature, dielectric loss factor, and power input density during the controlled pulsed microwave curing of the resin are shown in Figure 5.7. Dielectric loss factors can be measured when the power is on during the pulsed power processing. The dielectric loss factor increases with increasing temperature and decreases as the cure proceeds. Dielectric loss data of this epoxy/amine mixture as a function of temperature and extent of cure at 2.45 GHz have been obtained previously [6]. Measurements of dielectric loss factor and temperature can be used to predict the extent of cure and to monitor the cure process during the microwave processing [6]. However, a model of dielectric loss factor as a function of extent of cure and temperature at a given frequency needs to be developed.

Dielectric loss factor and temperature measurements were also made during microwave heating of pure epoxy at 2.45 GHz. This experiment was

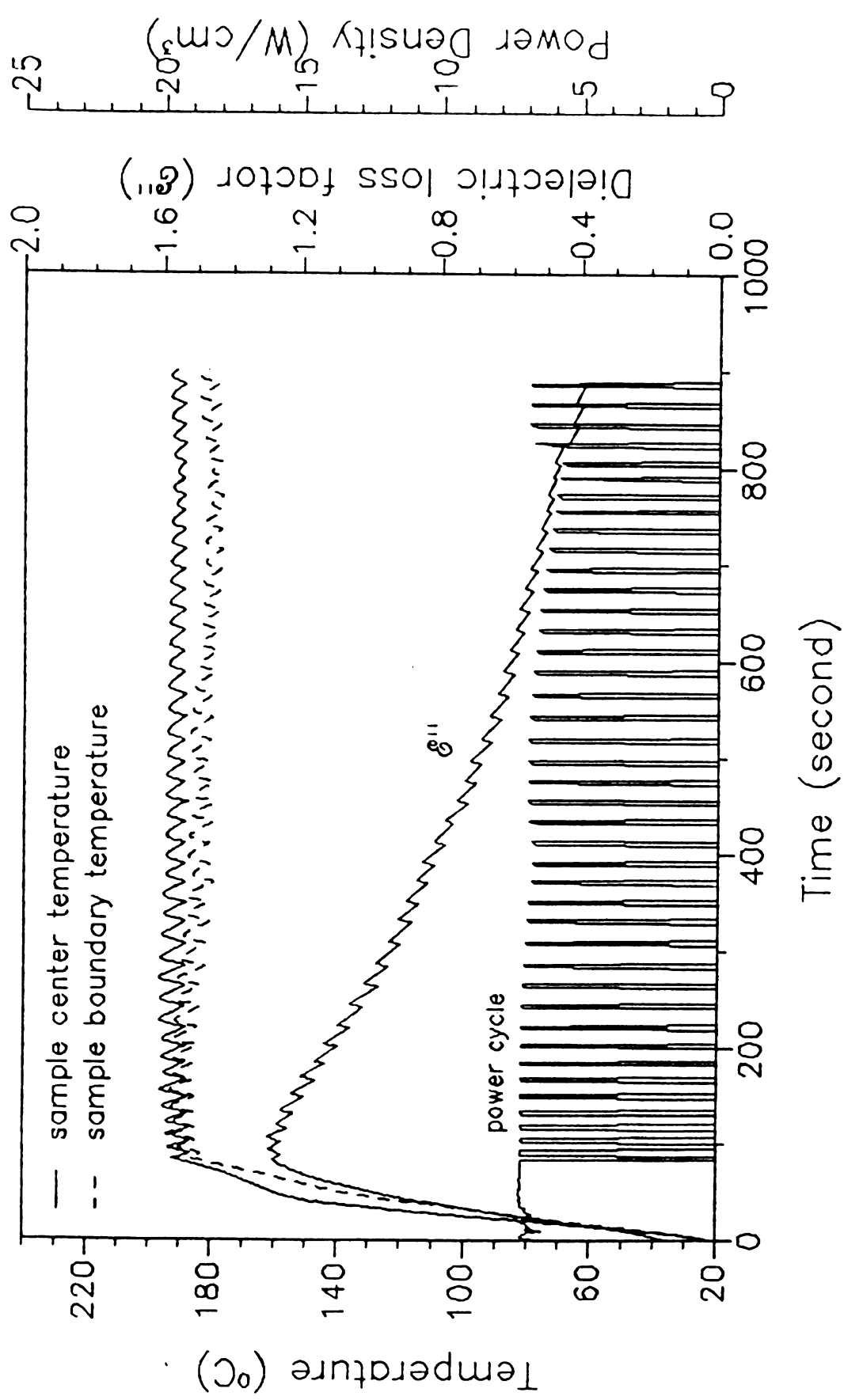

Figure 5.7: On-line measurements of temperature, dielectric loss factor, and input power density during pulsed microwave curing of DER 332/DDS resins

intended to illustrate the temperature-dependence of the dielectric loss factor of pure epoxy at 2.45 GHz. Dielectric loss factors versus temperature and average temperature between the sample center and boundary are shown in Figure 5.8. Dielectric loss factors of pure epoxy increase with increasing temperature before reaching the maximum loss but decrease thereafter. This is a characteristic of dielectric relaxation. As seen in Figure 5.8, dielectric loss versus temperature spectrum of pure epoxy is asymmetric due to interaction of neighboring dipoles. Again, the temperature difference between the sample center and boundary is significant due to heat transfer at the cold material boundary. Since the bulk value of dielectric loss factor of epoxy is always measured, an effective bulk sample temperature should be estimated in order to present dielectric loss factor versus temperature spectrum accurately during microwave heating.

5.3.3 Effect on cure kinetics

Fresh epoxy/amine samples were electromagnetically cured at three controlled cure temperatures of 190, 240, and 280 °C and thermally cured at an oven temperature of 190 °C. Temperature/time profiles at the boundary of pulsed microwave and thermally cured samples for a processing time of 60 minutes are shown in Figure 5.9. Extents of cure at the boundary parts of these cured samples versus the curing time are shown in Figure 5.10. The temperature/time profiles indicate that the resins are heated faster using microwave energy than using thermal energy. However, the extent of cure for the pulsed microwave cure at 240 °C is lower than that for the thermal cure at 190 °C. A decrease in the reaction rate using pulsed microwave energy suggests the possibility

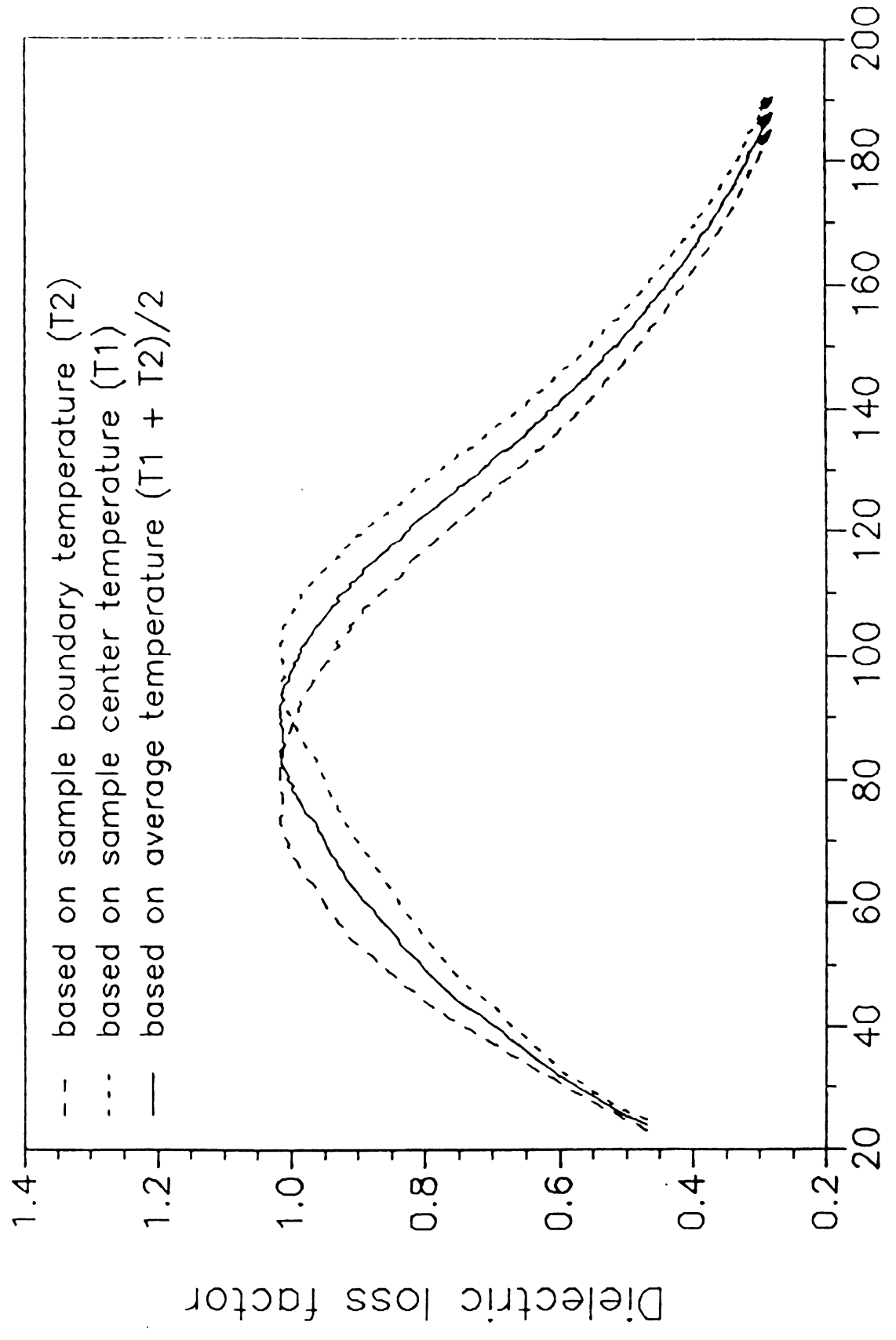

Figure 5.8: Dielectric loss factor versus temperatures of pure DER 332 at 2.45 GHz

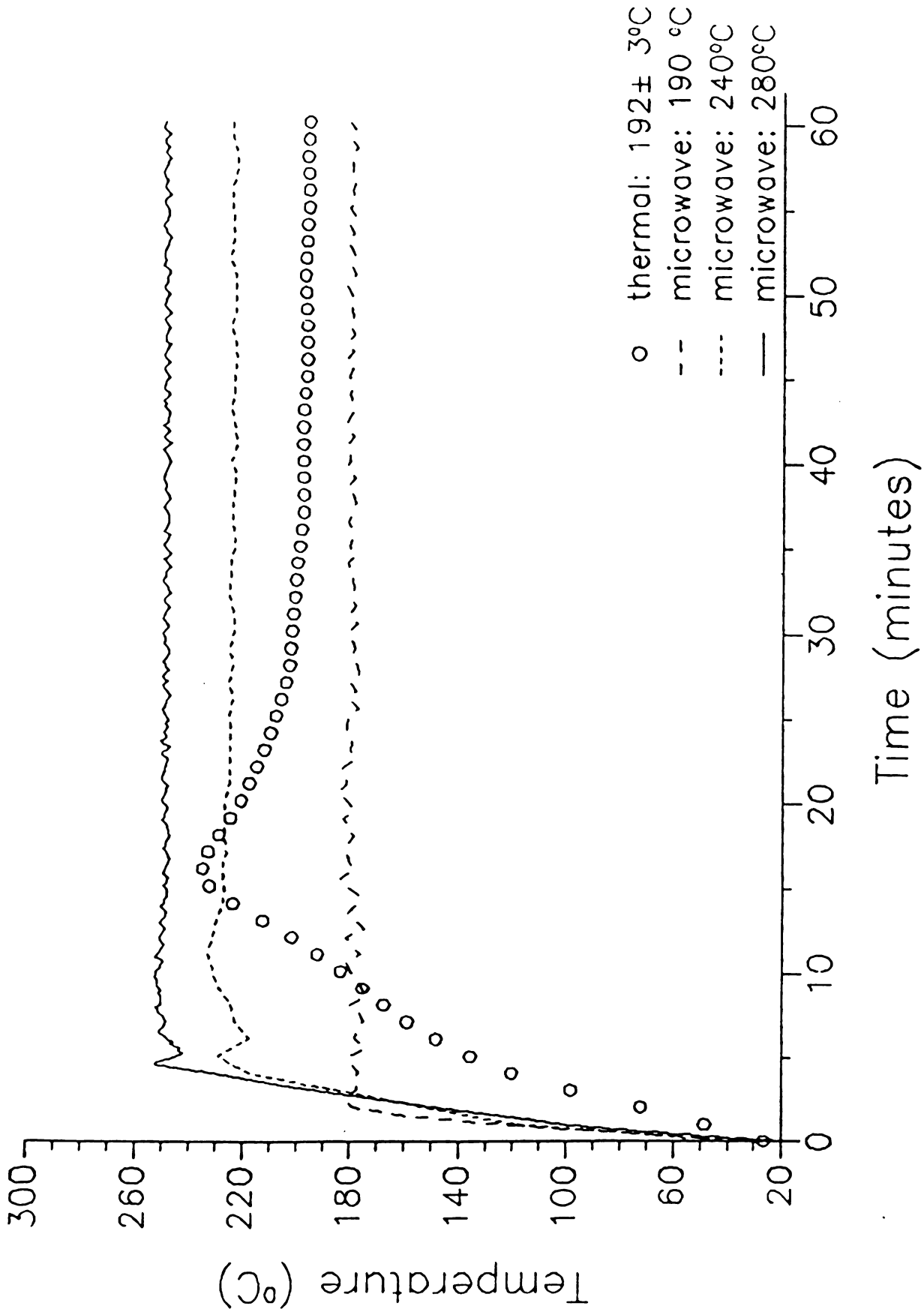

Figure 5.9: Temperature-time profiles for thermal and pulsed microwave curing of DER 332/DDS resins

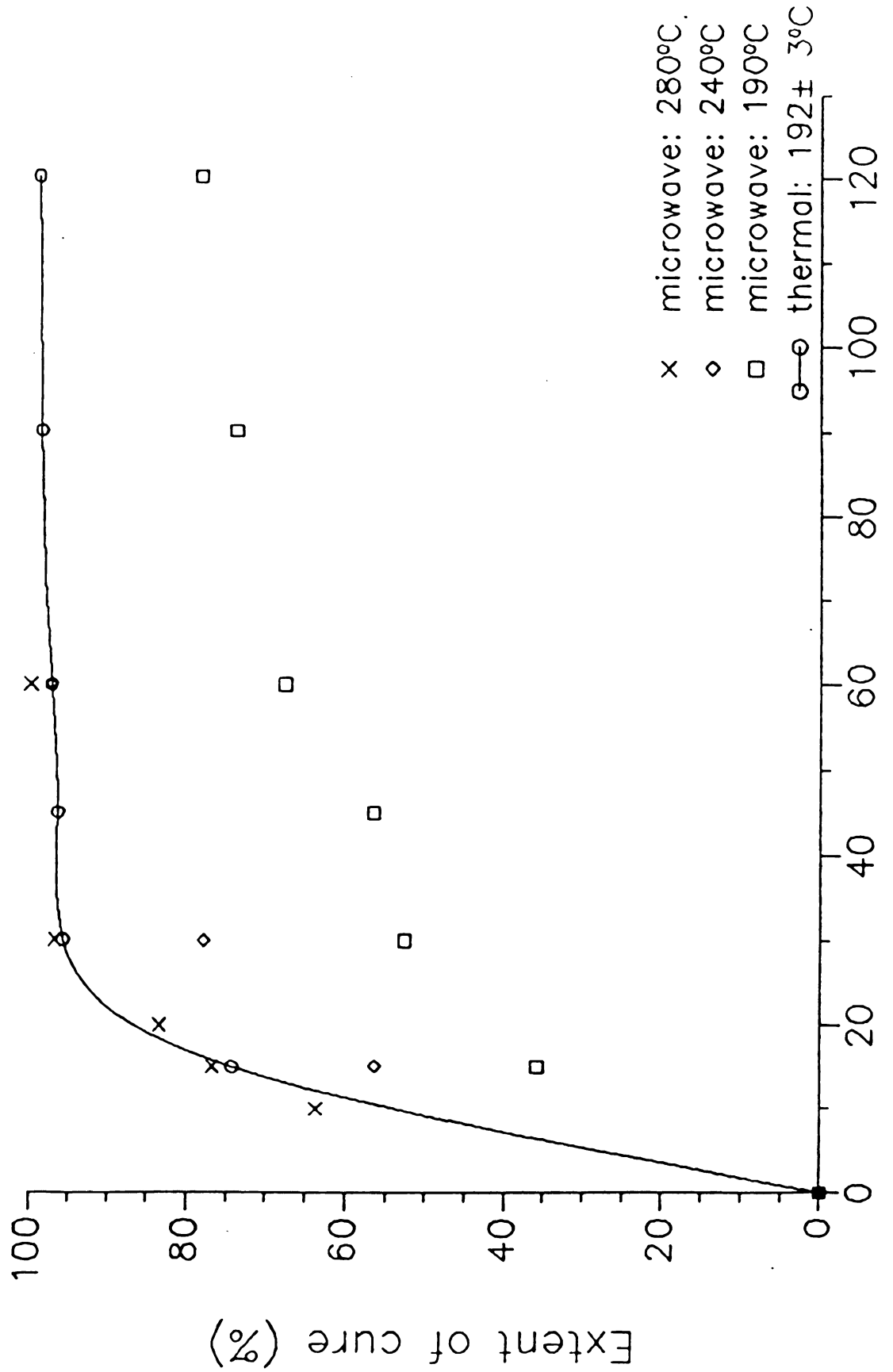

Figure 5.10: Extent of cure versus time for thermal and pulsed microwave curing of DER 332/DDS resins

that the entropy of the resin is decreased due to an increasing alignment of reactive polar groups in response to the electromagnetic field. However, higher cure temperature can be achieved using this controlled pulsed microwave heating in order to compensate for the slow reaction rate.

5.3.4 Effect on glass transition temperature

Glass transition temperatures of thermally and pulsed microwave cured samples were also determined using DSC. The samples were scanned in the DSC pans at a heating rate of 20 °C/min from 30 to 400 °C. Glass transition temperature (Tg) was defined as the inflection temperature of a step transition change on the DSC thermograph close to the residual exothermic peak. An example of glass transition temperature on the DSC thermograph for thermally and pulsed microwave cured samples at the extent of cure of 74% is shown in Figures 5.11 and 5.12, respectively. For thermally cured samples, glass transition temperature can be easily determined [57,58]. The glass transition temperature of 97.68 °C for 74% thermally cured samples was determined and shown in Figure 5.11. However, the transition changes on the DSC thermographs of these pulsed microwave cured samples were not so clear as thermally cured ones. The glass transition temperature of 137.82 °C for 74% pulsed microwave cured samples was determined and shown in Figure 5.12. The broad and slight decrease of heat flow on the DSC thermographs of pulsed microwave cured samples suggests that local molecular transitions caused by motions of groups of atoms in branches or at the ends may exceed a glass transition caused by the structural change. Data of glass transition temperature versus extent of cure for those thermally and pulsed microwave cured

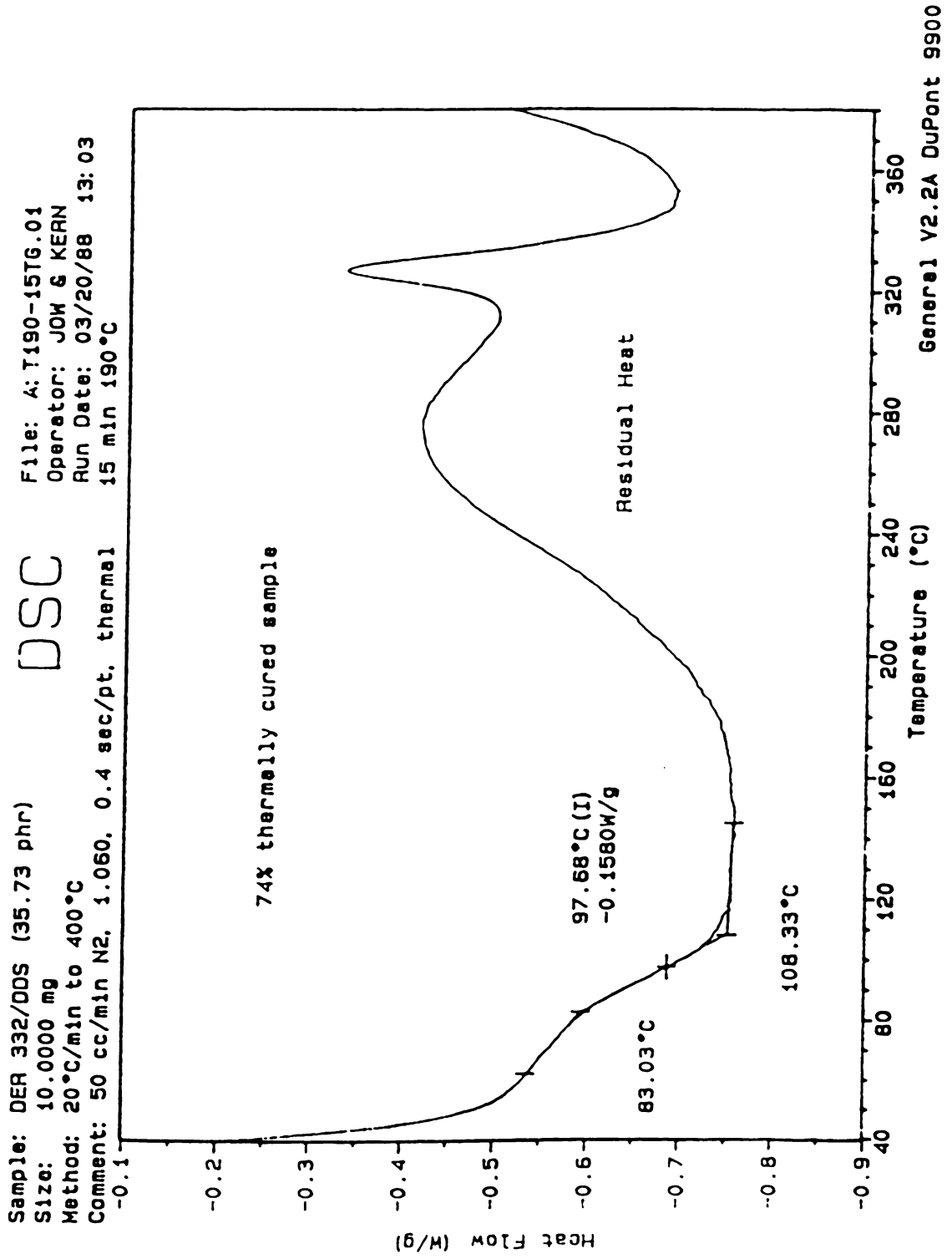

Figure 5.11: DSC thermograph of thermally cured DER 332/DDS resins

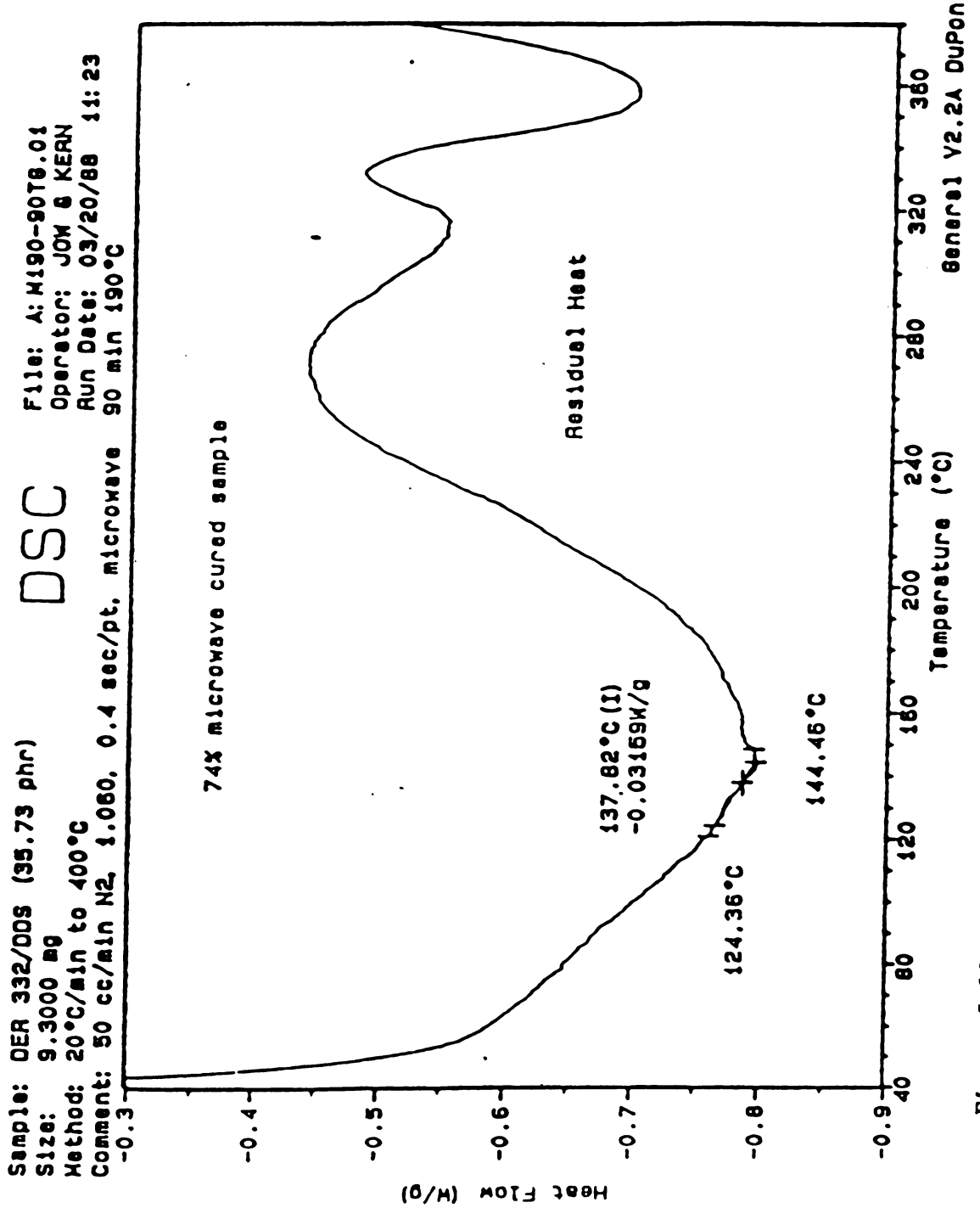

Figure 5.12: DSC thermograph of pulsed microwave cured DER 332/DDS resins

samples along with the literature results of thermally cured samples are shown in Figure 5.13, assuming that glass transition of pulsed microwave cured samples is defined at the inflection point of the small step change next to the residual heat peak. A significant increase in glass transition temperature is observed for pulsed microwave cured samples when compared with those thermally cured samples. However, glass transition temperatures of continuous microwave cured samples determined using TMA have been found to be slightly lower than those of thermally cured samples using DSC at the equivalent extent of cure [59]. The differences in Tg determination techniques, sample temperature/time profiles, microwave heating modes, sample shapes, and sample molds between pulsed and continuous microwave experiments have been extensively discussed by Singer [59]. The increase in Tg for pulsed microwave cured samples but the decrease for continuous microwave cured samples is not fully understood. This difference may be due to Tg interpretation, sample temperature/time history, and different cure kinetics and network formation between pulsed and continuous microwave cured samples. Since the step transition of pulsed microwave cured samples is different from that of thermally cured samples on the DSC thermograph, different techniques (such as TMA and DMA) are required to verify these glass transition temperature differences between thermally, continuous microwave, and pulsed microwave cured samples.

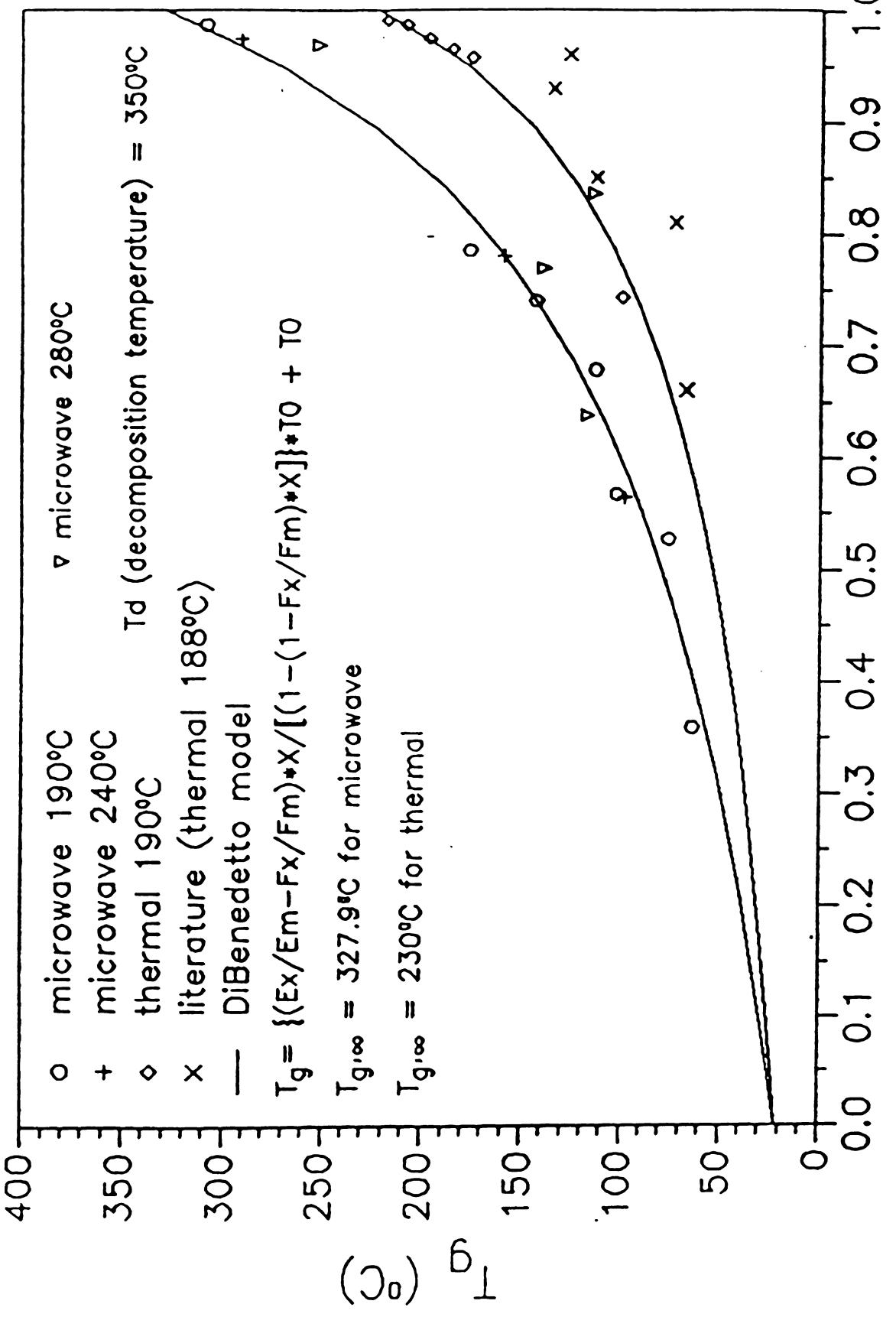

Figure 5.13: Glass transition temperature versus extent of cure for thermally and pulsed microwave cured epoxy/amine resins

5.4 Conclusion

A computer-controlled microwave processing and diagnostic system has been successfully developed and used to eliminate the exothermic temperature peak, maintain the same cure temperature at the end of reaction, and on-line measure dielectric loss factor and temperature during the pulsed power cure process. This work also shows that the controlled pulsed microwave processing is faster and can cure epoxy/amine resins at a higher temperature when compared with the continuous microwave or thermal processing. However, pulsed microwave curing time is longer than thermal curing time. The slow reaction rate using pulsed microwave energy can be compensated at a higher cure temperature. The glass transition temperatures on the DSC thermographs of pulsed microwave cured samples are found to be different from those of thermally cured samples. In addition, the temperature gradient inside low thermal conductivity materials is always built up due to the surface heat transfer and internal heat conduction during the microwave processing. Reduction of this temperature gradient is important for the microwave processing of low thermal conductivity materials. This work suggests that a combination of pulsed microwave and thermal processing should be used to heat low thermal conductivity polymers and composites quickly and uniformly.

CHAPTER SIX

PULSED MICROWAVE HEATING OF COMPOSITE MATERIALS

6.1 Introduction

The cure cycle for processing of composite materials is required to maintain uniform temperature inside the composites, and to complete cure in a shorter time. In the case of thermal processing of thermosetting polymeric composites, heat of reaction can produce a significant temperature gradient inside the composites. This temperature gradient can result in internal thermal stresses due to different thermal expansion inside the composites. Curing time using thermal energy is also very long when composites are thick. Therefore, microwave heating is an alternative method to heat composites fast and uniformly. Microwave processing can easily control the material temperature-time profile by pulsing power cycle. A computer-controlled pulsed microwave system has been successfully used to eliminate the exothermic temperature peak, to maintain constant temperature at a given position, and to cure epoxy/amine resins in a shorter time at a higher cure temperature [8]. However, the temperature gradient inside low thermal conductivity materials can be built up due to surface heat loss and slow internal heat conduction.

Microwave heating is dependent on the magnitudes of dielectric loss of constituents in composites. Schematics of heating mechanisms between thermal and microwave heating are illustrated in Figure 6.1. The arrows in Figure 6.1 represent the direction of heat flux. Microwave heating

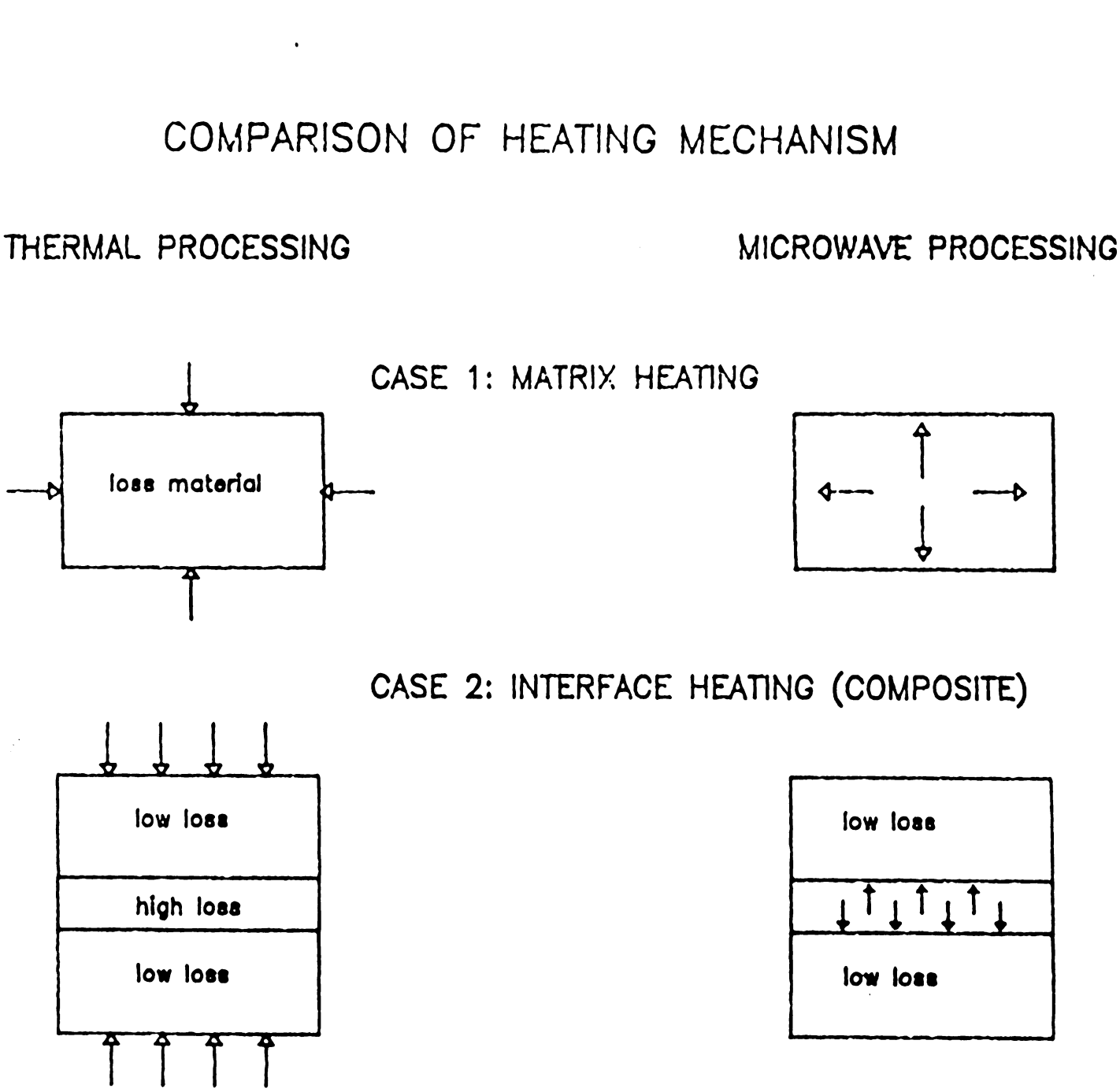

Figure 6.1: Comparison of heating mechanism between thermal and microwave processing

is selective and outward (heating from the hot interior material to the cold boundary). Thermal heating is nonselective and inward (heating from the boundary to the interior material). Selective microwave heating has been used to improve the interfacial bonding between fiber and matrix for the processing of carbon fiber/epoxy composites [53] and to modify the morphology of phase separation and toughening of blended materials [55]. The features between microwave and thermal processing are compared in Table 6.1. The unique features of microwave heating can be very important and critical in the processing of polymeric and composite materials.

The objectives of this chapter are to illustrate the selective microwave heating, to study the possibility of enhancing the boundary temperature using a high lossy sample mold, and to investigate temperature-position-time profiles of epoxy with and without conductive and non-conductive fiber powders using thermal and pulsed microwave heating. A hybrid processing technique of microwave and thermal heating is also developed to heat low thermal conductivity materials quickly and uniformly.

6.2 Experimental

A schematic diagram of the microwave and thermal processing system is shown in Figure 6.2. Microwave processing system aided with computer control and data acquisition has been described previously [1,4]. A cylindrical tunable cavity is resonated in a TM_{012} mode to efficiently couple microwave power into the processed composites at 2.45 GHz. All samples are always located at the center of the cavity. Temperatures of

Table 6.1 Comparison of features between thermal and microwave heating

Thermal Heating	Microwave Heating
* SLOW	* FAST
- Heating time is controlled by heat transfer	- Rapid heating is possible in thick lossy materials
* NONSELECTIVE	* SELECTIVE
- Temperature gradient	- Magnitude of loss factor
* INWARD	* OUTWARD
- Surface driven heating	- heat transfer at the cold material boundary
* NONCONTROLLABLE	* CONTROLLABLE
- Difficult in process control	- Adaptable for process control

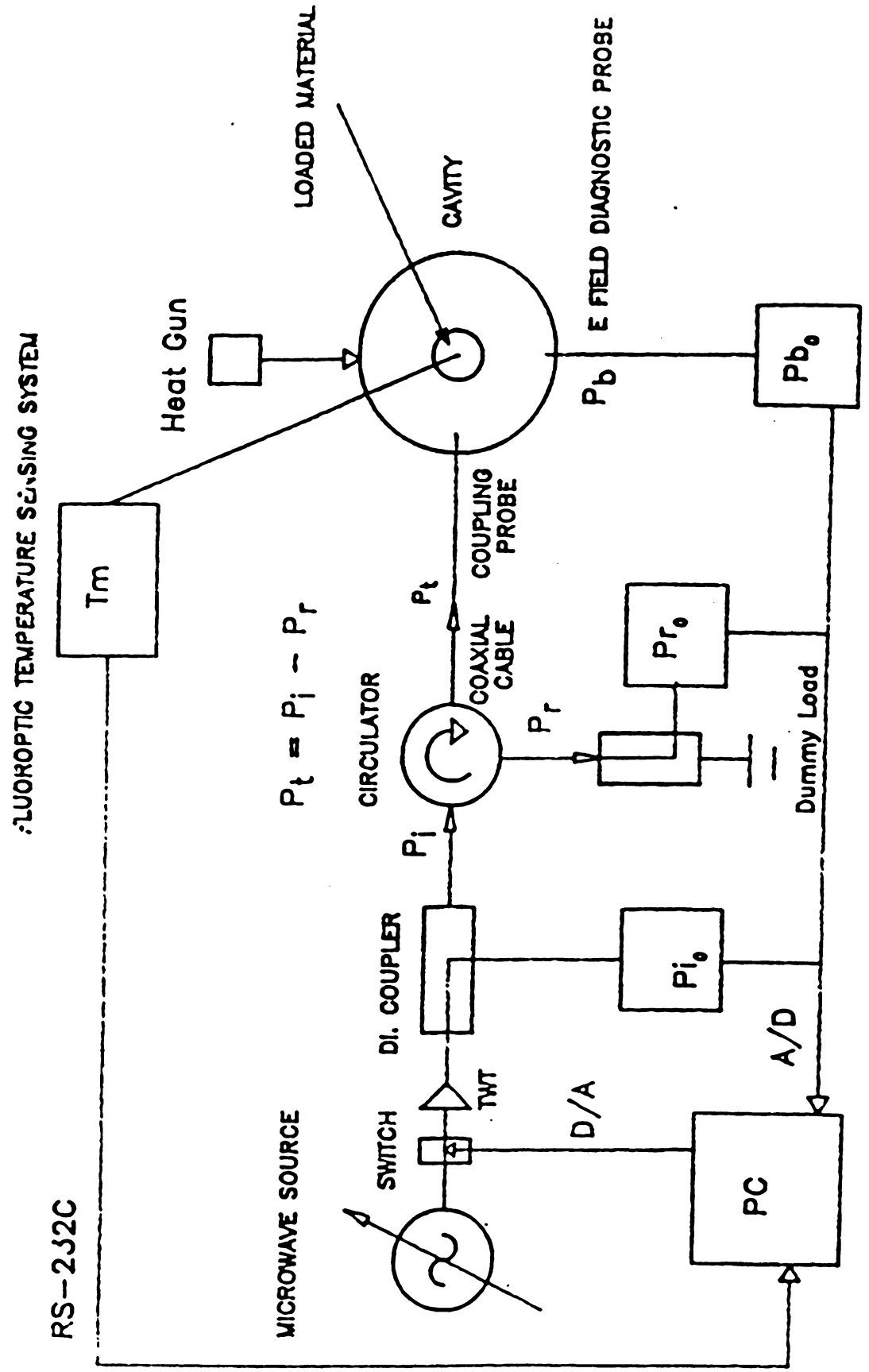

Figure 6.2: Microwave and thermal processing and diagnostic system

the sample are measured using fluoroptic thermometry. A prescribed temperature is selected to process these composites. The microwave power is turned on or off depending upon temperatures of the sample below or above the selected temperature. The hot air generated from a temperature controllable heat gun (Model VT-750B, Master Appliance Corp.) blows into the cavity whenever thermal heating is employed.

Nonreacting and microwave absorbing composites were used in this study. One rodlike graphite/Nylon composite with a length of 40.0 mm was made of a 4.0 mm diameter graphite rod in a Nylon 66 tube with the same inside diameter and thickness of 4.25 mm. This composite rod was used to illustrate selective microwave heating. Another same sized composite rod made of a Nylon 66 rod in a graphite tube was used to study the possibility of enhancing the material boundary by using a high lossy graphite as the sample mold. Epoxy composites were also prepared by well mixing liquid DGEBA epoxy (DER 332) with approximately 50% by weight finely ground AS4 graphite or glass fiber powders. A teflon holder (3/8" i.d., 1.5" long, and 1/16" thick) was used to contain these liquid composites. Epoxy composites were used to study temperature gradients inside epoxy with conductive and nonconductive additives under microwave radiation.

6.3 Results and Discussion

Rodlike composites of graphite/Nylon were electromagnetically heated in this controlled pulsed microwave resonant cavity. Temperatures at the interface and each constituent were measured during microwave heating. Temperature/time/position profiles during microwave

heating of the graphite rod in the Nylon tube are shown in Figure 6.3. Dielectric loss factors measured by the swept frequency perturbation method are 0.9 for graphite and 0.028 for Nylon at 25 °C and 2.45 GHz. Dielectric loss factor of graphite is fairly independent of temperature but dielectric loss factor of Nylon 66 significantly increases with increasing temperature before reaching the maximum loss [10]. The temperature in graphite is much higher than that in Nylon 66 during the entire microwave heating as shown in Figure 6.3. This illustrates that microwave heating is strongly selective in a manner dependent upon the magnitude of dielectric loss. However, a temperature gradient between the interface and Nylon is significant due to heat transfer at the cold boundary and slow internal heat conduction. Therefore, the use of a higher lossy material as a sample mold can enhance the material boundary temperature and reduce the temperature gradient during microwave heating of low thermal conductivity materials. Temperature/time/position profiles during microwave heating of a Nylon rod using graphite as a sample mold are shown in Figure 6.4. Figure 6.4 indicates that the high lossy graphite sample mold can enhance the boundary temperature of the Nylon rod so that the temperature gradient inside the Nylon rod is reduced during microwave heating.

Pure epoxy resins and epoxy resins with 50% by weight ground glass or graphite powders were heated using controlled pulsed microwave power. Temperatures at the center and boundary of the samples were measured. Temperature/time profiles of epoxy with and without glass are shown in Figure 6.5. Results indicate that the addition of the glass fiber has no effect on the temperature gradient and temperature/time profiles due to similar thermal conductivity of the constituents (1.04 W/m °C for glass and 0.21 W/m °C for epoxy). Temperature gradients are always

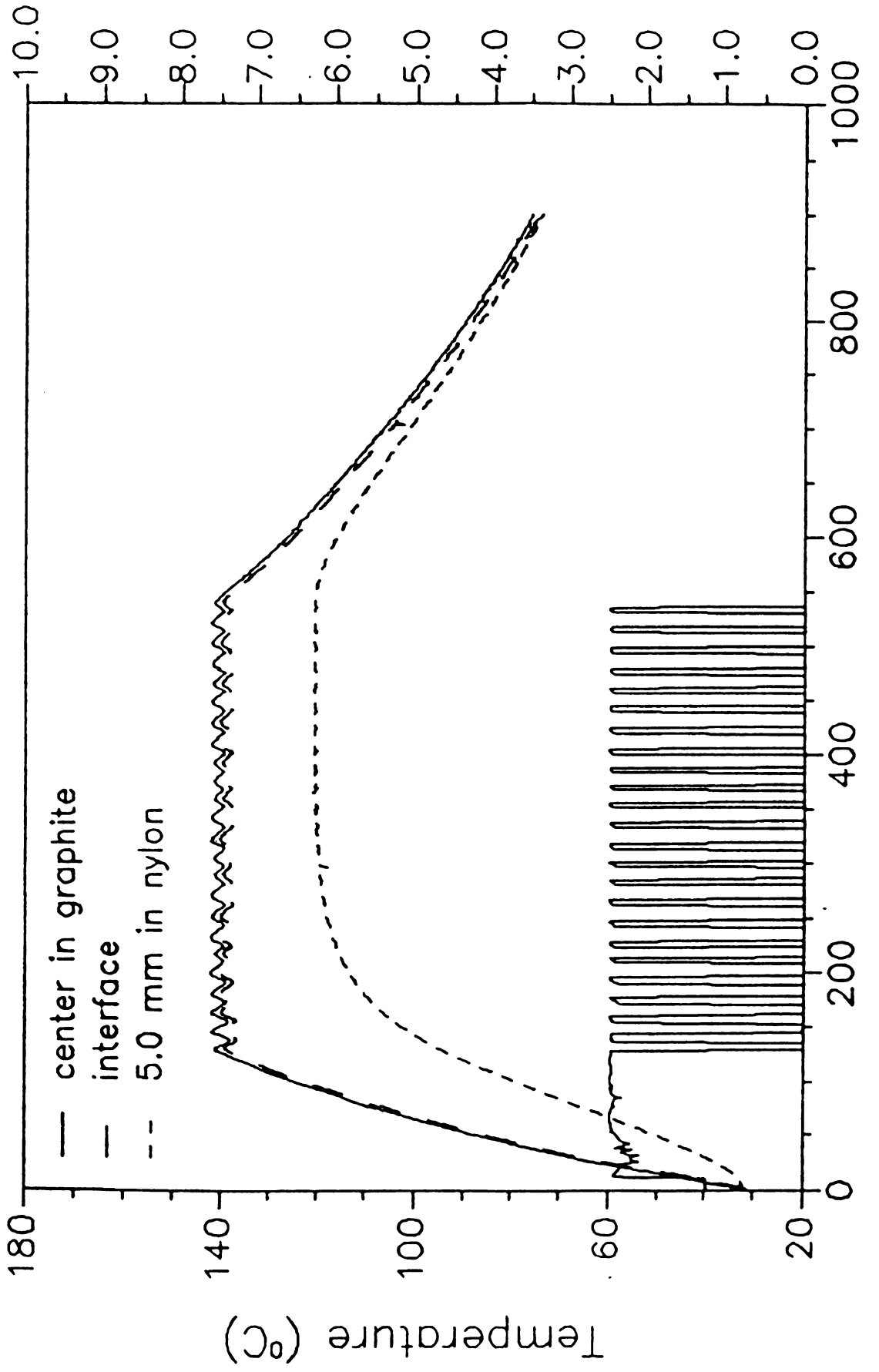

Figure 6.3: Temperature-time profiles during microwave heating of graphite in Nylon 66 rod

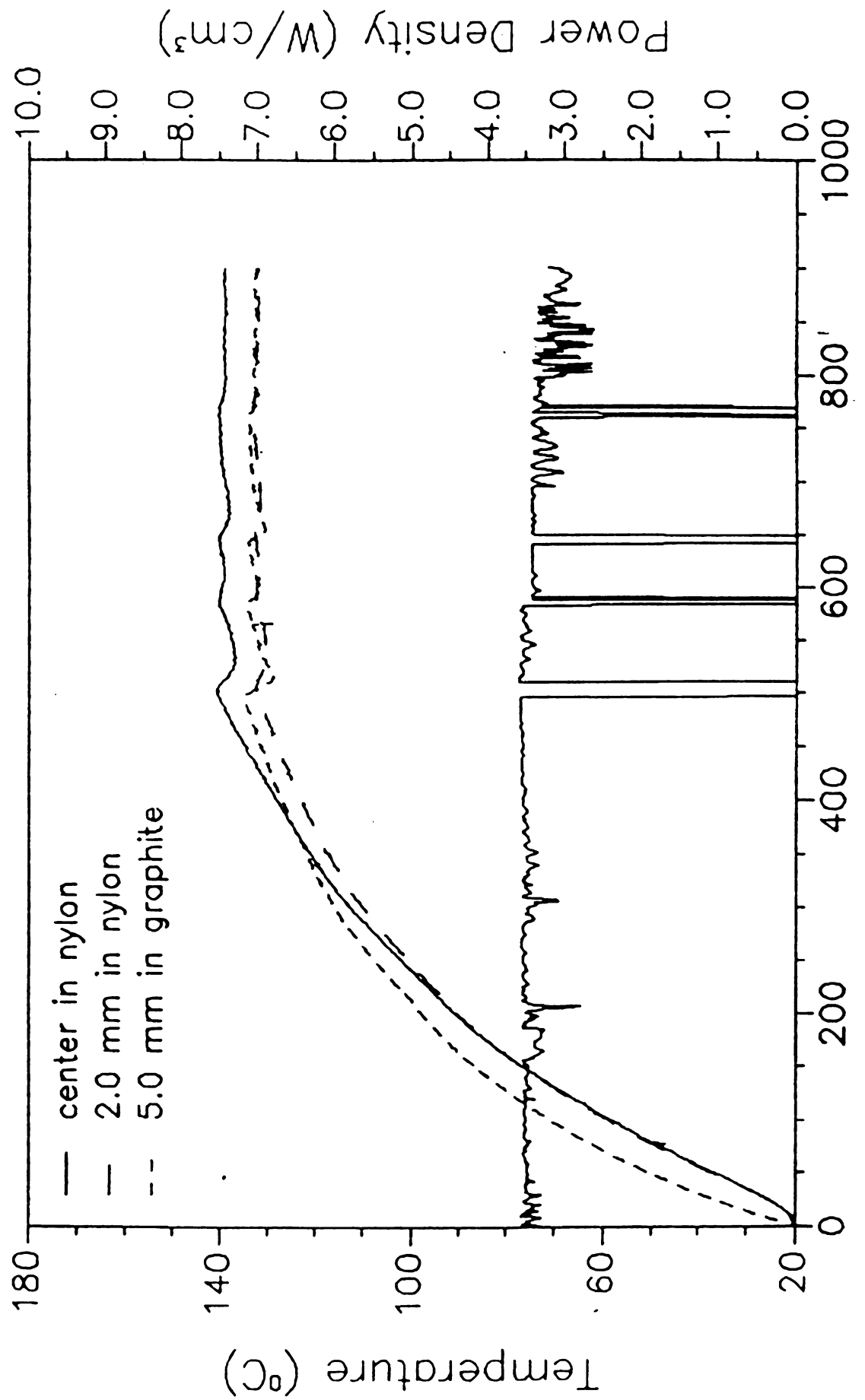

Figure 6.4: Temperature-time profiles during microwave heating of Nylon 66 in graphite rod

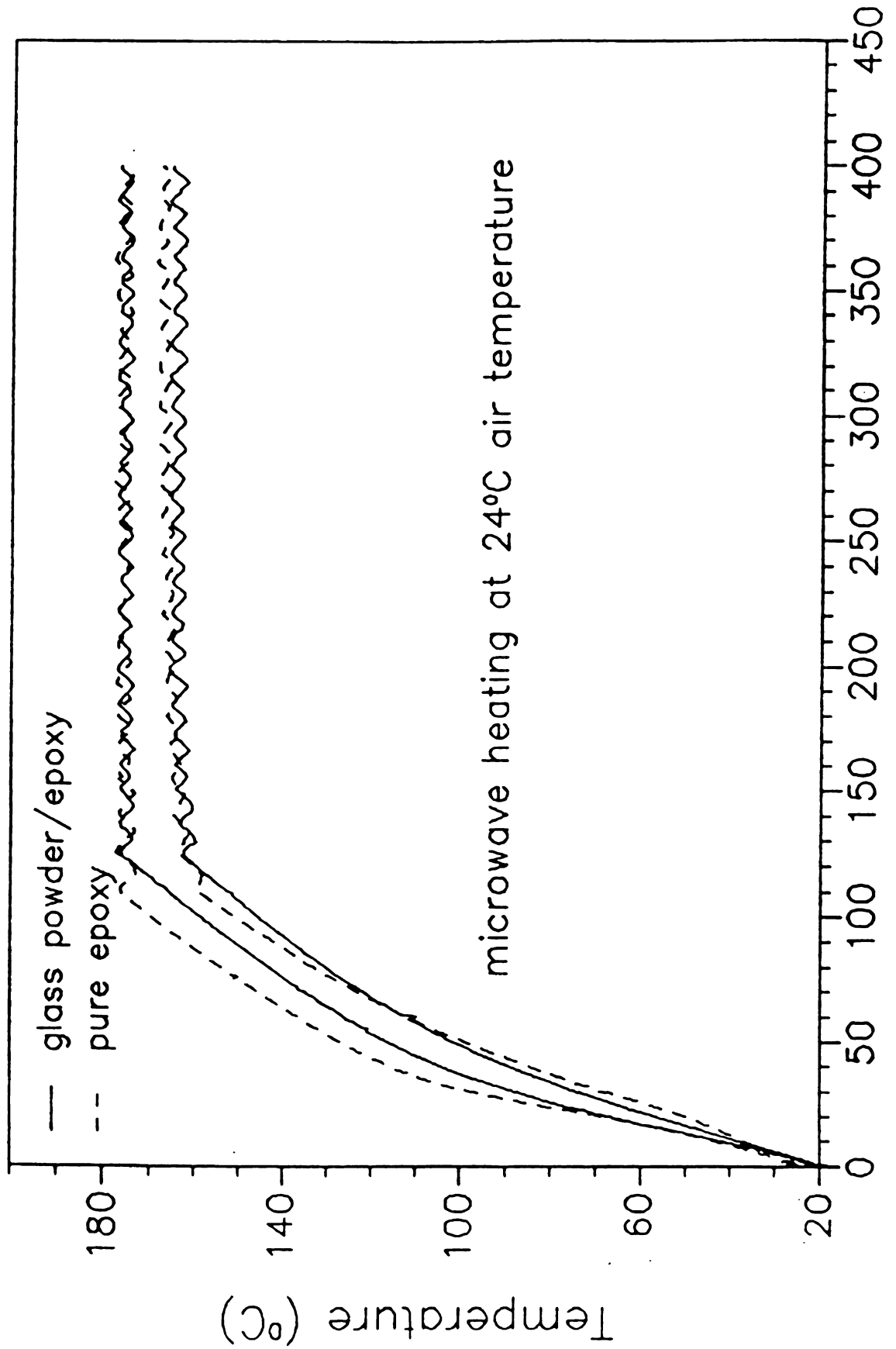

Figure 6.5: Temperature-time profiles for microwave heating of epoxy with and without glass fiber powders

built up due to heat transfer at the boundary and slow heat conduction [10]. Temperature/time profiles of epoxy with and without graphite fiber are shown in Figure 6.6. A reduction in the temperature gradient is found due to improvement of thermal conductivity (graphite, 105 W/m °C). However, a fluctuation in the boundary temperature of the epoxy/graphite samples occurs due to a lag time in the microwave on-off pulsed power cycle. This fluctuation can be reduced by adding a PID power control element in this microwave system circuit.

Pure epoxy resins were thermally and microwave heated. Temperature-time profiles at the center and boundary of epoxy during thermal and microwave heating are compared in Figure 6.7. Temperature at the sample center is higher than that at the boundary during microwave heating but is lower during thermal heating. Figure 6.7 indicates that microwave heating is outward due to surface heat loss and thermal heating is inward due to surface driven heating. The temperature gradient is greater in the early stage of thermal heating, gradually reduced, and eventually negligible. However, a temperature gradient is always built up and maintained during microwave heating of low thermal conductivity materials. Therefore, combination of microwave and thermal processing is a practical method to fast and uniformly heat low thermal conductivity materials such as epoxy and epoxy with nonconductive reinforced additives. Pure epoxy was heated in a combined microwave and thermal processing. Temperature/time profiles during the hybrid mode and thermal process are shown in Figure 6.8. For the hybrid mode, microwaves quickly heated the epoxy up to the prescribed temperature and were turned off. Thermal heating reduced the temperature gradient built up during microwave heating. Figure 6.8

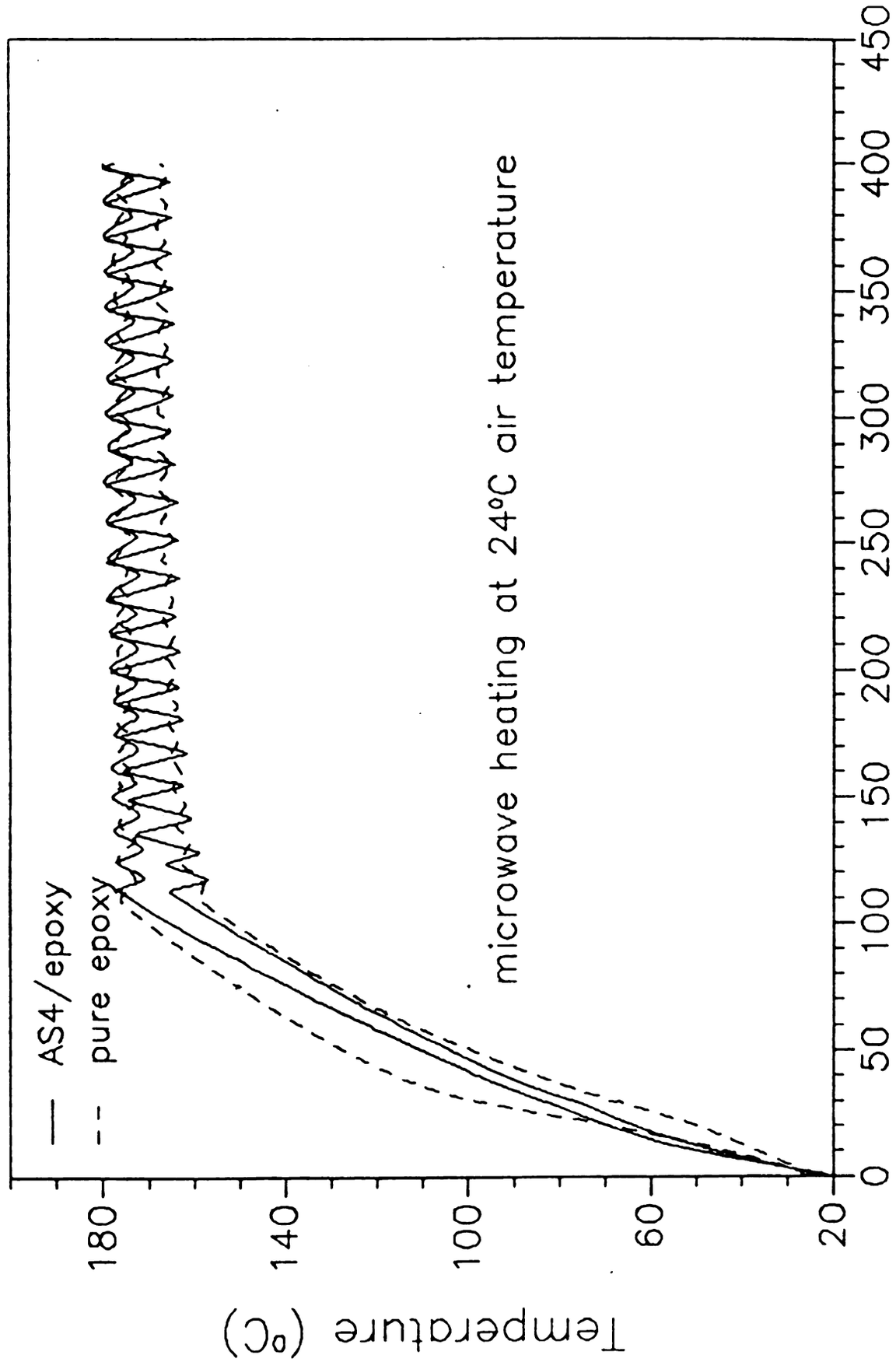

Figure 6.6: Temperature-time profiles for microwave heating of epoxy with and without graphite fiber powders

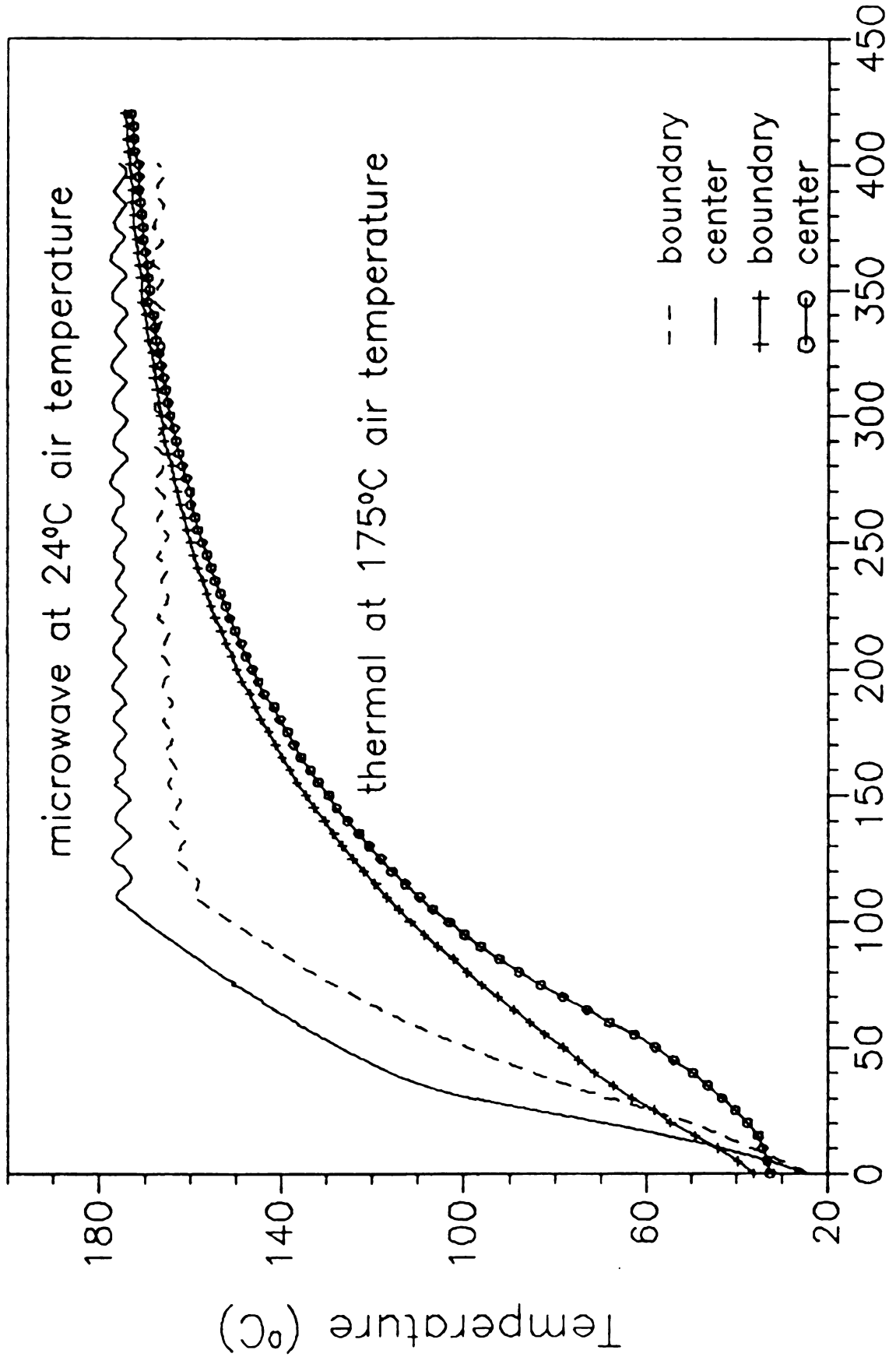

Figure 6.7: Temperature-time profiles for thermal and microwave heating of epoxy

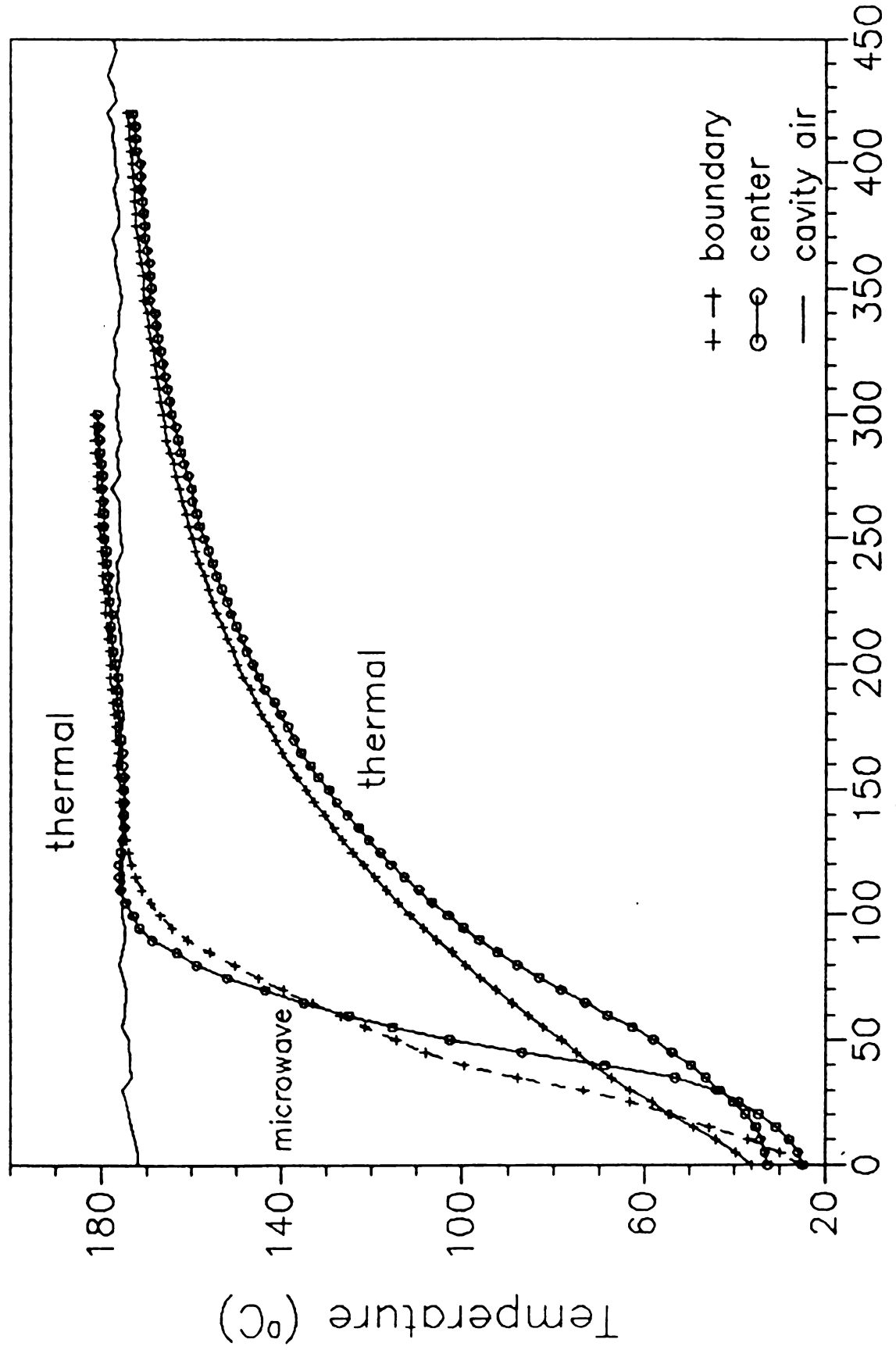

Figure 6.8: Temperature-time for thermal and the combined microwave and thermal heating of epoxy

indicates that the hybrid microwave/thermal processing can fast and uniformly heat thick materials with low thermal conductivity.

6.4 Conclusion

Microwave heating is fast, selective, and outward but not necessarily uniform for low thermal conductivity materials. The high thermal conductivity materials are usually lossy materials due to high electric conductivity. Microwaves can uniformly heat the highly conductive composites in a shorter time. However, for processing of low thermal conductivity composites, a hybrid mode of microwave and thermal processing should be used to heat the composites uniformly and quickly. Otherwise, a high lossy sample mold can be used to enhance the boundary temperature and reduce the temperature gradient during microwave processing of low thermal conductivity materials.

CHAPTER SEVEN

MICROWAVE POWER ABSORPTION AND HEATING CHARACTERISTICS

7.1 Introduction

Microwave heating of polymers has been extensively studied [32-36]. These experiments indicate that direct and fast heating can be accomplished using microwave energy. However, the change in the material dielectric loss during microwave heating causes impedance mismatch between the microwave circuit and the loaded material. This mismatch can reduce the power absorption efficiency and cause the control of the material temperature-time profile to be complex. The manifestation of this phenomena during microwave heating is discussed [60,61]. Three major factors which can cause non-uniform temperature distribution inside microwave heated materials are: (1) non-uniform electric fields, (2) low thermal conductivity of the absorbing material and heat transfer at the material boundary, and (3) variations of heating rate due to the changes in the dielectric loss characteristics within the material. The microwave energy absorption of the material is directly proportional to dielectric loss factor, the operating frequency, and the square of the electric field strength inside the material. The dielectric loss factor of materials depends on temperature, pressure, frequency, material structure and composition for liquid and solid materials. For a dielectric material at constant pressure and frequency, dielectric loss factor increases with increasing temperature before reaching the maximum dielectric loss but decreases

after passing through the maximum. However, the electric field strength in a microwave loaded cavity is always reduced as the dielectric loss factor of the loaded material increases. Heat transfer from the microwave heated material to the surroundings can build up the temperature gradient inside the material due to slow heat conduction during the course of microwave heating. Variation in the temperature-position profile causes a gradient in dielectric loss factor and field strength, thus producing different microwave heating rates at varying locations inside the material. These differences in heating rates accentuate temperature gradients inside the material. Therefore, relating microwave heating and power absorption of materials with heat transfer at the surface and heat conduction within the material is a highly nonlinear problem.

Nylon 66, a nonreacting and microwave absorbing polymer, was used in this study. Dielectric loss factor of Nylon 66 versus temperature was measured and characterized using a three-parameter dielectric relaxation model. The relative electric field strength inside the sample versus the material loss factor was also determined and characterized using a two-parameter model in a TM_{012}-mode resonant cavity. A small Nylon rod was loaded in a uniform electric field region of this resonant cavity. The nonuniform temperature distribution and the power absorption inside the low thermal conductivity rod are studied during microwave heating. Potential methods of obtaining uniform microwave heating are also described and discussed in this chapter.

7.2 Experimental

7.2.1 Apparatus

The microwave processing and diagnostic system along with the temperature sensing system is shown in Figure 2.1. An "internal-tunable" cylindrical cavity (7.62 cm in radius) is operated in a TM_{012} mode and resonated with an external microwave circuit at a single frequency of 2.45 GHz. A coupling probe is used to transfer the electromagnetic wave from a TEM-mode transmission line to this TM_{012}-mode cavity. The resonance at 2.45 GHz between the TM_{012}-mode cavity and the external circuit is always accomplished by adjusting the coupling probe depth L_p and the cavity length L_c so that the reflected power P_{r0} is negligible when compared with the incident power P_{i0}. A small E-field diagnostic probe located at the position of maximum magnitude of the TM_{012} radial wave is used to measure the power P_{b0} which is proportional to the square of the radial electric field strength inside the cavity ($P_{b0} = K_b |E_r|^2$). A fluoroptic temperature sensing system (Luxtron 750) with four sensor channels is used to measure temperatures of the material, the cavity wall, and the air inside the cavity. The detailed experimental system has been described earlier [1,4].

7.2.2 Materials

A nonreacting and microwave absorbing polymer used to study microwave power absorption and heating characteristics was Nylon 66, provided by Cadillac Plastics Co. The small size of Nylon rod (0.635 cm in radius and 4.0 cm in length) was selected so that determination of

dielectric loss factor using material-cavity perturbation theory is valid [2,4]. In this work, dielectric loss factor of Nylon 66 as a function of temperature at 2.45 GHz was measured and subsequently characterized using a Debye dielectric relaxation model.

7.2.3 Experimental methods

Temperature and dielectric loss factor were measured during thermal heating of Nylon 66 using the swept frequency method in order to determine the relationship between temperature and dielectric loss factor at 2.45 GHz. Dynamic and steady-state microwave heating experiments using Nylon rods suspended in a uniform electric field region of the TM_{012}-mode resonant cavity at 2.45 GHz were carried out. These microwave heating experiments were intended to show the dielectric loss dependence upon the electric field strength and the nature of non-uniform heating due to the boundary heat transfer and the slow internal heat conduction.

The Nylon rod was thermally heated and its dielectric loss factor measured using the swept frequency method with a low-power diagnostic cavity at 2.45 GHz [2]. Temperature measurements during heating were made using the fluoroptic temperature sensing system. The rod was loaded into this cavity and thermally heated using hot air. Hot air generated from a heating gun was blown into the cavity in order to maintain the temperature difference between the center and the boundary of the sample at a level less than 2 °C. Thus, the rod was maintained at an essentially uniform temperature during this thermal heating experiment.

In microwave heating experiments, small samples were always located in the position of the strongest electric field at the center of the

TM_{012}-mode resonant cavity as shown in Figure 2.4. The axial TM_{012}-mode electric field varied by less than one percent in the radial direction inside the sample and was therefore considered as essentially uniform. The maximum ratio of the square of the radial electric field strength to the axial electric field strength is much less than one percent. Therefore, the radial electric field inside the rod is also negligible. In the dynamic microwave heating experiment, on-line measurements of dielectric loss factors, temperatures, and power levels were made as Nylon 66 was heated in this cavity at an input power level of 5.0 W at 2.45 GHz. The same measurements were made in the steady-state experiments at several different input power levels of 1.0, 2.0, 3.0, 4.0, and 5.0 W. Dielectric loss factors were determined using material-cavity perturbation theory with a single frequency method [2].

7.3 Modeling on Microwave Heating

7.3.1 Power absorption model

The microwave power absorption of the material P_m is proportional to dielectric loss factor ϵ'', the angular frequency ω ($2\pi f_o$), and the square of the electric field strength $|E_m|^2$ inside the material. Dielectric loss factor used throughout this chapter is relative to free space permittivity ϵ_o (8.854×10^{-14} farad/cm). Therefore, microwave power absorption per unit volume of the material as a function of dielectric loss factor, frequency f_o, and electric field strength can be described as follows.

$$P_m = 1/2\ \omega\ \epsilon_o\ \epsilon''\ |E_m|^2 = \pi\ f_o\ \epsilon_o\ \epsilon''\ |E_m|^2 \qquad (7.1)$$

Dielectric loss factor of polar liquid and solid materials depends on temperature, frequency, pressure, and material composition and structure. Two most important variables for nonreacting materials in dielectric response are temperature and frequency. An "overall" single dielectric relaxation model proposed by Debye is commonly used to describe the relationship between dielectric loss factor, relaxation time τ, and angular frequency. It is assumed that a single overall dielectric relaxation time exists for all molecular species in the material. Typically, the temperature dependence of this overall relaxation time τ is assumed to be of Arrhenius type with positive temperature factor. This model is given below.

$$\epsilon''(T, \omega) = \epsilon \frac{\omega \tau}{1 + (\omega \tau)^2} \qquad (7.2)$$

where $\tau = k_o \exp(E/RT)$

Three parameters used in this model are the polar oscillation strength ϵ, the activation energy of the dipole motion E, and the pre-exponential factor k_o. The polar oscillation strength ϵ is the difference between the relative relaxed and unrelaxed permittivities. The gas constant is represented by R (1.987 cal/mole/°K). The dielectric loss factor and temperature of the material are ϵ'' and T, respectively. At a constant frequency, dielectric loss of polar materials increases with increasing temperature before reaching the maximum dielectric loss but decreases after passing through the maximum.

The diagnostic power P_{b0} detected by the E-field coaxial probe is proportional to the square of the radial electric field at the cavity wall. Since the loaded cavity always resonates in the TM_{012} mode at

2.45 GHz, an effective coupling coefficient K_p of this diagnostic probe can be defined in this study [62]. Therefore, the square of the axial TM_{012}-mode electric field strength inside the material can be directly related to the diagnostic power and described in Equation 7.3.

$$|E_m|^2 = K_p \quad P_{b0} \tag{7.3}$$

The measured power ratio P_e, which is defined as the ratio of the diagnostic power P_{b0} to the incident power P_{i0}, is proportional to the cavity Q factor [2]. A typical power ratio P_e versus different input power levels for an empty TM_{012}-mode cavity in resonance with the external microwave circuit is shown in Figure 7.1. Since the empty resonant cavity Q factor is constant, the power ratio is constant as shown in Figure 7.1, regardless of input power levels. The relationship between the power ratio and the cavity Q factor for the resonant cavity with and without the sample can be described in Equation 7.4. The power ratio and the cavity Q factor are P_e and Q_s for the loaded resonant cavity, and P_{e0} and Q_0 for the empty resonant cavity.

$$\frac{P_e}{P_{e0}} = \frac{Q_s}{Q_0} \tag{7.4}$$

The loaded cavity Q factor decreases as the dielectric loss factor of the loaded material increases. The relationship between the cavity Q factor and the material dielectric loss factor based on material-cavity perturbation can be described in Equation 7.5 [2]. The dimensionless constants for TM_{012}-mode material-cavity perturbation are A, B, and G. The sample and cavity volumes are V_s and V_c, respectively.

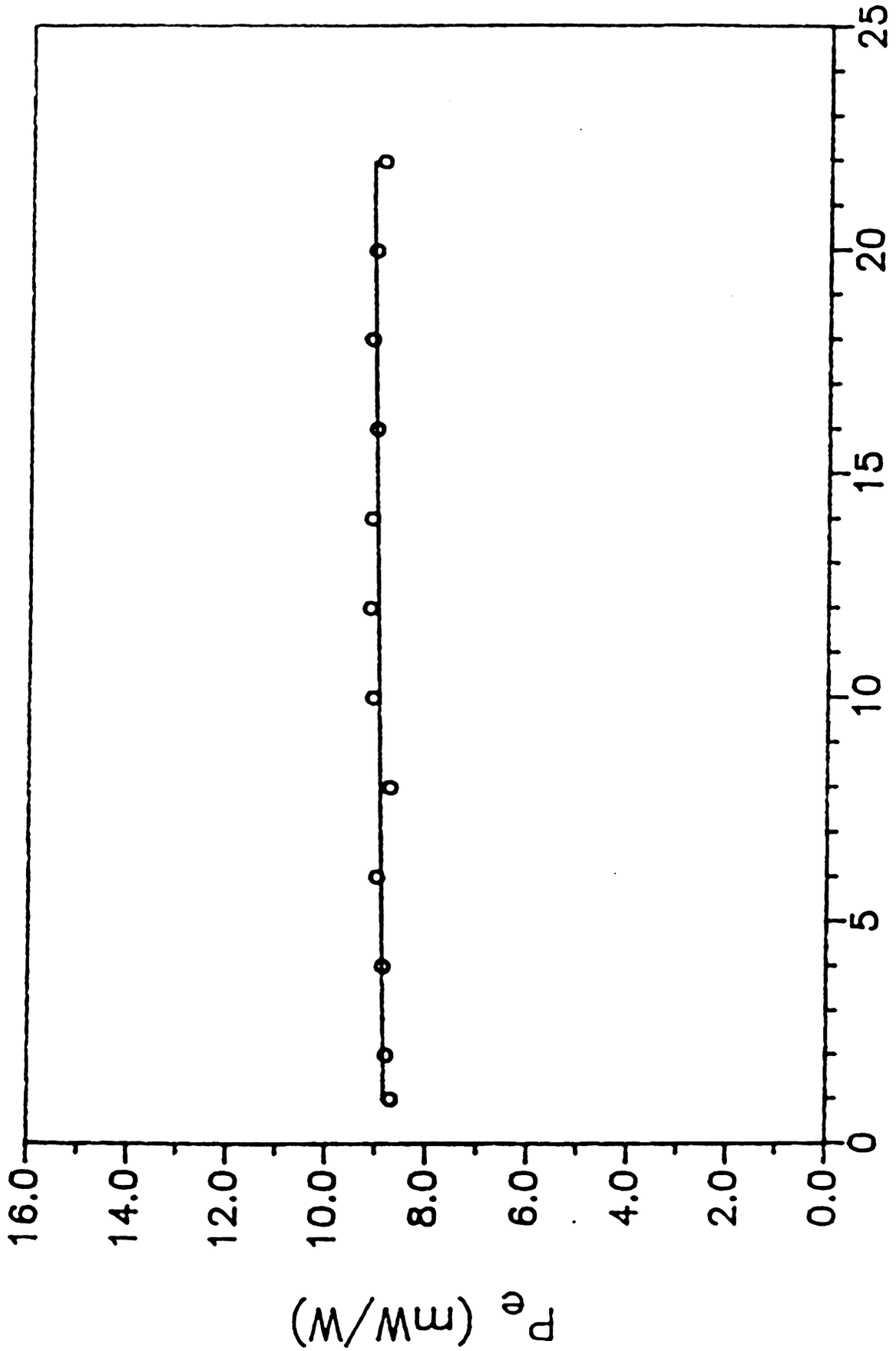

Figure 7.1: Power ratio P_e versus input power P_{io} for an empty cavity resonated with the external microwave circuit in a TM_{012} mode at 2.45 GHz

$$Q_s = \frac{1}{2\ \epsilon''\ ABGV_s/V_c + 1/Q_0} \tag{7.5}$$

Therefore, the power ratio P_e decreases as material dielectric loss increases. The relationship between the power ratio P_e and material dielectric loss factor ϵ'' at a resonant frequency is described as follows.

$$P_e(\epsilon'') = Q_s\ P_{e0}\ /\ Q_0 = (B_1\ \epsilon'' + B_2)^{-1} \tag{7.6}$$

$$\text{where}\quad B_1 = 2ABGV_sQ_0\ (V_cP_{e0})^{-1}\ \text{and}\ B_2 = (P_{e0})^{-1}$$

By combining Equations 7.3, 7.4, 7.5, and 7.6, the square of the electric field strength inside the material can be determined by the material dielectric loss factor and the input power level. The relationship is described below.

$$|E_m|^2 = K_p\ P_{b0} = K_p\ P_e(\epsilon'')\ P_{i0} = K_p\ (B_1\ \epsilon'' + B_2)^{-1}\ P_{i0} \tag{7.7}$$

Therefore, microwave power absorption per unit volume of the material as a function of dielectric loss factor and electric field strength at a constant frequency is then described in Equation 7.8.

$$P_m = \pi\ f_o\ \epsilon_o\ \epsilon''\ |E_m|^2 = P_k\ \epsilon''(T)\ P_e(\epsilon'')\ P_{i0} \tag{7.8}$$

$$\text{where}\ P_k = \pi\ f_o\ \epsilon_o\ K_p$$

7.3.2 Energy balance model

A one-dimensional energy balance is used to describe non-uniform microwave heating due to the effects of heat conduction, convection, radiation, and changes in dielectric loss and electric field strength inside the material. Physical properties such as heat capacity, density, thermal conductivity, and free convective and radiant heat transfer coefficients are assumed to be temperature-independent in this study. The partial differential equation and boundary conditions in the cylindrical coordinate describing temperature as a function of radial position and time are given below.

$$C_p \rho \frac{\delta T}{\delta t} = \frac{k\delta(r\delta T/\delta r)}{r\,\delta r} + P_m \qquad (7.9)$$

$t = 0 \quad T = T_0 \quad$ for all r

$t > 0 \quad r = 0 \quad \delta T/\delta r = 0$

$r = R_s \quad - k\delta T/\delta r = h_c (T - T_s) + h_r (T^4 - T_c^4)$

Initially, the rod is at the temperature of T_0. The air temperature T_s and the cavity wall temperature T_c are assumed to be constant. The temperature at the center of the rod is symmetrical. Energy accumulation inside the sample element is equal to heat conduction and microwave power absorption. Heat transfer at the material boundary is equal to free heat convection and radiation.

7.4 Results and Discussion

Measurements of dielectric loss and temperature were made during thermal heating of Nylon 66 at 2.45 GHz. Dielectric loss data as a function of temperature at 2.45 GHz were fit using a simple three-parameter Debye dielectric relaxation model. Power ratios and dielectric loss factors of Nylon 66 were also measured during the dynamic and static microwave heating. The parameters in the model of power ratio and dielectric loss of the loaded material were then determined using nonlinear regression. The temperature/position/time profiles during microwave heating of Nylon were simulated and compared with the experimental data. Methods of obtaining uniform microwave heating are proposed and discussed.

7.4.1 Power absorption model

Dielectric loss factor of Nylon 66 as a function of temperature was measured at 2.45 GHz using a low-power diagnostic swept frequency method during thermal heating. The three-parameter dielectric relaxation model, Equation 7.2, as a function of temperature at a constant frequency was used to fit the experimental dielectric loss data of Nylon as shown in Figure 7.2. The estimated values of these three parameters of Nylon 66 were 1.393 for the polar oscillation strength ϵ, 7.75 Kcal/mole for the activation energy E, and 0.255×10^{-13} sec for the pre-exponential factor k_o. Figure 7.2 shows that dielectric loss factor of Nylon increases with increasing temperature before reaching the maximum dielectric loss and decreases thereafter.

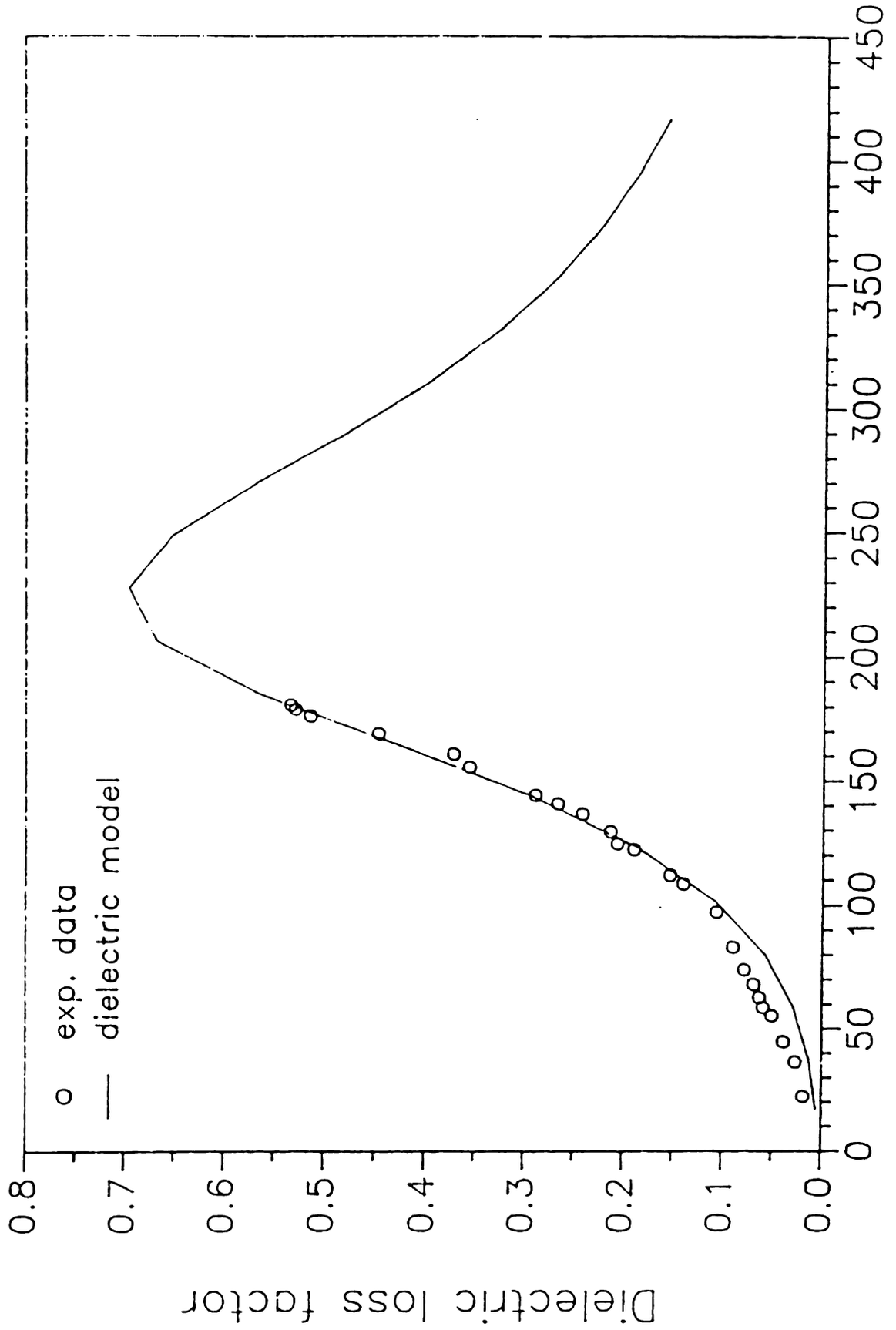

Figure 7.2: Dielectric loss factor versus temperature of Nylon 66 at 2.45 GHz and atmospheric pressure

The power ratio P_e as a function of dielectric loss of Nylon was measured from both dynamic and steady-state experiments at different input power levels. A two-parameter model, Equation 7.6, was used to fit the experimental data as shown in Figure 7.3. The estimated values of these two parameters were 4.610 for B_1 and 0.0885 for B_2. Figure 7.3 indicates that the power ratio is inversely proportional to the material loss factor, regardless of input power levels. However, the square of the electric field inside the sample is directly proportional to the product of the power ratio and the input power level as described in Equation 7.7. Therefore, the electric field strength inside the material decreases as the material dielectric loss increases at a given input power level.

7.4.2 Energy balance model

Temperature/position/time profiles for microwave heating of Nylon at an input power level of 5.0 W were measured. Temperature-dependent dielectric loss and dielectric loss-dependent electric field strength were determined and discussed in the previous section. Radiant and convective heat losses at the boundary during microwave heating of Nylon were experimentally determined and shown in Figure 7.4. The computer-simulated temperature-position-time profiles were directly calculated at an input microwave power level of 5 W and 2.45 GHz using the one-dimensional energy balance equation and boundary conditions. The parameters used in this computer simulation of microwave heating of Nylon 66 are listed in Table 7.1. Temperatures inside the rod were directly calculated using the partial differential energy balance equation and boundary conditions. These equations were solved using the

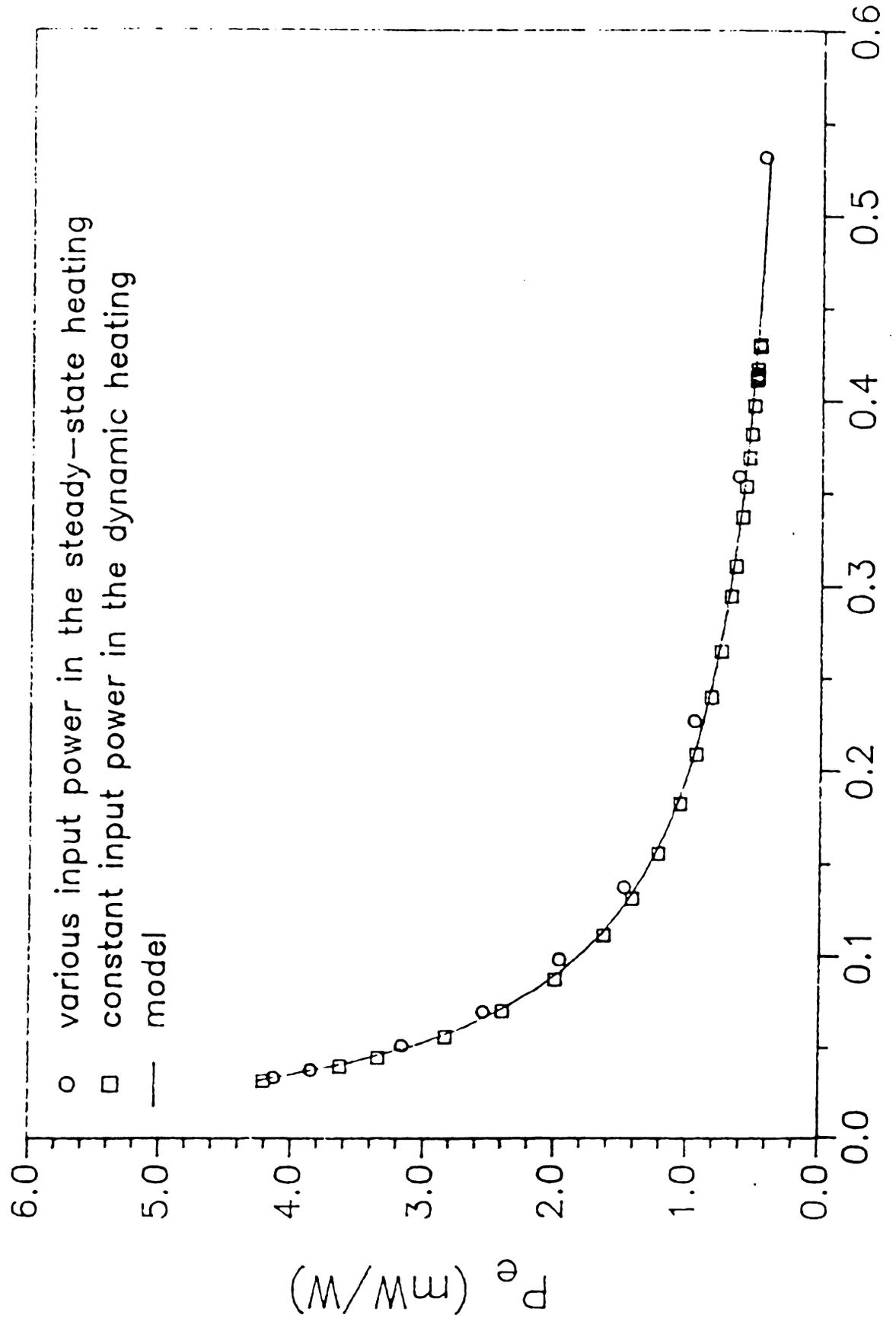

Figure 7.3: Power ratio of P_{bO} to P_{iO} versus dielectric loss factor of Nylon 66 in a resonant TM_{012}-mode cavity

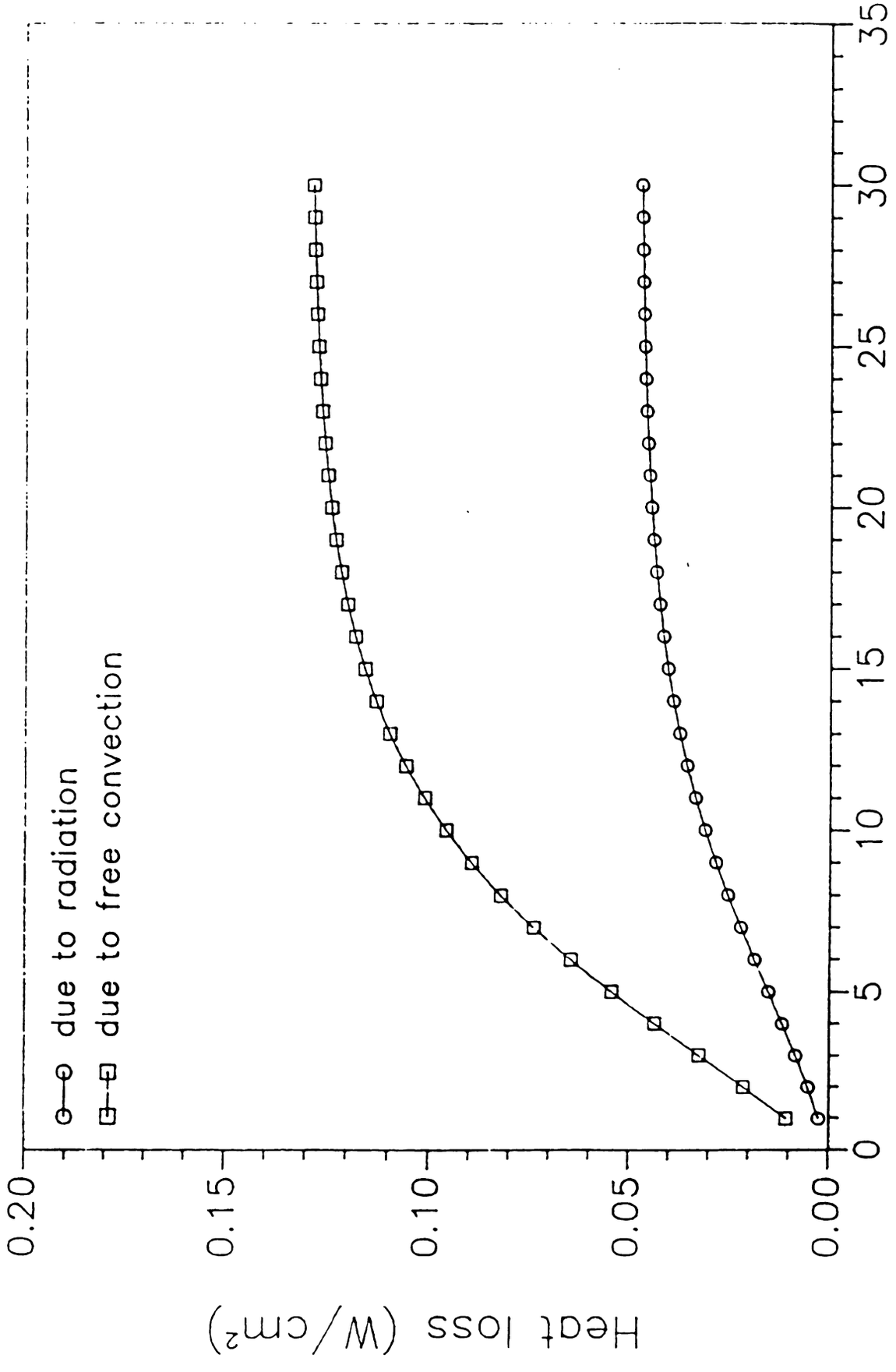

Figure 7.4: Radiant and convective heat loss during microwave heating of Nylon 66

Table 7.1: Simulation parameters on microwave heating of Nylon 66

Parameters	Symbol	Value	Unit
Heat capacity	C_p	0.35	cal/g/°K
Density	ρ	1.145	g/cm^3
Thermal conductivity	k	0.00058	cal/cm/sec/°K
Convective heat transfer	h_c	0.0003	$cal/cm^2/sec/°K$
Radiant heat transfer	h_r	0.610×10^{-12}	$cal/cm^2/sec/°K$
Polar oscillation strength	ϵ	1.393	-
Pre-exponential factor	k_0	0.255×10^{-13}	sec
Power absorption constant	B_1	4.610	-
Power absorption constant	B_2	0.0885	-
Activation Energy	E	7.75	Kcal/mole
Radius of nylon rod	R_s	0.635	cm
Initial nylon temperature	T_0	301.5	°K
Cavity air temperature	T_s	302.0	°K
Cavity wall temperature	T_c	301.5	°K
Incident input power	P_{i0}	5.0	W
Power absorption coefficient	P_k	0.65	cm^{-3}

forward finite difference method with a time step of 1.0 sec and five spatial elements. Temperature at the material boundary was directly calculated using the boundary condition. The boundary condition was solved using the Newton-Raphson method with a tolerance of 1.0×10^{-4} for a convergence criterion. An example of temperatures calculated at each node for heating times of 2.5, 5.0, 7.5, 10, 15, and 30 minutes is shown in Figure 7.5.

The experimental and computer-simulated temperature/position/time profiles are shown in Figure 7.6. The temperatures are slightly over-estimated from 90 to 160 °C but under-estimated before 90 °C and after 160 °C. These deviations between the predicted and experimental temperature measurements may be due to the temperature-independent assumptions on the physical properties, the numerical errors on the forward finite difference and Newton-Raphson methods, and/or the accuracy on the dielectric relaxation model. However, it is important to point out that temperature gradients always build up inside this low thermal conductivity material, even though the sample is initially located in the uniform electric field. The effects of slow internal heat conduction and heat transfer at the material boundary cause a temperature gradient inside the material. The temperature gradient then induces variations in the dielectric loss and electric field strength, and produces different microwave heating rates inside the sample. Greater differences in heating rates inside the material make the temperature gradient even larger.

The microwave power absorption in each element for different heating times was also calculated and shown in Figure 7.7. Figure 7.7 indicates that the microwave energy absorption is non-uniform inside the

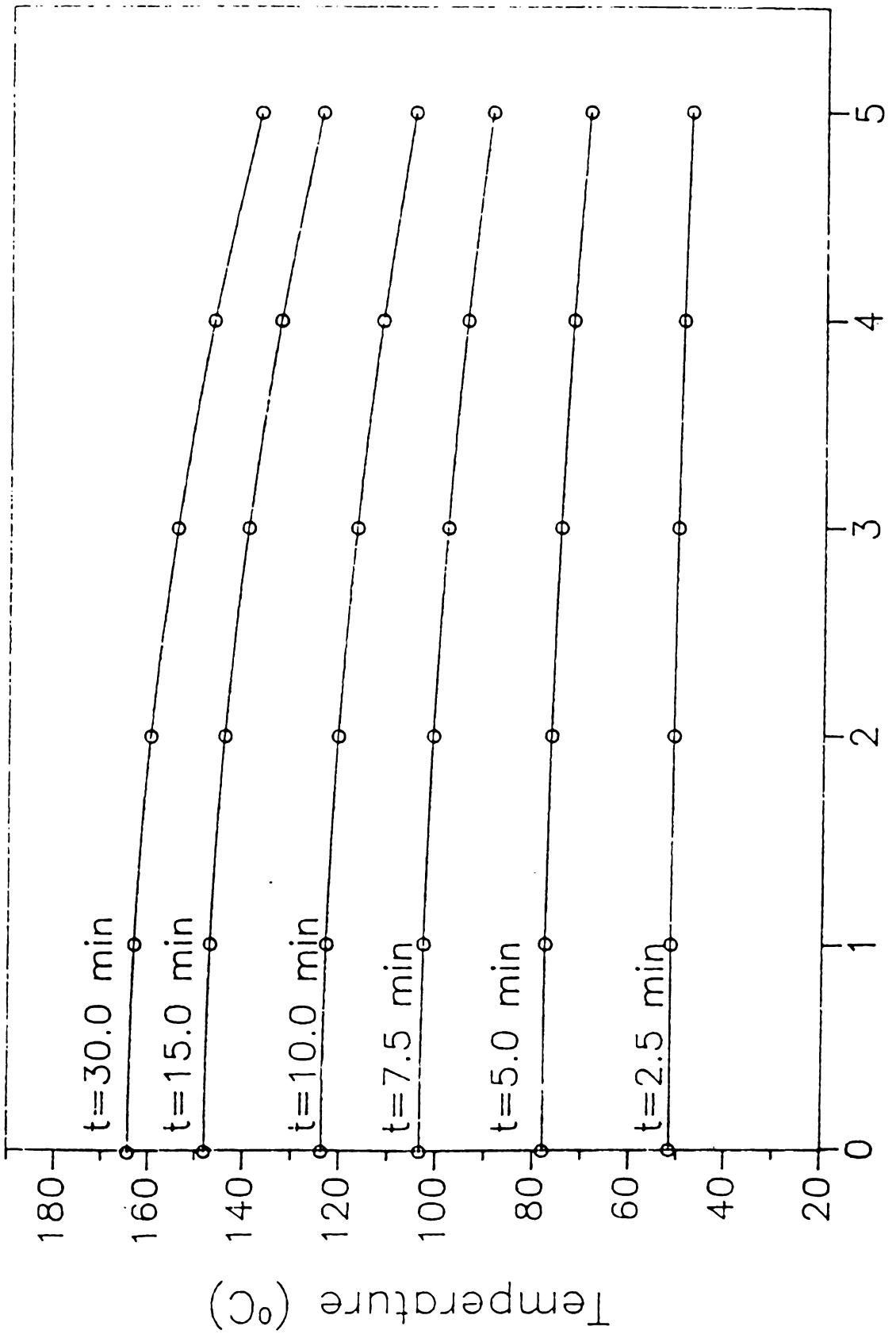

Figure 7.5: Computer-simulated temperatures of the Nylon 66 rod at each spatial node for different microwave heating times at an input power level of 5 W and 2.45 GHz

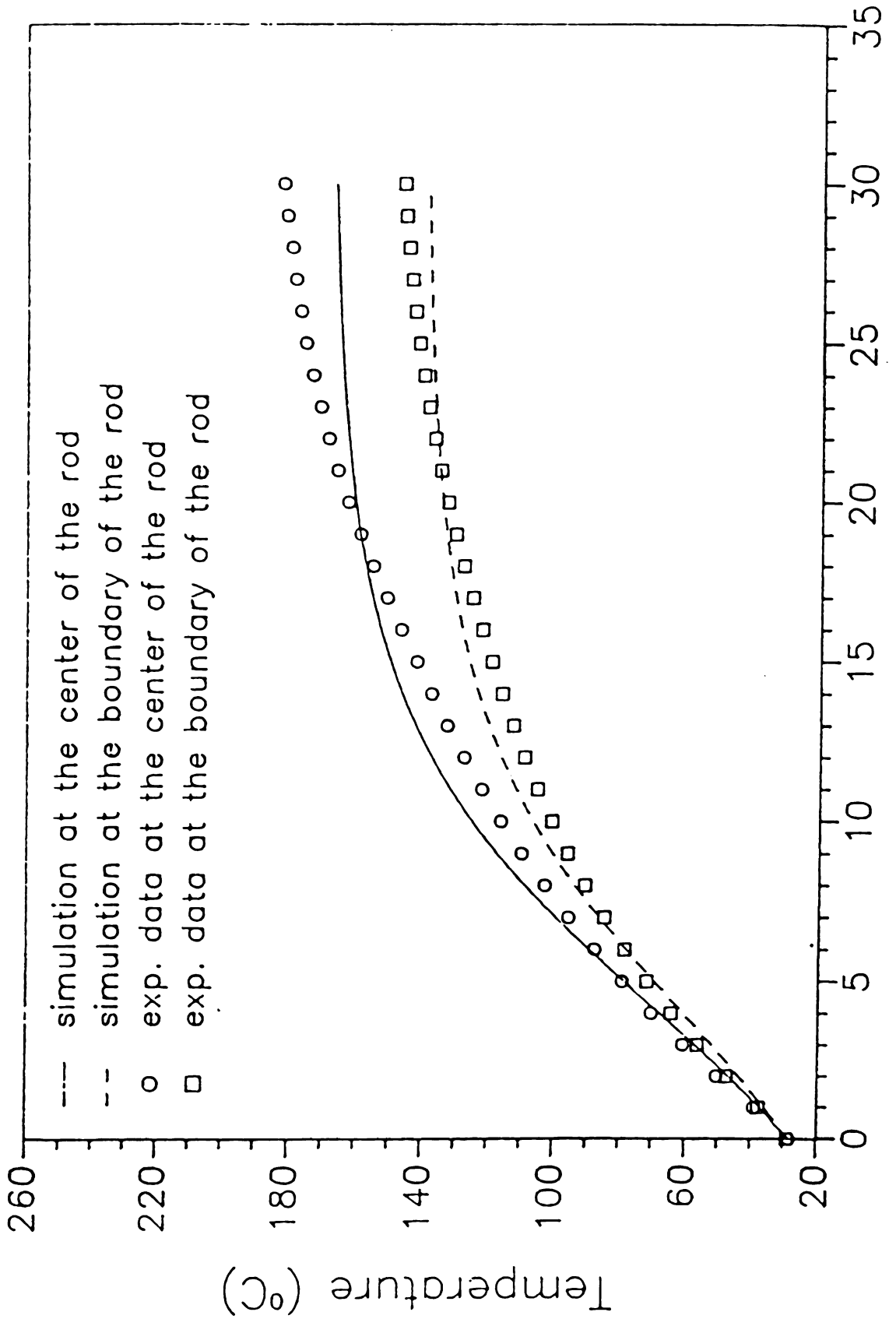

Figure 7.6: Experimental and Computer-simulated temperatures of Nylon 66 as a function of time at center and boundary location during continuous microwave heating

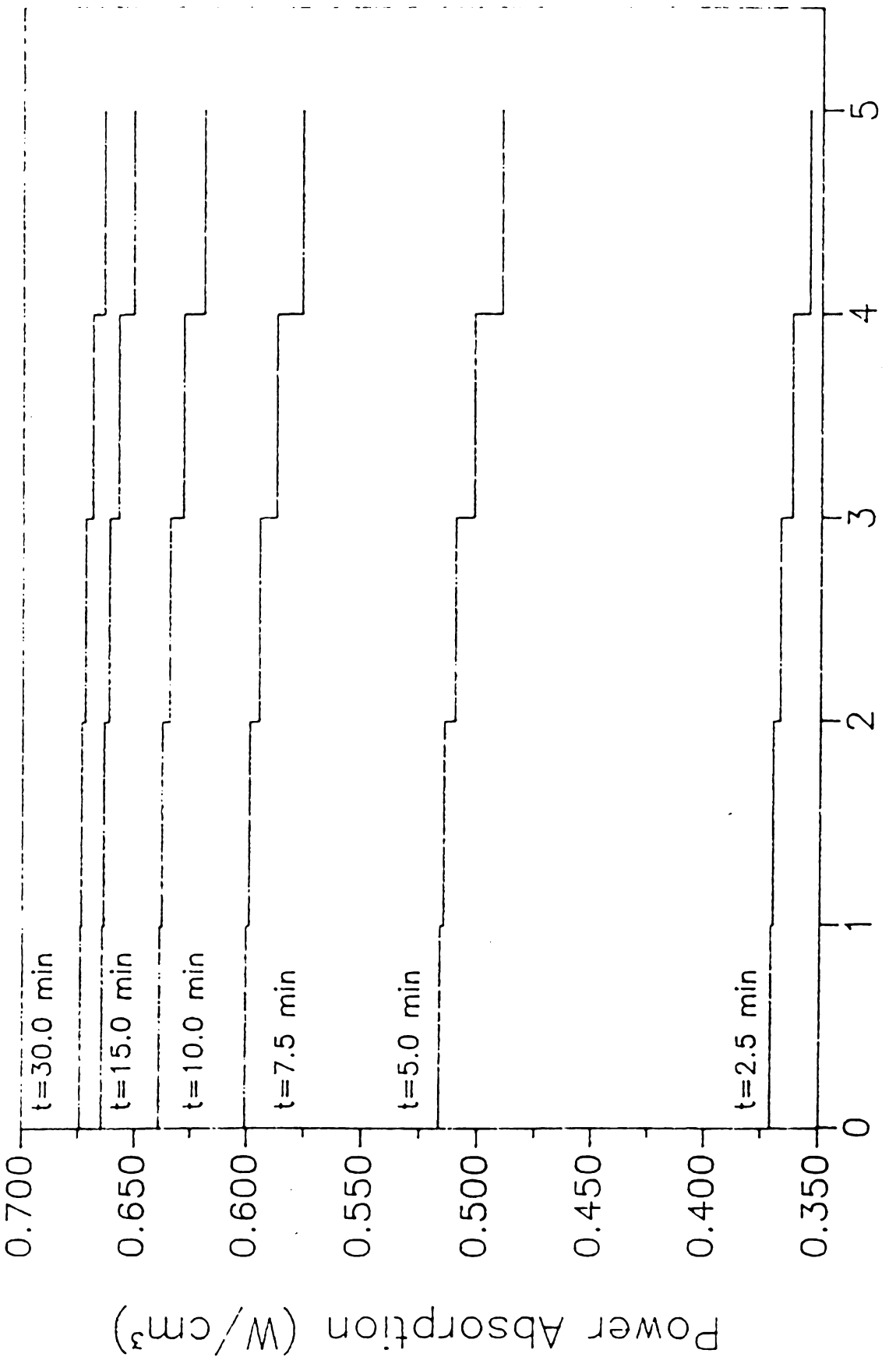

Figure 7.7: Calculated power absorption of the Nylon 66 rod in each spatial element for different microwave heating times at an input power level of 5 W and 2.45 GHz

sample and increases with increasing temperature. Again, the non-uniformity of power absorption inside the material during microwave heating is due to the variations in dielectric loss with temperature and electric field with dielectric loss.

7.4.3 Methods of obtaining uniform microwave heating

Since a temperature gradient is built up due to heat transfer at the boundary and slow internal heat conduction during microwave heating of low thermal conductivity materials, the gradient can be reduced by insulating the boundary or enhancing the material thermal conductivity. Computer-simulated temperatures during microwave heating of low thermal conductivity materials with the insulated boundary and of high thermal conductivity materials with free heat convection and radiation at the boundary are shown in Figure 7.8. Figure 7.8 indicates that no temperature gradient is built up for these two cases. Therefore, modification is required in order to obtain uniform temperature distribution inside low thermal conductivity materials electromagnetically heated in a uniform electric field region.

Uniform microwave heating can be improved by increasing the thermal conductivity of the material. Small samples of a low thermal conductivity epoxy (DER 332) and epoxy with 50.9 % by weight highly conductive powder (AS4 graphite) added were heated in the same cavity. The temperature/position/time profiles are shown in Figure 6.6. The temperature gradient during microwave heating of epoxy can be reduced by adding this highly conductive powder. Another highly conductive pure graphite rod was also electromagnetically heated in the same cavity.

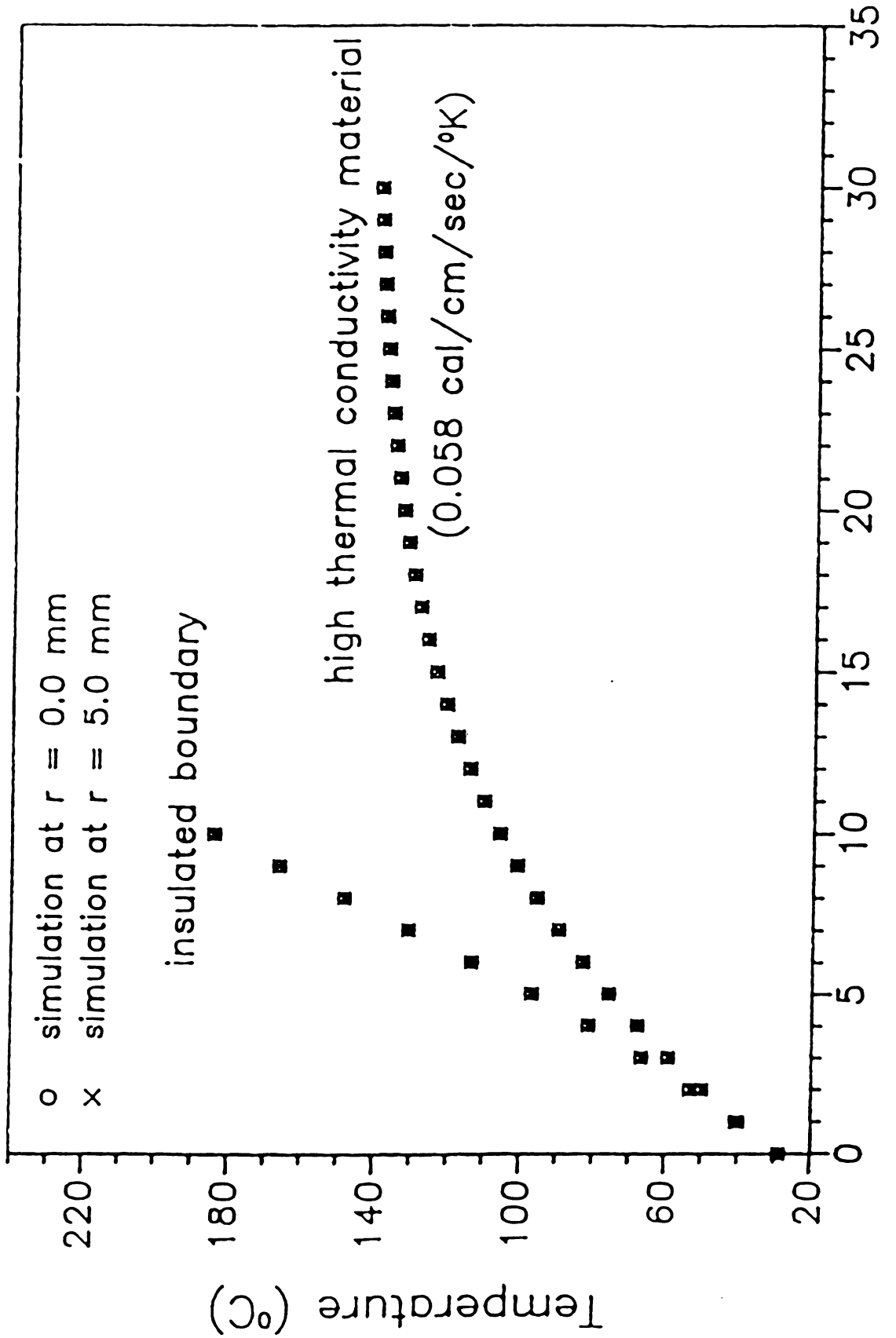

Figure 7.8: Computer-simulated temperature/position/time profiles for low thermal conductivity materials with the insulated boundary and high thermal conductivity materials with free surface heat transfer

The temperature/position/time profiles of this microwave heated graphite are shown in Figure 7.9. It indicates that the temperature inside a highly conductive material is uniform during microwave heating, if the material is located in a region of uniform electric field.

The boundary insulation requires selection of an insulated material with much lower thermal conductivity compared with that of the target material or heating a sample of low surface-to-volume ratio so that the surface heat transfer can be negligible. Sometimes, it is difficult to find the material which has a much lower thermal conductivity than that of the target material. An alternative method of insulating the material boundary is to heat materials in a vacuum environment to prevent convective heat transfer and to provide greater boundary insulation. Otherwise, uniform heating may be potentially accomplished by heating a larger material volume with relatively small surface-to-volume ratio in the same uniform field region of a larger cavity operated at a lower frequency (such as 915 MHz). Therefore, the heat transfer at the surface can be reduced.

Uniform heating can also be accomplished by using fast microwave heating for the material located in a uniform electric field region so that the temperature rise is controlled by microwave bulk heating instead of a thermal conduction process. A small Nylon rod is heated at different power levels in the same microwave cavity. Temperature-position-time profiles of Nylon heated at different power densities are shown in Figure 7.10. This illustrates that the temperature gradient between the center and the boundary of the rod is reduced as the microwave power density increases.

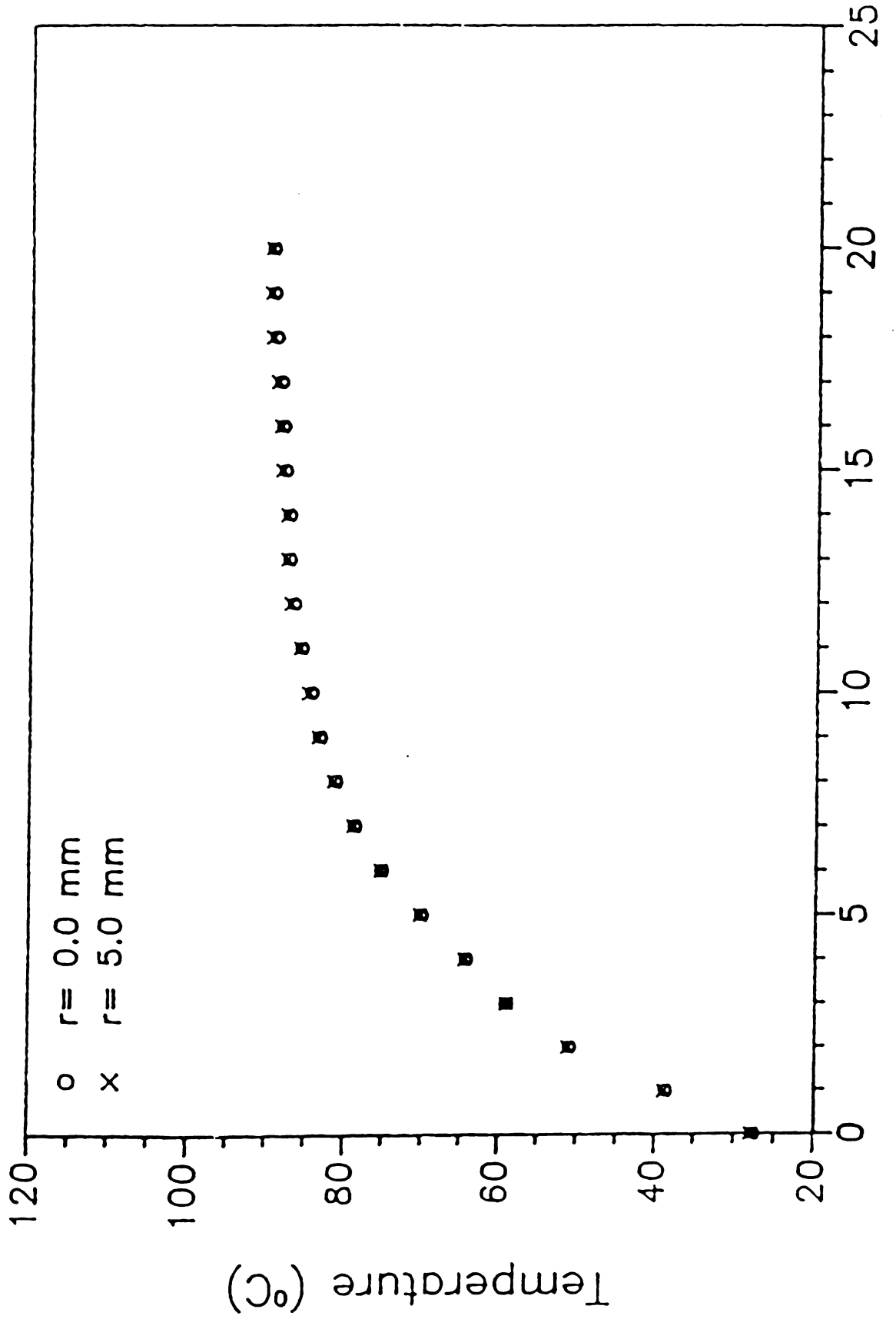

Figure 7.9: Temperature/position/time profile of a graphite rod during microwave heating

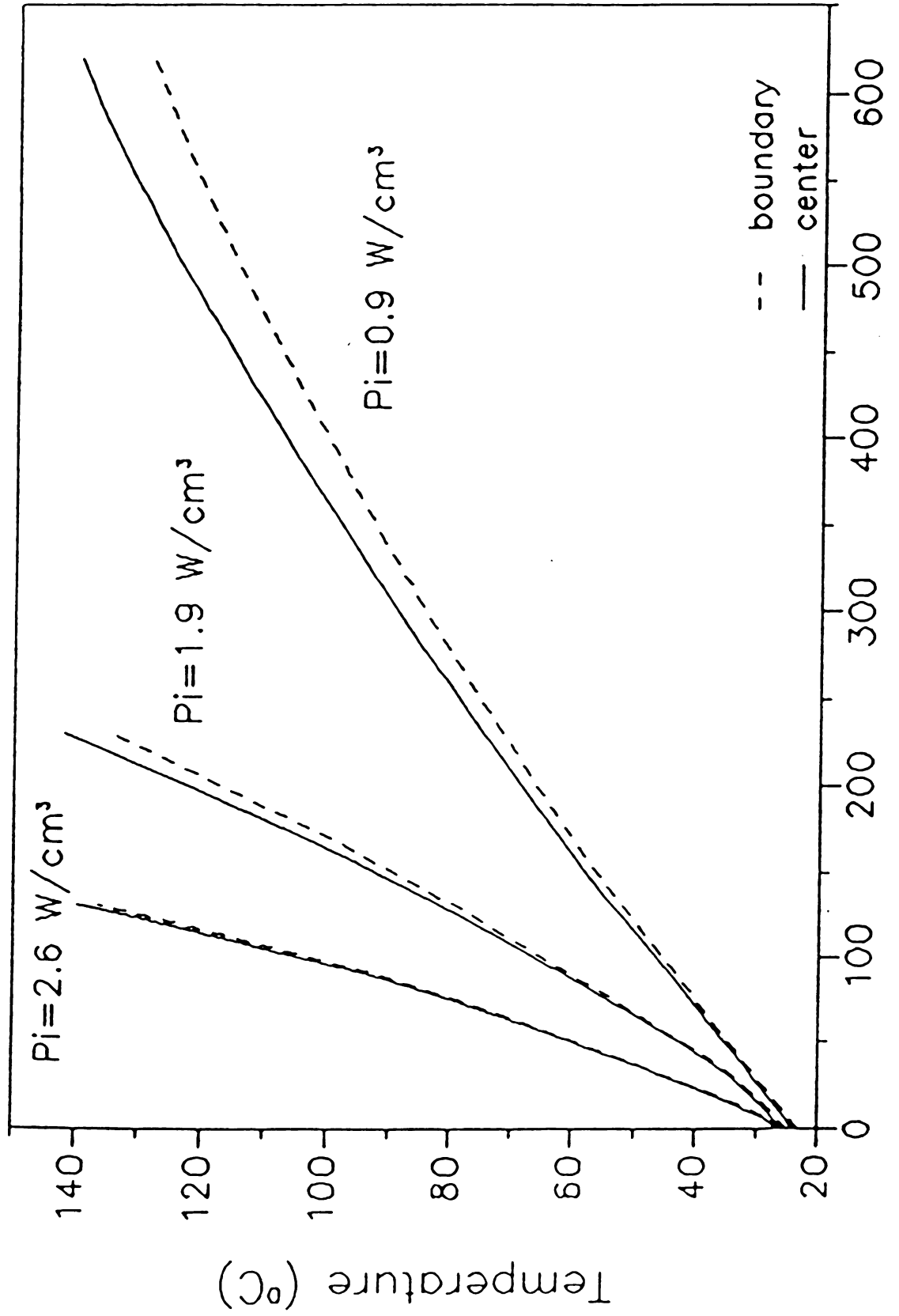

Figure 7.10: Microwave heating of Nylon 66 at different input power density levels

Microwave heating may provide fast and uniform heating initially, but a temperature gradient will eventually be developed and maintained due to heat transfer at the material boundary and slow heat conduction inside the dielectric material. On the other hand, thermal heating produces a temperature gradient in the early stage of heating due to slow surface driven heating processes, with all material temperatures eventually equilibriating at the boundary temperature. Therefore, it is very practical to combine the advantages of microwave and thermal heating. A comparison of temperature-position-time profiles between thermal and combined microwave/thermal heating of pure epoxy is shown in Figure 6.8. Microwave energy quickly raises the epoxy temperature up to a pre-set oven temperature (175 °C) and shuts off. Using thermal heating reduces the temperature gradient which is always established during microwave heating of low thermal conductivity materials by elevating the boundary temperature. Uniform temperature inside the heated material can be maintained in this manner.

An alternative method of enhancing the boundary temperature without using thermal heating is to select a lossy material which can be simultaneously heated up by microwaves to the same temperature as the target material. Otherwise, using different electric field patterns can balance lower temperature spots with higher heating rates in order to reduce the temperature differences.

7.5 Conclusion

Microwave heating is fast, controllable, selective, and outward, but not necessarily uniform. The temperature gradient inside low

thermal conductivity materials can be built up due to the combined effects of the surface heat transfer and slow heat conduction during the slow microwave heating. However, uniform microwave heating for processing of these low thermal conductivity materials can be achieved by increasing the material thermal conductivity, insulating the material boundary, fast heating, or combining microwave and thermal methods during the heating process.

CHAPTER EIGHT

CONCLUSIONS

8.1 Research Achievements and Findings

This research is directed toward development and investigation of microwave energy coupling and diagnostic measurement system for processing of polymers and composites. The specific objectives are to develop a single-mode microwave processing and dielectric diagnosis technique to process polymers and composites, to obtain dielectric data of selected polymers (epoxy/amine resins, Nylon 66, and pure epoxy), to develop a controlled-pulsed microwave processing technique with feedback control of material temperature measurements, to investigate microwave processing of composites, and to understand microwave energy coupling and heat transfer in polymer materials.

A microwave heating and dielectric measurement technique using a TM_{012}-mode resonant cavity has been developed to simultaneously heat the material and measure the material complex permittivity. Two experimental methods (single and swept frequency method) are used to measure the material complex permittivity during microwave processing of nonreacting (Nylon 66) and reacting (epoxy/amine resin) polymers. This research shows that dielectric measurements using the single and swept frequency method are repeatable and consistent. However, the single frequency method is faster, more accurate, more efficient and adaptable to control power coupled into the loaded materials when compared with the swept frequency method. Therefore, the single frequency method is

more useful than the swept frequency method in a dynamic microwave heating process.

Permittivity and dielectric loss factor of stoichiometric mixtures of epoxy/amine resins (DER 332/DDS) as a function of temperature and extent of cure have been obtained at a microwave frequency of 2.45 GHz. Permittivity and dielectric loss factor of these resins increase with increasing temperature and decrease with increasing extent of cure. Dielectric loss factor is more dependent on temperature in the early stages of cure but becomes less dependent on temperature as the cure proceeds. Measurements of temperature- and cure-dependent dielectric loss factor during the microwave curing of epoxy/amine resin show three material structure stages and significant changes in dielectric loss factor at the extent of cure about 40%. Dielectric loss factor is also found to be the same for both thermally and microwave cured samples. This work suggests that dielectric loss data can be related to extent of cure in order to monitor the cure process. However, dielectric loss measurement may strongly depend on the presence of primary amine due to a significant dielectric loss change in the early stages of cure. Measurements of dielectric loss factor of nonreacting polymers (pure DER 332 and Nylon 66) are also made at 2.45 GHz. Dielectric loss factor for these nonreacting materials increases with increasing temperature before reaching the maximum dielectric loss but decreases after passing through the maximum. However, the dielectric loss versus temperature spectrum of epoxy is asymmetric.

The single-mode resonant cavity technique using continuous and computer-controlled pulsed microwave power has been developed and used to simultaneously cure epoxy/amine resins and measure dielectric loss factor. A significant exothermic temperature peak is always found in

continuous microwave curing of the epoxy/amine resins. The controlled pulsed microwave processing system can heat the resins quickly and maintain constant temperature-time profile through the entire curing process. Glass transition temperatures of pulsed microwave cured samples are different from those of thermally cured samples on the DSC thermographs. Curing time using pulsed microwave energy is longer than that using thermal energy. However, the slow reaction can be compensated at a higher cure temperature using this pulsed power system.

The controlled pulsed microwave system is also used to heat Nylon/graphite composites and epoxy with conductive and nonconductive additives. Microwave heating is selective and outward. This work shows that microwaves can uniformly heat the composites with conductive additives in a shorter time. On the other hand, a temperature gradient is always built up and maintained during microwave processing of low thermal conductivity composites. A hybrid mode of microwave and thermal processing is developed and used to heat these low thermal conductivity materials quickly and uniformly.

Microwave power absorption and heating characteristics of low thermal conductivity materials are modeled and verified with experimental data on microwave heating of Nylon 66. Nonuniform temperature distribution and power absorption inside these materials are due to the combined effects of the surface heat transfer, the slow internal heat conduction, and the variations in dielectric loss factor and electric field strength. The electric field strength in a microwave loaded resonant cavity is always reduced as the dielectric loss factor of the loaded material increases. However, uniform microwave heating for processing of low thermal conductivity materials can be achieved by increasing the material thermal conductivity, heating fast, insulating

the material boundary, or combining microwave and thermal methods during the heating process.

This research shows that microwave heating is outward due to heat transfer at the cold material boundary, direct and selective depending upon the loss factor of constituents in processed materials, fast and controllable depending on input power levels and cycles, and adaptable for control of power with feedback diagnostic measurements. These unique features may cause microwave cured materials to have superior thermal or mechanical characteristics when compared with thermally cured materials. It would be a very promising technique using microwave energy to process thermoplastics, thermosets, and composite materials.

8.2 List of Conclusions

The above research achievements and findings are summarized and listed as follows.

1. A microwave processing and dielectric diagnosis technique using a TM_{012}-mode resonant cavity has been developed using the single and swept frequency method.
2. Single frequency method is more accurate, more efficient and adaptable for control of power coupled into materials.
3. Data base of dielectric properties as a function of temperature and extent of cure for the stoichiometric mixture of epoxy/amine resins has been obtained at 2.45 GHz.
4. Dielectric properties of epoxy/amine resins decrease with increasing extent of cure.
5. Dielectric loss factor of epoxy/amine resins is more dependent on

temperature in the early stages of cure but more dependent on extent of cure as the cure proceeds.

7. Dielectric loss measurement during microwave curing of epoxy/amine resins seems to depend on the presence of primary amine.
8. Dielectric loss factors of thermally and microwave cured epoxy/amine resins are the same at a given extent of cure, temperature, and frequency.
9. Dielectric loss factor of polymers increases with temperature before reaching the maximum loss but decreases thereafter.
10. The square of the electric field strength inside the resonant cavity decreases with increasing dielectric loss of the loaded material.
11. A controlled pulsed microwave processing and diagnostic technique has been developed.
12. Curing time of epoxy/amine resins using pulsed microwave energy is longer than that using thermal energy
13. Controlled pulsed microwave energy can process epoxy/amine resins at a higher cure temperature when compared with continuous microwave or thermal energy.
14. Glass transition temperature of pulsed microwave cured samples determined using DSC is different with that of thermally cured samples.
15. Nonuniform temperature distribution during microwave heating of low thermal conductivity materials is eventually built up due to surface heat transfer, slow heat conduction, and variations of heating rates inside materials.
16. Nonuniform heating rate and power absorption inside the materials are due to the variations in dielectric loss and electric field strength inside the materials.

17. Reduction in temperature gradient during microwave heating of low thermal conductivity materials has been achieved by increasing the material thermal conductivity, heating fast, and enhancing the material boundary temperature.
18. Microwaves can heat highly conductive materials fast and uniformly.
19. A hybrid mode of microwave and thermal processing has been used to heat low thermal conductivity materials quickly and uniformly.

CHAPTER NINE

RECOMMENDATIONS

Suggestions for future study based on current research work are presented in this chapter. Three research directions are proposed: (1) technique and system development, (2) experiments, and (3) theoretical modeling.

9.1 Technique and System Development

In this single-mode processing and diagnostic technique, a cavity of 7.62 cm in radius is used to resonate in a TM_{012} mode at 2.45 GHz. Two diagnostic techniques used in this system are: dielectric and temperature measurement. Dielectric measurements are made using the material-cavity perturbation technique. Only small samples are allowed to be processed and diagnosed due to the limitations of perturbation and the cavity size. A bigger size cavity operated at 915 MHz or a controlled multi-mode technique can be used to process large samples. For the controlled multi-mode technique, a dual-mode method should be developed to heat the materials in the high-power controlled multi-modes and diagnose the heating process in another low-power diagnostic mode. Another dielectric diagnostic method should be developed for a wide range of sample volumes and shapes.

A fluoroptical temperature sensing system has been successfully used to measure material temperature. However, it is required to contact the sample surface or to be immersed into samples to measure the

surface or bulk temperature. Liquid epoxy/amine resins are converted into cured solids through the crosslinking reaction. Therefore, a capillary tube is always used to protect the expensive fiber probe and stuck in the cured samples. Nondestructive temperature techniques should be instead used to process the mechanical testing samples. An IR thermometer, which does not need to contact the surface, can be used for nondestructive surface temperature measurement. For microwave processing of composites, an embedded optical fiber sensor technique associated with optical time-domain instrumentation can be used to on-line monitor temperature, pressure, and strain during curing of fiber composites [63]. Another nondestructive temperature measurement technique using temperature-dependent ultrasonic wave velocity [64] can be used to measure temperature distribution inside the samples. Otherwise, low-cost disposable optical fiber may be considered for the fluoroptic thermometer.

A field-transparent pressurized sample mold should be designed in order to expel excessive resins and to evacuate voids inside the composite specimen. However, for microwave processing of low thermal conductivity composites, temperature gradients are always built up and maintained due to heat transfer at the sample surface and slow internal heat conduction. Therefore, a fairly high lossy material can be a good sample mold to enhance the boundary temperature and to reduce the surface heat loss. Otherwise, a hybrid mode of thermal and microwave processing technique should be developed to heat thick composites with low thermal conductivity fast and uniformly. The development of a microwave processing technique associated with on-line measurements of temperature, pressure, and dielectric properties is also needed to continuously process polymers and composites.

Development of an on-site microwave cure of thin sample films in the FTIR analyzer associated with temperature measurement and control of the sample is a convenient technique to study microwave kinetics. Combination of the microwave processing and diagnostic resonant cavity with a differential scanning calorimeter can be used to study dielectric property changes and extent of cure in either thermal or microwave cure runs.

9.2 Proposed Experiments

Dielectric loss factor of epoxy/amine resins depends on population and mobility of reactive polar groups during crosslinking reaction. Dielectric measurements and cure experiments on monofunctional epoxy (such as phenyl glycidyl ether)/DDS resins compared with those of crosslinked epoxy/amine resins are proposed. The purpose of these experiments is to study the effect of crosslinking on the dielectric measurement. Comparison of product distribution, dielectric loss factor change, and rate of reaction for both uncrosslinked and crosslinked epoxy/amine reaction is also helpful to understand the reaction mechanism and network formation.

In epoxy/primary amine mixtures, dielectric loss factor seems to strongly depend upon the presence of primary amine during microwave curing [6,65]. Dielectric loss measurement during the epoxy/amine cure is believed to be dominated by the concentration of primary amine. On-line measurements of dielectric loss factors during curing of different ratios of primary amine to epoxy are proposed to investigate this relationship.

Curing time using pulsed microwave energy is shown to be longer

than that using thermal energy for the epoxy/amine reaction. Experiments on controlled pulsed microwave and thermal curing of epoxy/amine resins at three cure temperatures are proposed to study microwave and thermal kinetics using the computer-controlled microwave cavity and DSC. Rates of reaction, rate constants, and activation energies will be evaluated and compared. Different techniques (such as TMA and DMA) are also used to determine the glass transition temperatures of these cured samples.

In addition, different thermosetting (such as polyimide) and thermoplastic (such as PEEK) polymers can be investigated using current microwave processing and diagnostic technique. Experiments on microwave processing of thick polymeric composites with long conductive and nonconductive fibers will be conducted. The mechanical and thermal properties of the microwave cured polymers and composites will be evaluated and compared with those of thermally cured samples.

9.3 Theoretical Modeling

Since data of dielectric properties of epoxy/amine resins as a function of temperature and extent of cure are obtained at 2.45 GHz, the relationship between dielectric loss, temperature, and extent of cure can be modeled in order to monitor the cure process.

After dielectric model of epoxy/amine resins has been developed, microwave power absorption by these matrix resins can also be simulated and verified with experimental data in order to develop the fundamental knowledge and understanding of microwave energy coupling, chemical reaction, and heat transfer for these chemically reacting materials.

Further, it is recommended that thermochemical model associated

with microwave power absorption model be developed and applied to microwave processing of polymeric and composite materials. The optimal cure cycles and process criteria based on these research findings would be useful to develop an AI controlled cure process.

For microwave processing of low thermal conductivity materials, nonuniform temperature distribution and power absorption are found due to the effects of heat transfer and the nonlinear changes in dielectric loss and electric field strength. Therefore, theoretical simulation for uniform microwave heating of low thermal conductivity materials is proposed using different electric field patterns in order to balance low temperature spots with high heating rates.

9.4 List of Suggestions

The above suggestions are summaried and listed as follows.

1. to develop a dielectric diagnostic technique applicable for a wide range of sample volumes and shapes.
2. to develop a dual-mode processing and diagnostic technique to heat the materials in high power controlled multimodes and measure the material complex permittivity in a low power diagnostic mode.
3. to design an alternative temperature sensing technique for microwave processing without physical damages in the specimen.
4. to design a pressurized sample mold to expel excessive resins and to evacuate voids inside the specimen.
5. to develop a hybrid mode of thermal and microwave processing for low thermal conductivity polymers and composites.
6. to develop a continuous microwave processing technique associated with on-line temperature, pressure, and dielectric measurements.

7. to develop an on-site microwave processing chamber in an FT-IR analyzer.
8. to develop a combined experimental device with a dielectric analyzer and a differential scanning calorimeter.
9. to study the effect of network formation on dielectric measurement using monofunctional epoxy with DDS or epoxy with monofunctional DDS.
10. to study the relationship between the dielectric loss and the concentration of primary amine in the epoxy/amine resins.
11. to study microwave cure kinetics of epoxy/amine resins.
12. to study different polymers using a microwave resonant cavity.
13. to illustrate microwave curing of composites.
14. to evaluate glass transition temperatures between thermally and pulsed microwave cured samples.
15. to model dielectric loss factor of epoxy/amine resins as a function of temperature and extent of cure at 2.45 GHz.
16. to model microwave curing processing of polymers and composites.
17. to develop AI cure cycles for thermal and microwave processes.
18. to theoretically simulate uniform microwave heating for low thermal conductivity materials using different field patterns.

APPENDIX A

DERIVATION OF TM_{012}-MODE MATERIAL-CAVITY PERTURBATION EQUATIONS

APPENDIX A

DERIVATION OF TM_{012}-MODE MATERIAL-CAVITY PERTURBATION EQUATIONS

A rodlike sample is concentrically loaded into a cylindrical TM_{012}-mode resonant cavity. The distance from the center of the sample to the bottom of the cavity is H. The radius, length, and volume of the cavity are R_c, L_c, and V_c. The radius, length, and volume of the sample are R_s, L_s, and V_s. A diagram of the cavity with the sample rod is shown in Figure A.1. Using standard material-cavity perturbation assumptions, the perturbation equations for the material complex permittivity in the TM_{012}-mode resonant cavity can be derived as follow.

The scalar Helmholtz wave equation in a source-free region for cylindrical coordinates is given below.

$$\frac{1}{\rho}\frac{\partial(\rho\partial\psi/\partial\rho)}{\partial\rho} + \frac{1}{\rho^2}\frac{\partial^2\psi}{\partial\phi^2} + \frac{\partial^2\psi}{\partial z^2} + k^2\psi = 0 \qquad (A.1)$$

Using the method of separation of variables and matching boundary conditions for a cylindrical cavity with the radius of R_c and the length of L_c, the wave function for the TM_{012} mode is then obtained and listed as follows.

$$\psi = J_0(X_{01}\rho/R_c)\cos(2\pi z/L_c) \qquad (A.2)$$

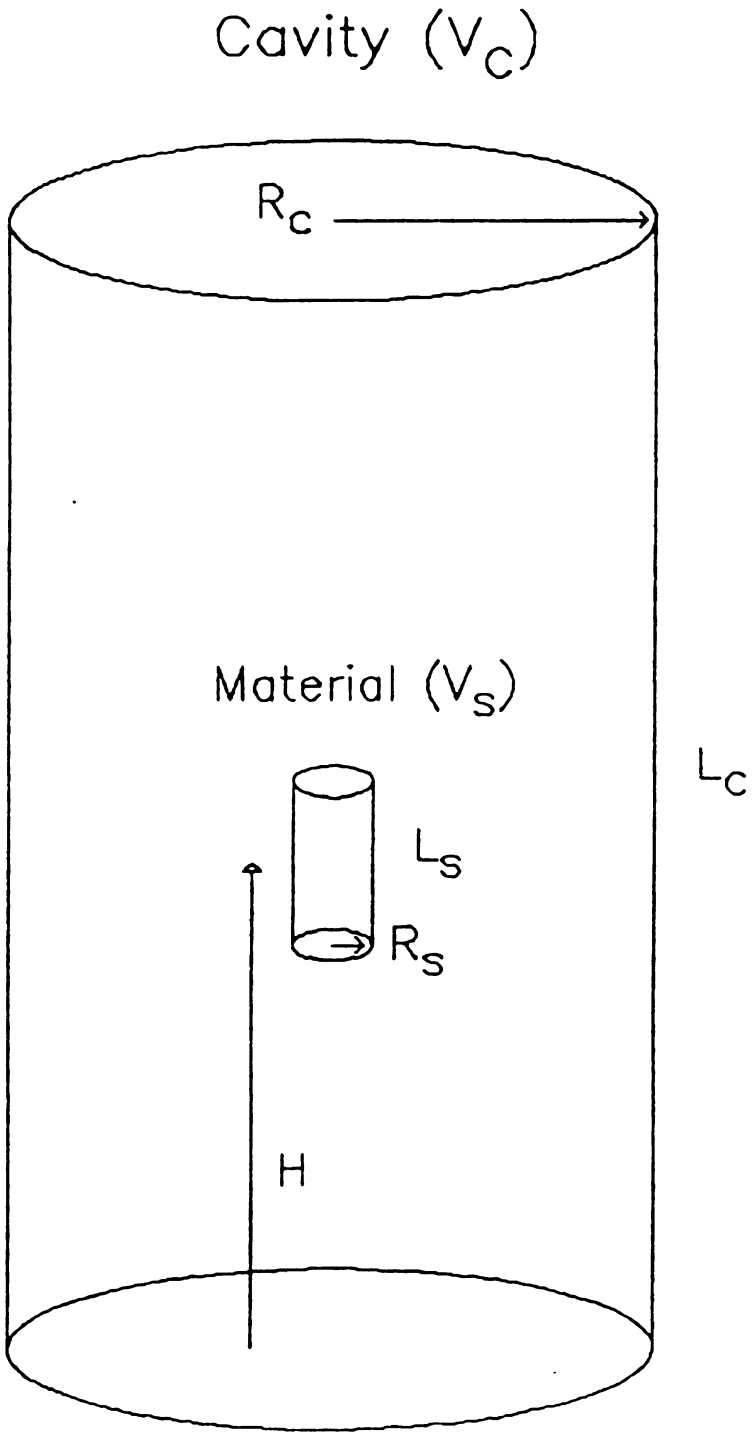

Figure A.1: A sample rod loaded in a cylindrical cavity

The electric fields for TM mode waves can be expressed in terms of the wave functions and are given below.

$$E_\rho = \frac{1}{j\omega\epsilon} \frac{\partial^2 \psi}{\partial\rho\partial z} \tag{A.3}$$

$$E_\phi = \frac{1}{j\omega\epsilon} \frac{\partial^2 \psi}{\partial\phi\partial z} \tag{A.4}$$

$$E_z = \frac{1}{j\omega\epsilon} (k^2 + \partial^2/\partial z^2)\, \psi \tag{A.5}$$

$$\text{where} \quad k^2 = k_\rho^2 + k_z^2$$

Therefore, the electric fields in the TM_{012}-mode cavity can be expressed as follows.

$$E_\rho = \frac{1}{j\omega\epsilon} (X_{01}/R_c)\, (2\pi/L_c)\, J_0'(X_{01}\rho/R_c)\, \sin(2\pi z/L_c) \tag{A.6}$$

$$E_\phi = 0 \tag{A.7}$$

$$E_z = \frac{1}{j\omega\epsilon} (X_{01}/R_c)^2\, J_0(X_{01}\rho/R_c)\, \cos(2\pi z/L_c) \tag{A.8}$$

If the diameter of the sample rod is much less than the free space wavelength, the quasi-static approximation of the electric field can be applied inside the sample. Using quasi-static approximation, the electric field components inside the rodlike material ($E_{z,int}$ and $E_{\rho,int}$) can be expressed in terms of the electric field components in the cavity (E_z and E_ρ).

For tangential component

$$E_{z,int} = E_z \tag{A.9}$$

For normal component

$$E_{\rho,int} = 2\, E_\rho \,/\, (1 + \epsilon) \tag{A.10}$$

The material-cavity perturbation with quasi-static correction has been formulated [31] and is given below.

$$\frac{\omega^* - \omega_0^*}{\omega_0^*} \approx \frac{1 - \epsilon^*}{2} \frac{\int \vec{E}_{int} \cdot \vec{E}\, \delta v'}{\int |\vec{E}|^2\, \delta v}$$

$$= \frac{1 - \epsilon^*}{2} \frac{\int 2\,|E_\rho|^2/(1+\epsilon)\, \delta v' + \int |E_z|^2\, \delta v'}{\int |E_\rho|^2\, \delta v + \int |E_z|^2\, \delta v} \tag{A.11}$$

Since the material has much smaller radius than the cavity and is loaded at the center of the cavity, the radial electric field inside the material is negligible when compared with the axial electric field inside the material. Therefore, the material-cavity perturbation can be simplified as follows.

$$\frac{\omega^* - \omega_0^*}{\omega_0^*} = \frac{1 - \epsilon^*}{2} \frac{\int |E_z|^2\, \delta v'}{\int |E_\rho|^2\, \delta v + \int |E_z|^2\, \delta v} \tag{A.12}$$

For lossy materials, the quantities ω^*, $\omega_0{}^*$, and ϵ^* are complex and can be expressed as follows.

$$\omega^* = \omega + j\,\omega/2Q$$

$$\omega_0{}^* = \omega_0 + j\,\omega_0/2Q_0$$

$$\epsilon^* = \epsilon' - j\,\epsilon''$$

If $Q_0 \gg 1$, $Q > 1$ and $\omega/\omega_0 \approx 1$, the complex material-cavity perturbation is then separated into the real and imaginary part [66].

$$\frac{\omega - \omega_0}{\omega_0} = -\frac{1 - \epsilon'}{2} \frac{\int |E_z|^2\, \delta v'}{\int |E_\rho|^2\, \delta v + \int |E_z|^2\, \delta v} \tag{A.13}$$

$$\frac{1}{2Q} - \frac{1}{2Q_0} = -\frac{\epsilon''}{2} \frac{\int |E_z|^2\, \delta v'}{\int |E_\rho|^2\, \delta v + \int |E_z|^2\, \delta v} \tag{A.14}$$

Integration of the square of the electric field over the material volume is given below. .

$$\int |E_z|^2\, \delta v' = \frac{(X_{01})^4}{(\omega\epsilon_0 R_c{}^2)^2} \frac{V_s}{2} A\, B \tag{A.15}$$

where $A = [J_1{}^2(X_{01}R_s/R_c) + J_0{}^2(X_{01}R_s/R_c)]$

$B = [1 + L_c \sin(2\pi L_s/L_c)/2\pi L_s \cos(4\pi H/L_c)]$

$V_s = \pi R_s{}^2 L_s$

Integration of the square of the electric field over the entire cavity volume is given below.

for E_ρ component

$$\int |E_\rho|^2 \, \delta v = \frac{1}{(\omega\epsilon_0)^2} \frac{X_{01}^4}{R_c^4} \frac{V_c}{2} [J_1(X_{01})^2] \tag{A.16}$$

for E_z component

$$\int |E_z|^2 \, \delta v = \frac{2}{(\omega\epsilon_0)^2} \frac{(\pi X_{01})^2}{(L_c R_c)^2} V_c \, J_1(X_{01})^2 \tag{A.17}$$

where $V_c = \pi R_c^2 L_c$

$$\int |E_\rho|^2 \, \delta v + \int |E_z|^2 \, \delta v = \frac{(X_{01})^2}{2(\omega\epsilon_0 R_c^2)^2} \left\{ X_{01}^2 + \frac{(2\pi R_c)^2}{(L_c)^2} \right\} V_c \, J_1(X_{01})^2$$

Since the cavity is resonated in the TM_{012} mode, the square of the resonant frequency f_0 is equal to $(v_0/2\pi R_c)^2 [X_{01}^2 + (2\pi R_c/L_c)^2]$.

$$\int |E_\rho|^2 \, \delta v + \int |E_z|^2 \, \delta v = \frac{(X_{01})^2}{2(\omega\epsilon_0 R_c^2)^2} \frac{(2\pi f_0 R_c)^2}{(v_0)^2} V_c \, J_1(X_{01})^2 \tag{A.18}$$

Therefore, the ratio of integration of the square of the electric field over the material volume to the cavity can be expressed below.

$$\text{Let} \quad G = \frac{X_{01}^2}{2\,[2\pi\, J_1(X_{01})]^2} \frac{(v_0)^2}{(f_0 R_c)^2} = 0.2718\, [v_0/(f_0 R_c)]^2$$

where $X_{01} = 2.405$ and $J_1(X_{01}) = 0.51915$

$$\frac{\int |E_z|^2 \, \delta v'}{2\left(\int |E_\rho|^2 \, \delta v + \int |E_z|^2 \, \delta v\right)} - \frac{X_{01}^2}{2\,[2\pi\, J_1(X_{01})]^2} \frac{(v_0)^2}{(f_0 R_c)^2} \frac{A\ B\ V_s}{V_c} \qquad (A.19)$$

$$= G\ A\ B\ V_s/V_c$$

By combining Equations A.13, A.14, and A.19, the material-cavity perturbation equations for the TM_{012} mode are then simplified as follows.

$$\frac{1}{2Q} - \frac{1}{2Q_0} = \epsilon''\ A\ B\ G\ V_s/V_c \qquad (A.20)$$

$$\frac{\omega - \omega_0}{\omega_0} = (1 - \epsilon')\ A\ B\ G\ V_s/V_c \qquad (A.21)$$

Since $\omega = 2\pi\ f_s$ and $\omega_0 = 2\pi\ f_0$

$$(f_0 - f_s)/f_0 = (\epsilon' - 1)\ A\ B\ G\ V_s/V_c \qquad (A.22)$$

where $A = J_0(X_{01}R_s/R_c)^2 + J_1(X_{01}R_s/R_c)^2$

$B = 1 + [L_c/(2\pi L_s)]\sin(2\pi L_s/L_c)\cos(4\pi H/L_c)$

$G = 0.2718\ [v_0/(f_0 R_c)]^2$

The resonant frequency and the Q factor of the cavity without the sample are f_0 and Q_0. The resonant frequency and the Q factor of the cavity with the sample are f_s and Q. Permittivity and dielectric loss factor of the sample are ϵ' and ϵ''. The speed of light is v_0.

APPENDIX B

ONE-DIMENSIONAL ENERGY BALANCE PROGRAM FOR MICROWAVE HEATING OF NYLON 66

APPENDIX B

ONE-DIMENSIONAL ENERGY BALANCE PROGRAM FOR MICROWAVE HEATING OF NYLON 66

A one-dimensional energy balance is used to describe non-uniform microwave heating of a Nylon 66 rod due to the effects of heat conduction, convection, radiation, and changes in material dielectric loss and electric field strength. Physical properties such as heat capacity, density, thermal conductivity, and free convective and radiant heat transfer coefficients are assumed to be temperature-independent in this study. The partial differential equation describing temperature as a function of radial position and time, the microwave power coupling equation, and boundary conditions are given below.

$$C_p \rho \frac{\delta T}{\delta t} = \frac{k\delta(r\delta T/\delta r)}{r\,\delta r} + P_m$$

$$P_m = P_k \epsilon''(T)\, P_e(\epsilon'')\, P_{i0}$$

$$P_e(\epsilon'') = (B_1 \epsilon'' + B_2)^{-1}$$

$$\epsilon''(T, \omega) = \epsilon \frac{\omega \tau}{1 + (\omega \tau)^2}$$

where $\tau = k_o \exp(E/RT)$

$t = 0 \quad T = T_0 \quad$ for all r

$t > 0 \quad r = 0 \quad \delta T/\delta r = 0$

$$r = R_s \quad -k\delta T/\delta r = h_c (T - T_s) + h_r (T^4 - T_c^4)$$

The square of the electric field strength inside the material as a function of material dielectric loss and dielectric loss as a function

of temperature were experimentally determined. Temperature inside the rod is calculated using the forward finite difference method with a time step of 1.0 sec and five spatial elements. Temperature at the material boundary is calculated using the Newton-Raphson method with a tolerance of 1.0×10^{-4} for a convergence criterion. This energy balance computer program is written in FORTRAN language and is listed as follow.

```
      PROGRAM   N66E2PB
      DIMENSION T(100,3),B(5),P(5)
      CHARACTER AN
      REAL K,B,P,T,E2,TP,TE,T1,T2,T3,TOL,AR1,ER1,HT,HR
      OPEN(UNIT=31,FILE='N66JMPTC.DAT',STATUS='NEW')
      OPEN(UNIT=32,FILE='N66JMPTM.DAT',STATUS='NEW')
      OPEN(UNIT=33,FILE='N66JMPTB.DAT',STATUS='NEW')
      OPEN(UNIT=34,FILE='N66JMP.DAT',STATUS='NEW')
      OPEN(UNIT=35,FILE='N66JMPPMT.DAT',STATUS='NEW')
      OPEN(UNIT=36,FILE='N66JMPHTT.DAT',STATUS='NEW')
      OPEN(UNIT=37,FILE='N66JMPHRT.DAT',STATUS='NEW')
C     REM ************************************************************
C     REM  Non-uniform power absorption: P=PK*E2(T)*PB(E2)
C     REM  Non-uniform field strength
C     REM
C     REM  E2(T)= B(1)*B(2)*EXP(B(3)/T)/[1+ B(2)**2*EXP(2*B(3)/T)]
C     REM  PB(E2)= 1 / (P(1)* E2 + P(2) )
C     REM  where T: OC
C     REM ************************************************************
C     REM ***** Parameters of models ******************
      B(1) = 1.393
      B(2) = 0.392E-3
      B(3) = 3900
      P(1) = 4.610
      P(2) = 0.0885
C     REM ********************************************
C     REM ***** PHYSICAL PROPERTIES OF NYLON 66  ******
      D = 1.145
      CP = 0.35
      K = 0.00058
      HT = 0.0003
      HR = 1.355E-12
      ER1 = 0.45
      AR1 = 0.45
C     ************************************************
      print *, '              '
      PRINT *, 'Material Properties as follows:'
      print *, '              '
      PRINT *, '1. Thermal Conductivity (K;cal/cm/sec/OK):        ',K
      print *, '2. Heat Transfer Coefficient (HT;cal/cm2/sec/OK): ', ht
      print *, '3. Density of Material (D;g/cm3):                 ', d
```

```
      print *, '4. Heat Capacity (CP;cal/g/0K):                    ', cp
      print *, '      '
C     ******* CHANGE YOUR VARIABLE ? *****************
150   WRITE(5,151)
151   FORMAT(1X,'Do you want to change material properties (Y/N)? ',$)
      READ(5,200) AN
200   FORMAT(A1)
      IF ((AN .EQ. 'Y') .OR. (AN .EQ. 'y')) GOTO 300
      IF ((AN .EQ. 'N') .OR. (AN .EQ. 'n')) GOTO 310
      WRITE(5,152)
152   FORMAT(1X,'Mistype! Try again.')
      GOTO 150
310   CONTINUE
C     ************************************************
C     ********** EXPERIMENTAL CONDITIONS ************
      C = 0.635
      PI0 = 5.0
      PK = 0.65
      PKI = PI0*PK
      T0 = 28.5
      T0 = T0 + 273.0
      TS = 29.5 + 273.0
      TC = 28.5 + 273.0
C     ************************************************
      print *, '      '
      print *, 'Experimental Condition as follows:'
      print *, '          '
      print *, '1. Radius of the material            (C;cm):  ',c
      print *, '2. Initial material temperature      (T0;0C): ',t0-273.0
      print *, '3. Power per unit volume in material (W/cm3): ',PKI
      print *, '4. Surrounding temperature           (TS:)C): ',ts-273.0
      print *, '    '
C     ********* CHANGE YOUR EXPERIMENTAL CONDITIONS *******
160   WRITE(5,161)
161   FORMAT(1X,'Do you want to change curing conditions (Y/N)? ',$)
      READ(5,200) AN
      IF ((AN .EQ. 'Y') .OR. (AN .EQ. 'y')) GOTO 400
      IF ((AN .EQ. 'N') .OR. (AN .EQ. 'n')) GOTO 410
      WRITE(5,152)
      GOTO 160
      410 CONTINUE
C     ************************************************
C     ********* CALCULATION OF EQUATION PARAMETERS **
      A1 = D*CP*C**2/K
      A2 = PKI*C**2/K/4.18
      A4 = HT/K*C
      A5 = HR/K*C
C     ************************************************
C     ******** INPUT NUMERICAL METHOD PARAMETERS ****
      TM = 30.0
      MT = TM*60
      DN = 1.0
      NM = 5
      DM = 1.0/NM
      NN = MT/DN
```

```
      ND = 4
      TOL = 0.0001
C     ***********************************************
      print *, '                '
      print *, 'Numerical Sizes as follows:'
      print *, '                '
      print *, '1. Total reaction time (TM;min;real):           ', tm
      print *, '2. Step size of time (DN;sec;real):             ', dn
      print *, '3. Number of elements (NM;even integer):        ', nm
      print *, '4. Select the node to print out (ND; integer):  ', nd
      print *, '                '
C     ******* CHANGE YOUR NUMERICAL SIZES **********
170   WRITE(5,171)
171   FORMAT(1X, 'Do you want to change the numerical size (Y/N)? ',$)
      READ(5,200) AN
      IF((AN .EQ. 'Y') .OR. (AN .EQ. 'y')) GOTO 500
      IF((AN .EQ. 'N') .OR. (AN .EQ. 'n')) GOTO 510
      WRITE(5,152)
      GOTO 170
510   CONTINUE
C     ***********************************************
C     ****** STABILITY CHECK ***********************
      S1 = 1.0 - 2*DN/A1/DM**2
      S2 = 1.0 - 4*DN/A1/DM**2
      IF (S2 .LE. 0.0 ) THEN
      PRINT *,'Unstable Numerical Solution!'
      PRINT *,' Reduce time step or enlarge elements.'
      goto 500
      endif
      WRITE(34,*)B(1),B(2),B(3),K,HT,D,CP,C,T0-273,PKI,TS-273,TM,DN,NM,ND
C     ****** INITIALIZE THE SYSTEM EQUATION *******
      DO 10 J = 1, 2
        DO 10 I = 1, NM+1
          T(I,J) = T0
10    CONTINUE
      Z = 0.0
      PRINT*, 'TIME(MIN)','CENTER T','SELECTED T','BOUNDARY T'
      PRINT*, Z, T(1,2)-273.0, T(ND,2)-273, T(NM+1,2)-273.0
      WRITE (31,100) Z, T(1,2)-273.0
      WRITE (32,100) Z, T(ND,2)-273.0
      WRITE (33,100) Z, T(NM+1,2)-273.0
100   FORMAT(2F15.8)
C     ***********************************************
C     ** CALCULATION OF TEMPERATURE DISTRIBUTION **
      DO 60 N = 1, NN
C     ****** INTER NODES: 0 < Y < 1 ***************
        DO 20 M = 2, NM
        T1 = DN/A1/DM**2*(1.0 + 0.5/(M-1)) * T(M+1,1)
        T2 = S1 * T(M,1)
        T3 = DN/A1/DM**2*(1.0 - 0.5/(M-1)) * T(M-1,1)
        TE = T(M,1)
        E2 = B(1)*B(2)*EXP(B(3)/TE)/(1+B(2)**2*EXP(2*B(3)/TE))
        PB = 1 / (P(1) * E2  + P(2) )
        TP = DN*A2/A1*PB*E2
        T(M,2) = T1 + T2 + T3 + TP
```

```
20      CONTINUE
C     ***** AT THE NODE: Y = 0 ********************
        T(1,2) = S2 * T(1,1) + 4*DN/A1/DM**2 * T(2,1)
        TE = T(1,1)
        E2 = B(1)*B(2)*EXP(B(3)/TE)/(1+B(2)**2*EXP(2*B(3)/TE))
        PB = 1 / (P(1) * E2  + P(2) )
        TP = DN*A2/A1*PB*E2
        T(1,2) = T(1,2) + TP
C     ***** AT THE NODE: Y = 1 ********************
C      **** USING NEWTON-RAPHSON METHOD *****
        TE=T(NM,2)
        C1=ER1*A5*DM
        C2=1.0+DM*A4
        C3 = TE + DM*A4*TS + DM*A5*AR1*TC**4
40      FT = C1*TE**4+C2*TE-C3
        FT1 = 4*C1*TE**3 + C2
        TE1 = TE - FT/FT1
        FT2 = C1*TE1**4 + C2*TE1 - C3
        IF (ABS(FT2) .LT. TOL) GOTO 45
        TE = TE1
        GOTO 40
45      T(NM+1,2) = TE1
C     ************************************************
      NP = (N*DN)/60
      IF (N*DN .EQ. NP*60) THEN
      Z = DN*N
      Z = Z/60.0
      PRINT*, Z,T(1,2)-273.0, T(ND,2)-273.0,T(NM+1,2)-273.0
      WRITE (31,100) Z, T(1,2)-273.0
      WRITE (32,100) Z, T(ND,2)-273.0
      WRITE (33,100) Z, T(NM+1,2)-273.0
      WRITE (35,100) Z, PKI*E2*PB
      WRITE (36,100) Z, HT*(TE1 - T0)
      WRITE (37,100) Z, HR*(ER1*TE1**4 - AR1*TC**4)
      ENDIF
      DO 50 M = 1 , NM+1
      T(M,1) = T(M,2)
50    CONTINUE
60    CONTINUE
      CLOSE (31)
      CLOSE (32)
      CLOSE (33)
      CLOSE (34)
      CLOSE (35)
      CLOSE (36)
      CLOSE (37)
      GOTO 600
C     ****************************************************
C     REM
C     REM        SUBROUTINE FOR CHANGING INPUT DATA
C     REM
C     ********* CHANGE MATERAIL PROPERTIES ***************
300   PRINT *,'Select the following no. which you want to change!'
305   print *, ' '
      print *, '1. Thermal conductivity (K;cal/cm/sec/0K):        ',k
```

```
      print *, '2. Heat Transfer Coefficient (HT;cal/cm2/sec/0K): ', ht
      print *, '3. Density of Material (D;g/cm3):                 ', D
      print *, '4. Heat Capacity (CP;cal/g/0K):                   ', cp
      print *, '  '
      WRITE(5,331)
331   FORMAT(1X,'Input an integer of the above number: ',$)
      read(5,332)NA
332   FORMAT(I2)
      IF (NA .EQ. 1) THEN
      PRINT *, 'Input new thermal conductivity'
      read (5,*) k
      else if (na .eq. 2) then
      print *, 'Input new heat transfer coefficient'
      read (5,*) ht
      else if(na .eq. 3) then
      print *, 'Input new Density'
      read(5,*) d
      else if(na .eq. 4) then
      print *, 'Input new Heat Capacity'
      read(5,*) cp
      else
      WRITE(5,152)
      NA = 5
      endif
      IF (NA .EQ. 5) GOTO 300
340   WRITE(5,341)
341   FORMAT(1X,'Do you want to change more (Y/N) ? ',$)
      read(5,200) an
      if ((an .eq. 'Y') .or. (an .eq. 'y')) goto 300
      IF ((AN .EQ. 'N') .OR. (AN .EQ. 'n')) goto 310
      write(5,152)
      goto 340
C     ************************************************
C     ***** CHANGE EXPERIMENTAL CONDITION ***************
400   PRINT *, 'Select the following no. you want to change'
      PRINT *, '  '
405   print *, '1. Radius of the material            (C;cm):    ',  c
      print *, '2. Initial material temperature      (T0;0C):   ',t0-273.
      print *, '3. Power per unit volume in materail (Watt/cm3):', PKI
      print *, '4. Surrounding temperature           (TS;0C):   ',TS-273.
      print *, '  '
      WRITE(5,331)
      read(5,332) na
      if (na .eq. 1) then
      print *, 'Input new radius of the material'
      read(5,*) c
      else if (na .eq. 2) then
      print *, 'Input initial room temperature (0C)'
      read (5,*) t0
      t0 = t0 + 273.0
      else if (na .eq. 3) then
      print *, 'Input power per unit volume in material (Watt/cm3)'
      read (5,*) PKI
      else if (na .eq. 4) then
      print *, 'Input surrounding temperature (TS;0C)'
```

```
      read (5,*) TS
      TS = TS + 273.0
      else
      WRITE(5,152)
      NA = 6
      ENDIF
      IF (NA .EQ. 6) GOTO 400
440   WRITE(5,341)
      read (5,200) an
      IF ((AN .EQ. 'Y') .OR. (AN .EQ. 'y')) goto 400
      IF ((AN .EQ. 'N') .OR. (AN .EQ. 'n')) GOTO 410
      WRITE(5,152)
      goto 440
C     ***************************************************
C     ******* Change Numerical Sizes ********************
500   print *, 'Select the following no. you want to change:'
      PRINT *, ' '
505   print *, '1. Total reaction time (TM;min;real):        ', tm
      PRINT *, '2. Step size of time (DN;sec;inetger):       ', dn
      print *, '3. Number of elements (NM;even integer):     ', nm
      print *, '4. Select node to print out (NP; integer):   ', nd
      print *, ' '
      WRITE(5,331)
      read(5,332)na
      if (na .eq. 1) then
      print *, 'Input new total reaction time (min)'
      read(5,*)tm
      mt = tm*60
      NN = MT/DN
      else if (na .eq. 2) then
      print *, 'Input new step size of time'
      read(5,*) dn
      NN = MT/DN
      else if (na .eq. 3) then
      print *, 'Input new no. of elements'
      read(5,*) nm
      DM = 1.0/NM
      else if (na .eq. 4) then
      print *, 'Input selected mode to print'
      read(5,*) nd
      else
      WRITE(5,152)
      NA = 6
      endif
      IF (NA .EQ. 6) GOTO 500
540   WRITE(5,341)
      read(5,200) an
      if ((an .eq. 'Y') .or. (an .eq. 'y')) goto 500
      IF ((AN .EQ. 'N') .OR. (AN .EQ. 'n')) goto 510
      write(5,152)
      goto 540
C     ***************************************************
600   CONTINUE
      END
```

LIST OF REFERENCES

REFERENCES

1. J. Asmussen, H.H. Lin, B. Manring, and R. Fritz, "Single-mode or controlled multimode microwave cavity applicators for precision materials processing", Rev. Sci. Instrum., 58(8), 1477 (1987).

2. J. Jow, M.C. Hawley, M.C. Finzel, and J. Asmussen, "Microwave heating and dielectric diagnosis technique in a single-mode resonant cavity", Rev. Sci. Instrum., (in press, 1988).

3. J. Jow, M.C. Finzel, J. Asmussen, and M.C. Hawley, "Dielectric and temperature measurements during microwave curing of epoxy in a sweeping resonant cavity", 1987 IEEE MTT-S, International Microwave Symposium, June 9 - 11, 1987, Las Vegas, Nevada.

4. J. Jow, M.C. Hawley, M.C. Finzel, J. Asmussen, H.H. Lin, and B. Manring, "Microwave processing and diagnosis of chemically reacting materials in a single-mode cavity applicator", IEEE, Microwave Theory and Techniques, MTT-35(12), 1435 (1987).

5. J. Jow, M.C. Hawley, M.C. Finzel, J. Asmussen, and R. Fritz, "On-line measurement of temperature- and cure-dependent dielectric properties during single frequency microwave curing and comparison with thermal curing of epoxy resins", Conference on Emerging Technologies in Materials, August 1987, Minneapolis, MN.

6. J. Jow, M.C. Hawley, M.C. Finzel, and T. Kern, "Dielectric analysis of epoxy/amine resins using microwave cavity technique", Polymer Engineering and Science, (in press, 1988).

7. M.C. Hawley, J. Jow, C. Schwalm, S. Singer, and J.D. Delong, "Microwave curing of epoxy matrix", 4th Annual International Polymer Processing Society Meeting, May 8 - 11, 1988, Orlando, Florida.

8. J. Jow, J.D. DeLong, and M.C. Hawley, "Computer-controlled pulsed microwave processing of epoxy", SAMPE Quarterly, (submitted for publication, 1988).

9. J. Jow, M.C. Hawley, and J. Delong, "Microwave heating of polymer composites containing thermally conductive and non-conductive reinforcement", 3rd Technical Conference on Composite Materials, Sept. 26 - 29, 1988, Seattle, Washington.

10. J. Jow, M.C. Hawley, M.C. Finzel, and J. Asmussen, "Microwave power absorption and heating characteristics of polymers in a resonant cavity", J. Microwave Power, (submitted for publication, 1988).

11. D. Gouderc, M. Giroux, and R.G. Bosisio, "Dynamic high temperature microwave complex permittivity measurements on samples heated via microwave absorption", J. Microwave Power, 8(1), 69 (1973).

12. J.R. Rogers, "Properties of steady state, high pressure, argon microwave discharges", Ph.D. Thesis, Michigan State University, (1982).

13. Luxtron Technical Manual, Model 750, Luxtron Corp. (1986).

14. M. Sucher and J. Fox, Handbook of microwave measurements, Vol. II, 3rd, Polytechnic Press of the Polytechnic Institute of Brooklyn (1963).

15. E.G. Spencer, R.C. LeCraw, and L.A. Ault, "Note on cavity perturbation theory", J. of Applied Physics, 28(1), 130 (1957).

16. E.F. Labuda and R.C. LeCraw, "New technique for measurement of microwave dielectric constants", Rev. Sci. Instrum., 32(4), 391 (1961).

17. N.L. Conger and S. E. Tung, "Measurement of dielectric constant and loss factor of powder materials in the microwave region", Rev. Sci. Instrum., 35(3), 384 (1967).

18. H. Kobayashi and S. Ogawa, "Dielectric constant and conductivity measurement of powder samples by the cavity perturbation method", J. Applied Physics, 10, 345 (1971).

19. I.I. Eldumiati and G.I. Haddad, "Cavity perturbation techniques for measurement of the microwave conductivity and dielectric constant of a bulk semiconductor material", IEEE, MTT-20, 126 (1972).

20. W. Meyer, "Dielectric measurements on polymeric materials by using superconducting microwave resonators", IEEE, MTT-25, 1092 (1977).

21. A. Bonincontro and C. Cametti, "On the applicability of the cavity perturbation method to high-loss dielectrics", J. Physics E., 1232 (1977).

22. C. Akyel, R.G. Bosisio, and G. April, "An active frequency technique for precise measurements on dynamic microwave cavity perturbations", IEEE IM-27, 364 (1978).

23. A. Parkash, J.K. Vaid, and A. Mansingh, "Measurement of dielectric parameters at microwave frequencies by cavity-perturbation technique", IEEE, MTT-27(9), 791 (1979).

24. S. Lee, C. Akyel, and R.G. Bosisio, "Precise calculations and measurements on the complex dielectric constant of lossy materials

using TM_{010} cavity perturbation techniques", IEEE, MTT-29, 1041 (1981).

25. H.A. Buckmaster, C.H. Hansen, and H. Zaghloul, "Complex permittivity instrumentation for high-loss liquids at microwave frequencies", IEEE, MTT-33(9), 822 (1985).

26. S. Chao, "Measurements of microwave conductivity and dielectric constant by the cavity perturbation method and their Errors", IEEE, MTT-33(6), 519 (1983).

27. M. Martinelli, P.A. Rolla, and E. Tombari, "A method for dynamic dielectric measurements at microwave frequencies: applications to polymerization process studies", IEEE, IM-34, 417 (1985).

28. B. Terselius and B. Ranby, "Cavity perturbation measurements of the dielectric properties of vulcanizing rubber and polyethylene compounds", J. Microwave Power, 13(4), 327 (1978).

29. C.G. Montgomery, Technique of Microwave Measurements, Vol. 11, 384, Dover Pub., New York (1966).

30. D.M. Smith, "Relative humidity effects in microwave resonators", IEEE, MTT-15, 480 (1967).

31. R.F. Harrington, Time-harmonic electromagnetic fields, McGraw-Hill, New York (1961).

32. H.F. Huang, "Temperature control in a microwave resonant cavity system for rapid heating of nylon monofilament", J. Microwave Power, 11(4), 305 (1976).

33. A. Gourdenne, "Possible use of the microwaves in polymer science", International Conference on Reactive Processing of Polymers Proceedings, 23 (1982).

34. E. Karmazsin, P. Satre, and J.F. Rochas, "Use of continuous and pulsed microwaves for quick polymerization of epoxy resins: study of some thermomechanical properties", Thermochimica Acta, 93, 305 (1985).

35. L.K. Wilson, and J.P. Salerno, "Microwave curing of epoxy resins", Technical Report, AVRADCOM TR-78-46 (1978).

36. N.S. Strand, "Fast microwave curing of thermoset parts", Modern Plastics, 57(10), 64 (1980).

37. H. Lee and K. Neville, Handbook of Epoxy Resins, McGraw-Hill, New York (1972).

38. J. Delmonte, "Electrical properties of epoxy resins during polymerization", J. Applied Polymer Science, 2 (4), 108 (1959).

39. E.N. Haran, H. Gringras, and D. Katz, "Dielectric properties of an epoxy resin during polymerization", J. Applied Polymer Science, 9,

3505 (1965).

40. D. Kranbuehl, S. Delos, E. YI, J. Mayer, and T. Jarvie, "Dynamic dielectric analysis: nondestructive material evaluation and cure cycle monitoring", Polym. Eng. Sci., 26(5), 338 (1986).

41. D.R. Day, "Effects of stoichiometric mixing ratio on epoxy cure - a dielectric analysis", Polym. Eng. Sci., 26(5), 362 (1986).

42. J.W. Lane, J.C. Seferis, and M.A. Bachmann, "Dielectric studies of the cure of epoxy matrix system", Journal of Applied Polymer Science, 31, 1155 (1986).

43. J.W. Lane, J.C. Seferis, and M.A. Bachmann, "Dielectric modeling of the curing process", Polymer Engineering and Science, 26(5), 346 (1986).

44. N.F. Sheppard and S.D. Senturia, "Chemical interpretation of the relaxed permittivity during epoxy resins cure", Polym. Eng. Sci., 26(5), 354 (1986).

45. Z.N. Sanjana, "The use of microdielectrometry in monitoring the cure of resins and composites", Polym. Eng. Sci., 26(5), 373 (1986).

46. S.A. Bidstrup, N.F. Sheppard, and S.D. Senturia, "Dielectric analysis of the cure of thermosetting epoxy/amine systems", 45th Technical Conference, Society of Plastic Engineers, May, 1987.

47. S.D. Senturia and N.F. Sheppard, "Dielectric Analysis of Thermoset Cure", Advances in Polymer Science, 80, 1 (1986).

48. W.X. Zukas and S.E. Wentworth, "Microdielectric monitoring of prepreg cure", Polymer Composite, 8(4), 232 (1987).

49. Peter Hedvig, Dielectric Spectroscopy of Polymers, John Wiley & Sons, New York (1977).

50. J.J. Aklonis and W.J. Macknight, Introduction to Polymer Viscoelasticity, John Wiley & Sons, New York (1983).

51. Frank E. Karasz, editor, Dielectric Properties of Polymers, Plenum Press, New York (1972).

52. G.M. Bartenev and Y.V. Zelenev, editors, Relaxation Phenomena in Polymers, John Wiley & Sons, New York (1974).

53. R.K. Agrawal, and L.T. Drzal, "The characterization of the composite fiber-matrix interface formed under microwave curing", Conference on emerging technologies in materials, AICHE national summer meeting, Minneapolis, Minnesota (1987).

54. D.A. Lewis, J.C. Hedrick, T.C. Ward, and J.E. McGrath, "The accelerated curing of epoxy resins using microwave radiation", Polymer Reprint, 28(2), 330 (1987).

55. J.C. Hedrick, D.A. Lewis, T.C. Ward, and J.E. McGrath, "Morphology and fracture toughness of thermoplastic modified epoxy resin networks prepared via electromagnetic processing", Polymer Reprints, 29(1), 363 (1988).

56. M.C. Finzel, M.C. Hawley, R. Fritz, and J. Asmussen, "Comparison of multimode microwave and thermal methods for curing of epoxy/amine system", Conference on Emerging Technologies in Materials, August 18 - 20, 1987, Minneapolis, Minnesota.

57. H.E. Adabbo and R.J.J. Williams, "The evolution of thermosetting polymers in a conversion-temperature phase diagram", J. Applied Polymer, 27, 1327 (1982).

58. J.B. Enns and J.K. Gillham, "Time-temperature-transformation (TTT) cure diagram: modeling the cure behavior of thermosets", J. Applied Polymer, 28, 2567 (1983).

59. S.M. Singer, "Experimental study on some property effects and one-dimensional modeling of the cure and residual stress for thermal and electromagnetic curing of epoxy resin", Master Thesis, Michigan State University, 1988.

60. G. Roussy, A. Mercier, J.M. Thiebaut, and J.P. Vaubourg, "Temperature runaway of microwave heated materials: study and control", J. Microwave Power, 47 (1985).

61. R. Chahine, T.K. Bose, C. Akyel, and R.G. Bosisio, "Computer-based permittivity measurements and analysis of microwave power absorption instabilities", J. Microwave Power, 19(2), 149 (1984).

62. S. Burkhart, "Coaxial E-field probe for high-power microwave measurement", IEEE, MTT-33(3), 262 (1985).

63. R.W. Griffiths and G. Guard, "Composite Integration of optical fiber sensors", Conference on Composites in Manufacturing 7, Dec. 7 - 10, 1987, Long Beach, CA.

64. D. Ye and B. Ho, "Nondestructive probing of temperature profile inside layered composite material", Poster Paper, Open House, Composite Materials and Structures Center, Michigan State University, April 22 (1988).

65. L. Shechter, J. Wynstra, and R.P. Kurkjy, "Glycidyl ether reactions with amines", Ind. Eng. Chem., 48, 94 (1959).

66. H.H. Lin, research notes (1986).